# THERMODYNAMIC AND TRANSPORT PROPERTIES OF SIMPLE IONIC MELTS.

A THESIS

Submitted to

THE UNIVERSITY OF LONDON

by

CHRISTOPHER GEORGE JEFFREYS BAKER, B.Sc.(Eng.),A.C.G.I.

Candidate for the
Degree of Doctor of Philosophy
in the Faculty of Engineering.

Department of Chemical Engineering
and Chemical Technology,
Imperial College of Science and Technology,
London, S.W.7.

October, 1967.

ABSTRACT.

The thermodynamic and transport properties of molten salts are surveyed. The principal known causes of a.c. frequency dispersion in electrolytic cells, which severely limits the accuracy of electrical conductance measurements, are discussed.

A semi-phenomenological theory of diffuse layer relaxation in conductance cells is given for melts and solutions of pure salts. This relaxation gives rise to Debye type dispersion of the parallel resistance and capacitance components of the a.c. admittance at audio and radio frequencies. The polarization-free specific conductance, the Gouy capacitance, and the relaxation time may, in principle, be determined from experiment without assuming values for the parameters of the theory.

Equipment is described for measuring dispersion in conductance cells in the frequency range 0.1 - 200 KHz. Dispersion was measured in M-aqueous KCl solution (resistance to $\pm$ 0.002 %, capacitance to $\pm$ 0.015 %), and

in KCl, AgBr, and $CdCl_2$ melts (resistance to $\pm$ 0.003 %, capacitance to $\pm$ 0.06 %).

Results for KCl aq. in a 2.5 mm bore glass cell show excellent agreement with theory, but for narrower bores the dispersion depends on bore size, indicating extraneous effects.

Strong deviations are always found in the melts, the capacitance being too low and the conductance too high. In narrow bore cells the capacitance error is enlarged at low frequencies.

Saturation of AgBr and KCl melts with water produces an arrest in the conductance at 0.7 KHz, which may represent dielectric relaxation.

ACKNOWLEDGEMENTS.

I wish to express my sincere gratitude to Professor A.R.Ubbelohde, C.B.E., F.R.S., and to Dr.E.R.Buckle, to whom I am especially indebted for their valuable guidance and encouragement throughout this research.

I should also like to acknowledge the assistance of the members of the Electronics and Glassblowing workshops under the direction of Mr.L.Tyley and Mr.A.J.Jones respectively, without whose help much of this research could not have been accomplished.

Thanks are owed to the Science Research Council for a Research Studentship.

# CONTENTS.

# CHAPTER 1.

# THERMODYNAMIC AND TRANSPORT PROPERTIES OF SIMPLE IONIC MELTS.

## INTRODUCTION.

The study of molten salts is of great interest, since, as liquids, they are unique in that positive and negative ions coexist in them in the absence of solvent molecules. The structure of molten salts display considerable short range order, due to the presence of strong interionic forces[1]. The radial distribution functions have been determined by X-ray and neutron diffraction methods[2-6], and complex ion formation in melts has been investigated by Raman[7-10], infra-red[11-13], and ultra-violet[14,15] spectroscopy, and by electron spin[16] and nuclear magnetic[17,18] resonance. At present, no theory of the liquid state adequately describes the structure of ionic melts[19]. However, Bockris et al.[20-24] have applied the hole theory of Fürth[25] to pure molten salts, and have successfully calculated a number of thermodynamic properties. The empirical nature of this approach has led to a renewed interest in the compressed gas theory of McCall et al[26].

Molten salts are becoming increasingly important in technology. The recovery of certain metals by electrolysis of their molten salts[27,28] is a well established industrial process. The separation of isotopes by

electromigration in melts has been successfully carried out on a laboratory scale[29-31]. The possible use of molten salts in economical high temperature fuel cells[32,33] and as solvents for fissionable materials in homogeneous nuclear reactors[34,35] is at present being investigated.

An accurate knowledge of certain properties of molten salts is of great importance, both from a technological viewpoint, and in providing the foundations for new statistical theories of melts. Consequently, many physical, thermodynamic, and transport properties of both pure molten salts and their mixtures have been investigated. Early reviews include those by Lorenz[36](1905), Biltz and Klemm[37] (1926), Drossbach[38] (1938), and Mulcahy and Heymann[1] (1943). More recently, reviews have been published by Camescasse[39], Janz, Solomons and Gardner[40], Bloom[34], Voskresenskaya[41], Watelle-Marion[42], Blomgren and Van Artsdalen[43], Johnson and Pardee[44], Janz[45], and Laity[46]. Janz[47] and Morachevskii[48] have published bibliographies, and Buckle[49] has made a compilation of recent molten salt data. Books devoted to molten salts have been published by Delimarskii and Markov[50], Blander[51], and Sundheim[52]. In addition, there are useful chapters in the books of Bockris[53], and Bockris, White and Mackenzie[54]. Molten salts have also featured in the Discussions of the Faraday Society[55].

## THERMODYNAMIC PROPERTIES.

Maxwell's electromagnetic field equations have been solved only for the two extreme cases of a perfect conductor and a dielectric. Molten salts do not come under either of these categories, but for present purposes they will be treated as dielectrics. The thermodynamic functions for molten salts under the influence of an electric field are derived below.

### CALCULATION OF THE THERMODYNAMIC PROPERTIES.

Consider the molten salt contained between two parallel conducting plates, (e.g. the plates of a capacitor, or the electrodes of a capillary cell).

If the salt is considered as a dielectric, the Maxwell electromagnetic field equations give [56],

$$E = \frac{4\pi q}{\epsilon A} \quad , \qquad (1.1)$$

where E is the field, q is the charge on the plates of area A, and $\epsilon$ is the dielectric permittivity. The potential difference across the plates, V, is given by the relation,

$$V = \int_0^L E \, dx \quad , \qquad (1.2)$$

where x is the length co-ordinate between the plates, and L is their separation.

If the dielectric is homogeneous, E is constant, and it follows from Eqn.(1.2) that V = EL, and hence from Eqn.(1.1),

$$V = \frac{4\pi qL}{A\varepsilon} \qquad (1.3)$$

Now the work $dW_E$ required to transfer an element of charge dq from the negative to the positive plate is $dW_E = V.dq$, and from Eqns. (1.1), (1.3),

$$dW_E = \frac{LAE}{4\pi} d\,[\mathfrak{E}\cdot E]$$

$$= \frac{v_c E}{4\pi} d\,[\mathfrak{E}\cdot E] \; , \qquad (1.4)$$

where $v_c$ is the volume of fluid between the plates, and the quantity $[\mathfrak{E}\cdot E]$ is termed the electric displacement.

A variation in the internal energy U is given by the first law of thermodynamics as ,

$$dU = dQ - dW \; , \qquad (1.5)$$

where Q is the heat absorbed, and W is the total amount of work performed. Since U, Q and W, and also F,G, G', H, S, and v, which will be introduced later, are extensive properties, they will be defined, for convenience, in molar units.

Now, for a reversible, isothermal process, dQ = TdS, where T is the absolute temperature and S is the entropy. Using this relation and Eqns. (1.4), (1.5), we have,

$$dU = TdS - Pdv + \frac{v_c E}{4\pi} d\,[\mathfrak{E}\cdot E] \; , \qquad (1.6)$$

where P is the external pressure, and v the molar volume.

The Helmholtz free energy F is defined by the equation,

$$F = U - TS \,, \qquad (1.7)$$

and from Eqn. (1.6),

$$dF = dU - TdS - SdT$$

$$= -SdT - Pdv + \frac{V_c E}{4\pi} \, d\,[\,\varepsilon \cdot E]. \qquad (1.8)$$

It is now convenient to define the function[57]

$$G' = G - \frac{v_c \varepsilon E^2}{4\pi}$$

where $G = F + Pv$ is the Gibbs free energy.

Thus,
$$G' = F + Pv - \frac{v_c \varepsilon E^2}{4\pi} \,. \qquad (1.9)$$

Differentiating Eqn. (1.9), and using Eqn. (1.8) gives,

$$dG' = dF + Pdv + vdP - \frac{v_c E^2}{4\pi} d\varepsilon - \frac{v_c \varepsilon E}{2\pi} dE$$

$$= -SdT + vdP - \frac{v_c \varepsilon E}{4\pi} \, dE \,, \qquad (1.10)$$

and hence, $\left(\frac{\partial G'}{\partial T}\right)_{P,E} = -S \,; \qquad (1.11a)$

$$\left(\frac{\partial G'}{\partial E}\right)_{T,P} = -\frac{v_c \varepsilon E}{4\pi} \,, \qquad (1.11b)$$

$$\left(\frac{\partial G'}{\partial P}\right)_{T,E} = v \,. \qquad (1.11c)$$

Since, for exact differentials, the order of differentiation is immaterial, (cf. the Maxwell equations [58]), it follows from Eqns. (1.11a), (1.11b) that

$$\left(\frac{\partial S}{\partial E}\right)_{T,P} = \frac{v_c}{4\pi} \left(\frac{\partial [\varepsilon \cdot E]}{\partial T}\right)_{P,E} \,,$$

and if E is not a function of T then,

$$\left(\frac{\partial S}{\partial E}\right)_{T,P} = \frac{v_c E}{4\pi} \left(\frac{\partial \varepsilon}{\partial T}\right)_{P,E} . \quad (1.12)$$

Since, $Q = T.dS$, it follows from Eqn. (1.12) that,

$$\left(\frac{\partial Q}{\partial E}\right)_{T,P} = \frac{v_c T E}{4\pi} \left(\frac{\partial \varepsilon}{\partial T}\right)_{P,E} . \quad (1.13)$$

Similarly, from Eqns. (1.11b), (1.11c),

$$\left(\frac{\partial v}{\partial E}\right)_{T,P} = \frac{-v_c}{4\pi} \left(\frac{\partial [\varepsilon E]}{\partial P}\right)_{T,E} ,$$

and if E is not a function of P, then

$$\left(\frac{\partial v}{\partial E}\right)_{T,P} = \frac{-v_c E}{4\pi} \left(\frac{\partial \varepsilon}{\partial P}\right)_{T,E} . \quad (1.14a)$$

It follows directly from Eqn. (1.14a) that the coefficient of electrostriction, $\frac{1}{v}\left(\frac{\partial v}{\partial P}\right)_{T,P}$ is

$$\frac{1}{v}\left(\frac{\partial v}{\partial E}\right)_{T,P} = \frac{-E\, v_c}{4\pi v} \left(\frac{\partial \varepsilon}{\partial P}\right)_{T,E} . \quad (1.14b)$$

From Eqn. (1.6),

$$dU = TdS - Pdv + \frac{v_c E^2}{4\pi} d\varepsilon + \frac{v_c \varepsilon E}{4\pi} dE$$

$$\therefore \left(\frac{\partial U}{\partial E}\right)_{T,P} = T \left(\frac{\partial S}{\partial E}\right)_{T,P} - P \left(\frac{\partial v}{\partial E}\right)_{T,P} + \frac{v_c E^2}{4\pi} \left(\frac{\partial \varepsilon}{\partial E}\right)_{T,P} + \frac{v_c \varepsilon E}{4\pi} . \quad (1.15)$$

If the assumption is made that the permittivity is independent of the field strength then Eqn. (1.15) reduces to,

$$\left(\frac{\partial U}{\partial E}\right)_{T,P} = T \left(\frac{\partial S}{\partial E}\right)_{T,P} - P \left(\frac{\partial v}{\partial E}\right)_{T,P} + \frac{v_c \varepsilon E}{4\pi} . \quad (1.16)$$

This assumption is valid, for all practical purposes, for dielectrics except at field strengths greater than several thousand volts/cm [59].

Using Eqns. (1.12), (1.14a), (1.16), we have ,

$$\left(\frac{\partial U}{\partial E}\right)_{T,P} = \frac{v_c E}{4\pi}\left[\varepsilon + T\left(\frac{\partial E}{\partial T}\right)_{P,E} + P\left(\frac{\partial \varepsilon}{\partial P}\right)_{T,E}\right] \qquad (1.17)$$

The enthalpy H is defined by the equation,

$$H = U + Pv,$$

whence,

$$dH = dU + Pdv + vdP .$$

$$\therefore \left(\frac{\partial H}{\partial E}\right)_{T,P} = \left(\frac{\partial U}{\partial E}\right)_{T,P} + P\left(\frac{\partial v}{\partial E}\right)_{T,P} + v\left(\frac{\partial P}{\partial E}\right)_{T,P} ,$$

which reduces to,

$$\left(\frac{\partial H}{\partial E}\right)_{T,P} = \left(\frac{\partial U}{\partial E}\right)_{T,P} + P\left(\frac{\partial v}{\partial E}\right)_{T,P}$$

since the external pressure is not a function of the field. Using Eqns. (1.14a), (1.17) ,

$$\left(\frac{\partial H}{\partial E}\right)_{T,P} = \frac{v_c E}{4\pi}\left[\varepsilon + T\left(\frac{\partial \varepsilon}{\partial T}\right)_{P,E}\right] , \qquad (1.18)$$

where $\left(\frac{\partial H}{\partial E}\right)_{T,P}$ is the **electrocalorific coefficient.**

Since, $F = U - TS,$

and $dF = dU - TdS - SdT ,$

$$\left(\frac{\partial F}{\partial E}\right)_{T,P} = \left(\frac{\partial U}{\partial E}\right)_{T,P} - T\left(\frac{\partial S}{\partial E}\right)_{T,P} .$$

Therefore, using Eqns. (1.12), (1.17), we have,

$$\underline{\left(\frac{\partial F}{\partial E}\right)_{T,P} = \frac{V_c E}{4\pi}\left[\epsilon + P\left(\frac{\partial \epsilon}{\partial P}\right)_{T,E}\right]} \quad . \qquad (1.19)$$

Also, since $G = F + Pv$ ,

and $dG = dF + Pdv + vdP$ ,

$$\left(\frac{\partial G}{\partial E}\right)_{T,P} = \left(\frac{\partial F}{\partial E}\right)_{T,P} + P\left(\frac{\partial v}{\partial E}\right)_{T,P} + v\left(\frac{\partial P}{\partial E}\right)_{T,P}$$

$$= \left(\frac{\partial F}{\partial E}\right)_{T,P} + P\left(\frac{\partial v}{\partial E}\right)_{T,P} ,$$

since P is not a function of E.

Hence, from Eqns. (1.14a), (1.19),

$$\underline{\left(\frac{\partial G}{\partial E}\right)_{T,P} = \frac{V_c \epsilon E}{4\pi}} \quad . \qquad (1.20)$$

LIMITATIONS OF THE THERMODYNAMIC RELATIONS FOR POOR CONDUCTORS IN ALTERNATING FIELDS.

The above relations, Eqns. (1.12) - (1.14), (1.17) - (1.20), have been derived for a dielectric under the influence of a static field. They will apply only in the case of an alternating field if the charged particles can maintain statistical equilibrium with the applied field.

Landau and Lifshitz[60] have examined the conditions under which an alternating electromagnetic field can be treated as quasi-static for the purpose of obtaining correct solutions of Maxwell's electromagnetic field equations. These conditions are that the period of the field be large compared with the characteristic times of microscopic conduction, and

that the mean free path of the conducting species be small compared with the distance over which the field changes appreciably. The first condition is the more stringent, and requires that $\omega \ll 10^9$ $sec^{-1}$ for the solution to hold for a poor conductor (e.g. a molten salt) in a typical capillary cell.

## TRANSPORT PROPERTIES.

Transport properties are partly governed by the structure of the melt, and are consequently uniquely related to one another. The exact form of this relationship can only be determined from an accurate knowledge of the interionic forces. Since this is not yet available, transport processes are usually described by phenomenological laws.

### ELECTRICAL CONDUCTANCE.

The specific conductance of an electrolyte, $\kappa$, is formally defined as the reciprocal of the resistance of a cube of the material of side 1 cm, and is of the order of 1 $ohm^{-1}$ $cm^{-1}$ for most molten salts. The equivalent conductance, $\Lambda$, is related to the specific conductance by equation,

$$\Lambda = \kappa v^{eq} \text{ ohms}^{-1} \text{ cm}^2, \quad (1.21)$$

where $v^{eq}$ is the equivalent volume of the electrolyte. The interpretation of conductance data in mixed ionic melts has been discussed by Buckle and Tsaoussoglou[61], who stressed the need to separate the effect of specific volume changes on the ionic concentrations from the more important effects of structural or constitutional changes, which influence the mobilities.

Specific conductance is related to the resistance, R ohms, of a conductance cell of length L cm , and cross-

sectional area A $cm^2$ by the equation,

$$\kappa = \frac{1}{R} \cdot \frac{L}{A} = \frac{K}{R}, \quad (1.22)$$

where the ratio L/A = K is termed the cell constant. Silica capillary cells [62,63], normally having cell constants in the range 500 - 1000 $cm^{-1}$, are used for conductance measurements in most alkali halide melts. However, in molten fluorides, metallic [64] and hot pressed boron nitride [65] cells have been used, as these melts readily attack silica. Metallic cells have a very low resistance, and consequently, polarization can lead to serious errors [66].

Measurements of cell resistance are usually made with an a.c. bridge at audio-frequencies, to minimize polarization errors. The problems involved in making such measurements have been widely discussed [67-69]. D.c. methods have been reviewed by Gunning and Gordon [70], and applied to molten salts [71-73]. Conductances of metallic and semi-conductor melts have been measured using the transformer eddy current method [74,75]. This technique enables measurements spanning a very wide range of resistance to be made without the need for electrodes. However, the results are less accurate than those obtained by bridge measurements, when polarization effects are not serious.

The temperature and pressure coefficients of conductance in ionic melts are useful in determining which

of the theories of transport [76-79] are applicable to these media. Simple kinetic theory predicts the temperature dependence as being of the Arrhenius form,

$$\kappa = \kappa_\infty \exp\left[-\Delta H_\kappa / RT\right], \qquad (1.23a)$$

$$\text{or } \Lambda = \Lambda_\infty \exp\left[-\Delta H_\Lambda / RT\right], \qquad (1.23b)$$

where $\kappa_\infty$ and $\Lambda_\infty$ are the frequency factors, which are related to the entropy of activation [80], $\Delta H$ is the energy of activation for conductance, assumed to be independent of temperature, and R is the universal gas constant. Conductance measurements on ionic melts have shown that these equations are not generally obeyed. Van Artsdalen and Yaffe [81] found that, for the alkali halides at temperatures 50°C or more above their melting points, the activation energies at constant pressure decreased linearly with temperature. They attributed this to the lowering of the restricting potentials for migration as the liquid expands. Measurements on nitrate melts [82-84] have also shown a lowering of the activation energy with increasing temperature, although not linearly. This has been attributed by Ubbelohde et al.[85] to auto-complexing in these melts, which becomes less pronounced as the temperature is increased. Copeland and Zybko[86] measured the effect of pressure on the conductance of molten sodium nitrate. They found that this decreased with pressure and that, at 369°C, its value at 362

atmospheres was 5.7% lower than that at atmospheric pressure. This was attributed to the loss in the free volume for transport in the melt, mainly due to compression. This trend was confirmed by Fray[87] in his measurements on sodium and potassium nitrate melts. He showed that his results did not depend on the pressurizing gas, and that the temperature and pressure coefficients for conductance were best explained by the critical free volume theory of Cohen and Turnbull[79].

In a.c. measurements of the electrical conductance of electrolytes, the admittance of the cell changes with the applied a.c. frequency. This effect, which relaxes out at high frequencies, is termed dispersion, and is particularly serious in ionic melts[63]. The true electrical conductance has been allegedly obtained by the extrapolation to infinite frequency of the values obtained at a number of lower frequencies. However, the extrapolation procedures are empirical and it is probable that this has contributed to the wide scatter in the published conductance data [63]. In the research now described, dispersion has been studied with a view to achieving accurate conductance values for molten salts.

## ELECTROMIGRATION.

The motion of ions in an electrolyte under the influence of an electric field is termed electromigration.

The mobility of an ion is defined as its velocity, with respect to a stated frame of reference, under unit potential gradient. If ions of species i move with a velocity $\underline{v}_{ij}$ relative to ions j in an electric field $\underline{E}$, the internal mobility, $u_{ij}$, is defined by the equation,

$$\underline{v}_{ij} = u_{ij} \cdot \underline{E} \quad , \qquad (1.24)$$

and it follows that

$$\kappa = \sum_i e\, z_i\, c_i\, u_{ij} \qquad (1.25)$$

where e is the electronic charge, and $z_i$ and $c_i$ are respectively the valency and ionic concentration of ions i. The conductance is therefore independent of the choice of reference ion. The internal transport number, $t_{ij}$, is defined by the equation,

$$t_{ij} = \frac{u_{ij}}{\sum u_{ij}} = \frac{e\, z_i\, c_i\, u_{ij}}{\kappa} \quad . \qquad (1.26)$$

However, if the ionic velocities are measured relative to some point outside the electrolyte, (e.g. the wall of a capillary cell), this leads to the definitions of the external mobility, $u_{ie}$, and the external transport number, $t_{ie}$, given by the relations,

$$\underline{v}_{ie} = u_{ie} \cdot \underline{E} \quad , \qquad (1.27)$$

and

$$t_{ie} = \frac{u_{ie}}{\sum u_{ie}} = \frac{e\, z_i\, c_i\, u_{ie}}{\kappa} \quad , \qquad (1.28)$$

where $\underline{v}_{ie}$ is the velocity of ions i relative to the external point.

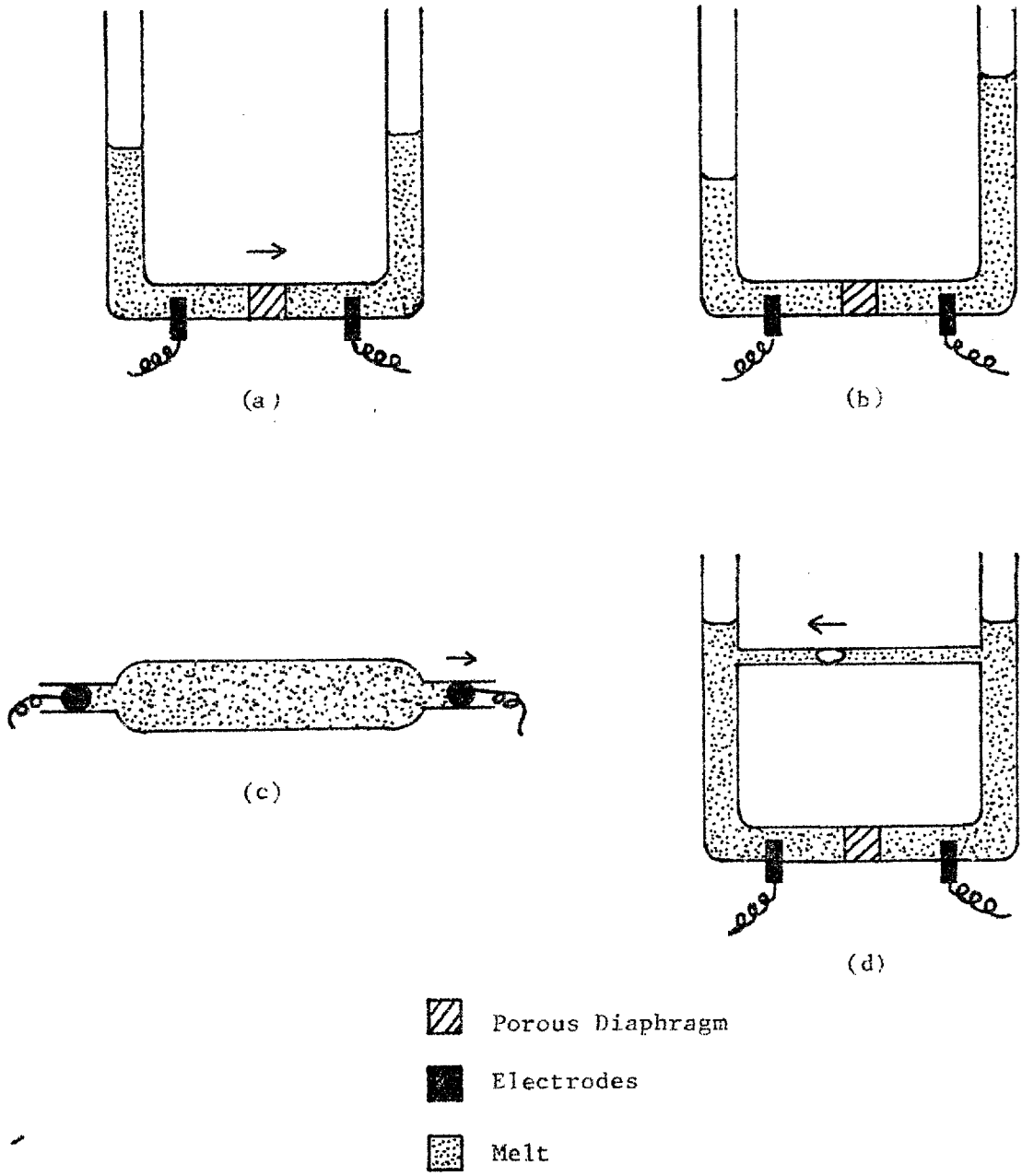


Figure 1: The Measurement of Mobilities in Hittorf Cells.

(a) Direct Weighing and Radiotracer Techniques.

(b) Measurement of Piezoelectric Coefficient.

(c) Measurement of the Displacement of Liquid Metal Electrodes.

(d) Measurement of the Velocity of an Indicator Bubble.

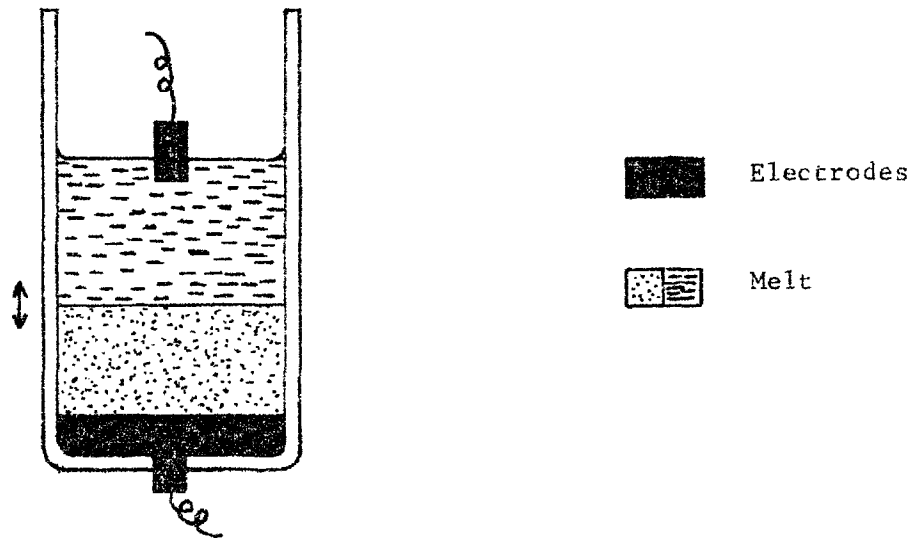


Figure 2: The Measurement of Mobilities by the Moving Boundary Method.

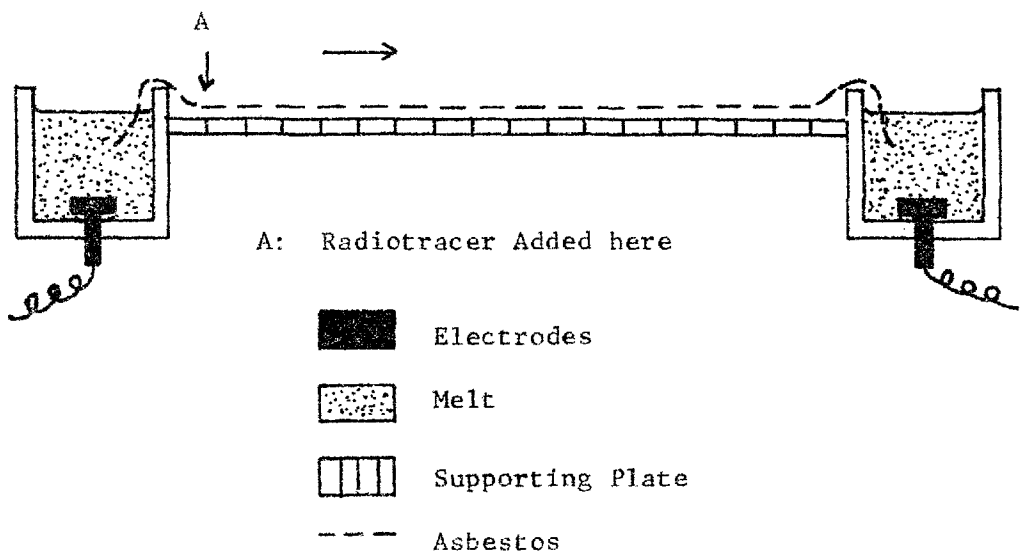


Figure 3: The Measurement of Mobilities by Electrophoresis.

External transport measurements are commonly made in Hittorf cells, in which bulk flow of melt between the electrode compartments is prevented by interposing a porous plug between the limbs (Fig.1). Transport numbers are evaluated from the changes in the amounts of the individual constituents in each half of the cell. These have been determined by direct weighing[89-92], by radiotracer methods[93-97] by the measurement of piezoelectric coefficients [98], by the displacement of liquid metal electrodes [99,100], and by the velocity of an indicator bubble [101-103]. Moving boundary methods, (Fig.2), have also been used [104,105] to measure external transport numbers in pure molten salts. These have also been measured in electrophoresis experiments[106,107], in which the displacement of radioactive ions along a sheet of asbestos joining the anode and cathode compartments of a molten salt cell is observed (Fig.3). Klemm[108] has indicated a method by which the absolute external mobilities could be determined by this technique.

At present there is no agreed interpretation of the results of molten salt electromigration experiments, and the concept of migration in pure molten salts has even been questioned[109,110]. The considerable scatter in existing data ($\sim$15%) probably results from the transport of ions by means other than electromigration. Measurements in Hittorf cells are particularly prone to errors of this kind.

Several workers [89,90,99,111] have devised methods to overcome bulk flow through the diaphragm due to a difference in the levels of the melt in the electrode compartments. Electro-osmosis is difficult to detect in electromigration experiments, as transport by this means is also proportional to the potential gradient[97]. This effect, which could lead to a time dependence in the results[97], has been investigated by altering the diaphragm[89]. Lundén[97] found that the sum of the independently measured cation and anion transport numbers in pure zinc chloride was not unity. He attributed this, and also the time effect in his results, to transport through the diaphragm by diffusion. Duke and Bowman [95] found that the transport numbers of alkali halides were not simple function of the mass[112] or the radius of the ions[113] or that they were independent of the anion[114]. They did not investigate the theoretical predictions of Klemm[115]. In the moving boundary[104,105] and the electrophoresis[106,107] experiments, electro-osmosis is of course absent, although transport by diffusion still occurs. Although this is not serious in the former method, it causes a widening of the migration zone in electrophoresis experiments, which severely limits the attainable accuracy[108]. Data on the temperature dependence of migration are scarce,but available experimental evidence [96,105] suggests that external transport numbers in molten salts are relatively insensitive to temperature. As

yet no data on the pressure dependence has been published.

Behl and Egan[116] have recently determined internal cation-anion mobilities in a number of mixed halide melts from measurements on an E.M.F. cell with transference[108]. Their results for the system LiCl-$PbCl_2$ agreed well with those of Klemm and Mønse[104], except at concentrations below 40%LiCl, wherethe two sets of results differed considerably. This can probably be explained by the fact that Behl and Egan assumed a linear relationship between equivalent volume and mole fraction for this mixture. In the light of results obtained for similar systems[19], this assumption is hardly likely to be valid.

## DIFFUSION.

Diffusion results from the natural transport of particles by Brownian motion. In one-dimensional steady state diffusion, the mass flux of species i across an interface, $N_i$, is related to the concentration of that species, $c_i$, (or, more correctly, to the chemical potential[117]) by Fick's first law:

$$N_i = -D_i \, dc_i/dx \, , \quad (1.29)$$

where $D_i$ is the Fick <u>diffusion coefficient</u>. The mass flux is normally defined using the melt container as the frame of reference for velocity. In unsteady state diffusion, Fick's second law applies :

$$\text{i.e.} \quad \partial c_i/\partial t = \frac{\partial}{\partial x}(D_i \partial c_i/\partial x), \quad (1.30a)$$

which simplifies to,

$$\partial c_i/\partial t = D_i \partial^2 c_i/\partial x^2 , \quad (1.30b)$$

if the dependence of $D_i$ upon concentration may be neglected. Szekely[118] has examined the effect of bulk flow on unsteady state diffusion, in which the diffusion coefficient is a function of concentration.

The methods for measuring diffusion coefficients in ionic melts have been very adequately reviewed by Yang and Simnad[117] and by Jost[119]. Radioactive tracer techniques are widely used in these measurements. In diffusion couple methods (Fig.4), two columns of melt containing different concentrations of the radioactive isotope of the component ion being studied are joined together, and diffusion is allowed to proceed for a suitable length of time. The couple is then quenched, and the distribution of radioactivity measured. This method is not particularly suitable for the alkali halides, since the distribution of radioactivity is altered on quenching, due to the shrinkage caused by the comparatively large volume change on fusion[120]. Attempts have been made to shear the liquid column into small sections at the diffusion temperature[121,122], but these have not been particularly successful[117]. The 'vacuum bubble' technique (Fig.5), devised by Angell and Bockris [123], has

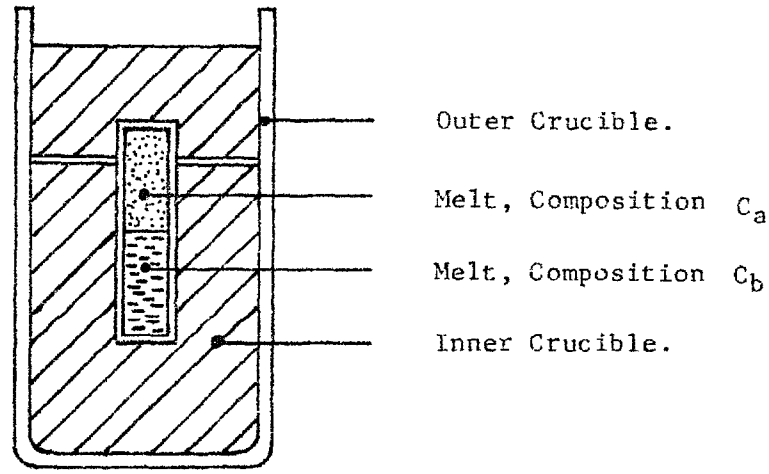


Figure 4: Measurement of Diffusion Coefficients in Melts by the Diffusion Couple Method.

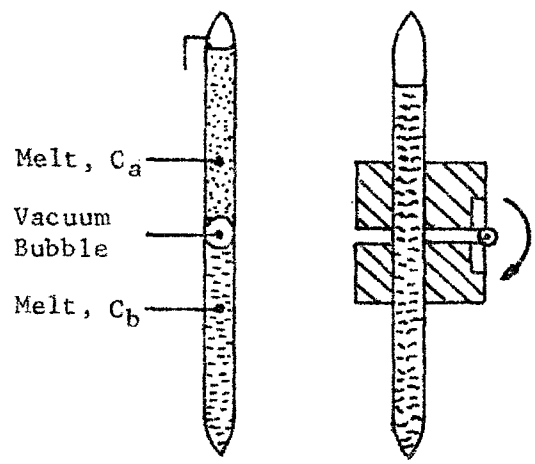


(a) Filled Diffusion Tube. (b) Breaking Mechanism

Figure 5: Measurement of Diffusion Coefficients by the Vacuum Bubble Technique.

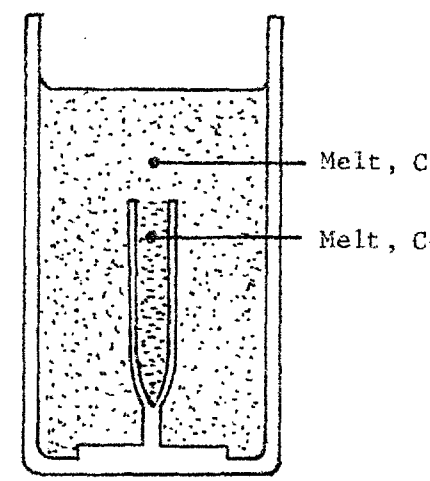


Figure 6: Measurement of Diffusion Coefficients by the Capillary Method.

proved far more successful in overcoming this difficulty. The two columns of melt are initially separated by a low pressure gas bubble, (Fig.5a), which, at the start of the experiment is compressed until it breaks away from the walls and floats to the surface. Diffusion then commences, and is allowed to continue for a suitable length of time. The tube is then broken at the original boundary, (Fig.5b), and the upper half removed for analysis. The capillary method (Fig.6) has been widely used for measuring diffusion coefficients. In this, a capillary, sealed at one end, is filled with molten salt and immersed in a bath containing melt having a different tracer ion concentration. Diffusion is allowed to proceed for a suitable length of time before the capillary is removed and quenched. The diffusion coefficient may be calculated from the total amount of component that has diffused into (or out of) the capillary[124]. It is usually necessary to stir the bath in order to keep the concentration at the interface effectively constant. This, however, could give rise to errors due to material being dragged out of the capillary[125]. Bockris and Hooper[126] examined this effect and found that the diffusion coefficient was independent of the stirring rate over a fairly wide range. In a number of cases, however, it has been reported that the bath was adequately stirred by convection[124,127,128]. Other methods used to measure diffusion coefficients include electrophoresis[129],

polarography[130], and diffusion through a porous diaphragm[131]. The likely errors in diffusion coefficient measurements in pure molten salts are far smaller (~5%) than those in electromigration experiments, due to less uncertainty in the mode of transport of the ions. The results generally obey the solution of Fick's second law relevant to the experimental method, with $D_i$ independent of concentration. In molten salt mixtures, however, the results are not as satisfactory, since they only obey the Fick's law solution for small concentration differences.

Bockris and co-workers [132-135] have measured tracer diffusion coefficients in a number of pure molten halides as a function of temperature, and have found that the Arrhenius equation is generally obeyed. The only exception[135] was zinc chloride, which exhibited curvature in the log $D_i$ versus 1/T plots. This was attributed to a network structure existing in the melt up to 100°C above the melting point. The validity[136] of the Stokes-Einstein[133,134], and of the Nernst-Einstein[132-134] equations,

$$D = kT/ar_i\eta \quad , \qquad (1.31)$$

$$\text{and} \qquad u/D = e/kT \quad , \qquad (1.32)$$

where k is the Boltzmann constant, a is a molecular shape factor, $r_i$ is the radius of the diffusing ion, and $\eta$ is the viscosity of the melt, were also investigated. They found that the Stokes-Einstein equation was obeyed within the limits of

experimental error, but that there were considerable deviations from the Nernst-Einstein equation. These deviations, also confirmed by other workers[137,138], were a function of the ionic radii[134], and were attributed to the occurrence of paired-ion diffusion[132,139]. Nagarajan and Bockris[140] have measured the tracer diffusion coefficients for sodium and caesium ions in their respective nitrate melts at a number of temperatures and pressures. The diffusion coefficients were found to decrease linearly with pressure, (15% per 1000 atmos.), to within the limits of the experimental error of 9%. From their results they were able to calculate the activation energies for diffusion at constant pressure and at constant volume, and from their difference determine the volume expansion work. This was found to predominantly determine the value of $(\Delta H_o)_p$, which was found to be independent of pressure. The formation of holes was the rate determining step for diffusion at constant pressure, and the results were adequately explained by the hole theory of Furth[25], (cf. Fray[87]).

## VISCOSITY.

In steady laminar flow, the velocity of a fluid at any point does not vary with time, and there is no bulk motion at right angles to the direction of flow (x). Under these conditions the <u>viscosity</u>, $\eta$, of the fluid may be

defined by the equation,

$$R_y = -\eta \frac{\partial v_x}{\partial y} \quad , \quad (1.33)$$

where $R_y$ is the shear stress at a given point in the fluid, and $(\partial v_x / \partial y)$ is the velocity gradient at right angles to the direction of flow. In 'Newtonian' fluids $\eta$ is independent of $R_y$.

The experimental techniques for measuring viscosities in melts have been reviewed by Mackenzie[141]. In molten salts and liquid metals, viscosities may be conveniently and accurately measured with a vertical capillary viscometer, provided a uniform temperature zone can be maintained over the height of the apparatus. Goodwin and Mailey[142] measured the viscosities of a series of pure molten salts using an Ostwald viscometer. This consisted essentially of a vertical platinum capillary, which was connected between two reservoirs, and immersed in a molten salt bath. The melt was forced into the upper reservoir under pressure, and allowed to fall back under gravity. Timing was accomplished by electrical contacts in the upper reservoir, and the apparatus was calibrated with water at room temperature. An improved viscometer was designed by Bingham and Ubbelohde, (Fig.7), in which the need for a kinetic energy correction for the head of melt was eliminated. This viscometer has been used in the measurement of the viscosities of pure

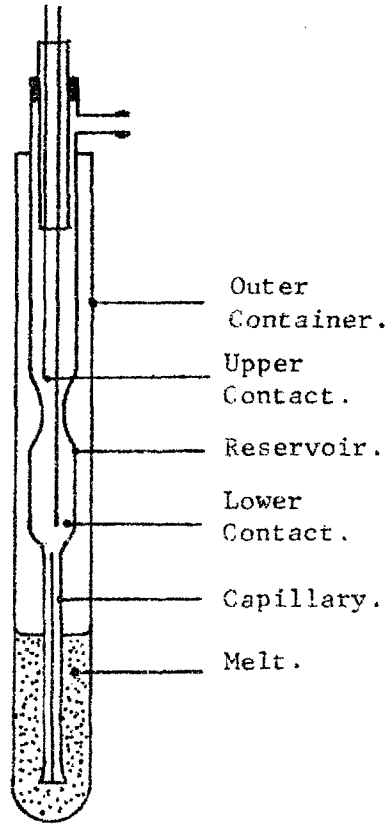


Figure 7: The Bingham - Ubbelohde Viscometer.

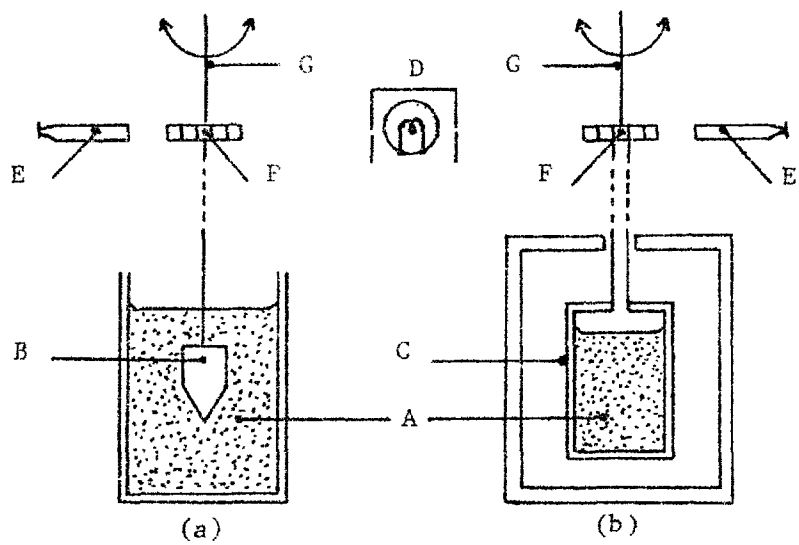


Figure 8: The Measurement of Viscosities by the Logarithmic Decrement Method.

(a) Oscillating Bob Method

(b) Oscillating Crucible Method.

molten salts[143] and mixtures[144] to an accuracy of ±1.5%. Horizontal capillary viscometers have also been used for measurements on molten salts[145] and liquid metals[146], but these offer no advantages over the vertical types, and, in addition, evaluation of the results requires an accurate knowledge of the density of the melt.

Logarithmic decrement methods, (Fig.8), have been widely used in the measurement of molten salt viscosities. The damping of simple harmonic motion performed by a bob suspended in a liquid, or by a crucible containing it, is a function of the viscosity of the liquid. Absolute measurements are rarely made owing to the complexity of this relationship, and, consequently, the apparatus has to be calibrated using liquids of accurately known physical properties.

Recently, Murgulescu and Zuca have measured the viscosities of the molten alkali halides[147,148] and some mixtures[149]. They found that the temperature dependence of their results for the pure salts was adequately described by the Arrhenius equation. This behaviour has been confirmed in viscosity determinations for alkali and alkali-earth halide melts[150], carbonate melts[151], and for a number of molten lead compounds[152]. Reeves and Janz[150] noted that the activation energies for viscous flow in alkali halide melts were approximately equal, and were considerably lower

than those of the alkali-earth halides, and the alkali salts with a doubly charged anion. This was attributed to the greater volume requirements for the flow of three particles rather than two, and to increased interionic attractions resulting from one of the ions being doubly charged. A comparison of viscosity and conductance data for molten alkali halides showed that the activation energy for viscous flow was always much larger than that for conductance. This indicates that, while electrical conductance is predominantly controlled by the smaller, more mobile cation, viscous flow depends largely on the motion of the anion. However, a co-operative anion-cation motion in viscous flow has not been ruled out[151]. The approximate equality of the activation energies for conductance and viscous flow in molten nitrates and thiocyanates has been attributed by Ubbelohde et al.[85] to association in these melts. The pressure dependence of the viscosities of molten salts has not, as yet, been measured. However, Jobling and Lawrence[153] have measured the viscosities of a number of organic liquids at constant volume. They found that the activation energy for viscous flow at constant volume increased with decreasing volume. This is to be expected, since the energy required to create a vacancy will increase as the molecules become closer packed.

## THERMAL CONDUCTIVITY.

The thermal conductivity of a material is defined as the rate of heat transfer through it per unit area under unit temperature gradient.

Thermal conductivity data for molten salts are scarce, probably because of the experimental difficulties encountered in making accurate measurements at high temperatures. The earlier measurements on melts[154,155] were subject to uncertainties of the order of 25%. More recently, Turnbull[156] measured the thermal conductivities of a number of molten salt eutectics, using a transient heating method. A constant current was passed through a platinum wire immersed in the melt, and the rate of heating followed from the change in its resistance. The maximum experimental error was given as $\pm$ 2.8%, but measurements on liquids at room temperature indicated that the actual errors were probably much smaller than this. Bloom et al.[157] measured the thermal conductivities of some molten nitrates and their mixtures by a steady state method. The melt was contained between two concentric silver cylinders, and heat was generated at the base of the inner one with a heating coil. The temperature difference between the two cylinders was measured after equilibrium had been attained. The uncertainty of 5% in the measurements was due principally to

inaccuracies in measuring the small temperature difference across the melt. It is of interest to note that in only one mixture studied ($AgNO_3$-$KNO_3$) was the thermal conductivity a linear function of composition to within the limits of experimental error.

A theory of thermal conductivity for molten salts has been given by Turnbull[158]. He considered that the melt could be represented by a quasi-crystalline lattice, and that heat was transferred by diffusion and vibrational mechanisms alone. He measured the thermal conductivities of a number of low melting point salts, both in the solid and the liquid state. On melting, a drop in the conductivity was observed, and the ratio of the liquid to the solid conductivity at the melting point was found to be $0.86 \pm 0.13$, for all the salts investigated. All the liquids had positive temperature coefficients of thermal conductivity, indicating that association occurred in these salts.

This Chapter is intended as a general survey of the thermodynamic and transport properties of molten salts. The topics of particular interest in the present research are the electrostrictive and electrocalorific effects (pp.11 and 12) and electrical conductance (p.15).

## REFERENCES.


1. M.F.R.Mulcahy and E.Heymann,
   J.Phys.Chem., 1943, 47, 485.

2. H.A.Levy, P.A.Agron, M.A.Bredig and M.D.Danford,
   Ann.N.Y.Acad.Sci., 1960, 79, 762.

3. J.Zarzycki,
   Compt. rend., 1957, 244, 758.

4. idem.,
   J.Phys.radium, (Supp.Phys.Appl., 1957, 18, 65A; 1958, 19, 13A).

5. idem.,
   Verres et Refractaires, 1957, 11, 3.

6. E.H.Henninger,R.C.Bushert and L.Heaton,
   J.Chem.Phys., 1966, 44, 1758.

7. J.R.Moyer, J.C.Evans and G.Y-S.Lo,
   J.Electrochem.Soc., 1966, 113, 158.

8. R.B.Ellis,
   ibid., 1966, 113, 485.

9. K.Balasubrahmanyam,
   J.Chem.Phys., 1966, 44, 3270.

10. G.P.Smith, C.R.Boston and J.Brynestad,
    ibid., 1966, 45, 829.

11. J.S.Fordyce and R.L.Braum,
    ibid., 1966, 44, 1159, 1166.

12. A.Bandy, J.P.Devlin, R.Burger and B.McCoy,
    Rev.Sci.Instr., 1964, 35, 1206.

13. J.P.Devlin, K.Williamson and G.Austin,
    J.Phys.Chem., 1966, 44, 2202.

14. E.Rhodes and A.R.Ubbelohde,
Proc.Roy.Soc., 1959, A251, 156.

15. B.Cleaver, E.Rhodes and A.R.Ubbelohde,
Disc.Faraday Soc., 1962, 32, 22.

16. J.S.Van Wieringen and J.G.Rensen,
Proc.Colloq.A.M.P.E.R.E., 1963, 12, 229.

17. S.Hafner and N.H.Nachtrieb,
J.Chem.Phys., 1964, 40, 2891.

18. idem.,
Rev.Sci.Instr., 1964, 35, 680.

19. P.E.Tsaoussoglou,
Ph.D.Thesis, London, 1965.

20. J.O'M.Bockris and D.C.Lowe,
Proc.Roy.Soc., 1954, A226, 423.

21. J.O'M.Bockris, J.W.Tomlinson and J.L.White,
Trans. Faraday Soc., 1956, 52, 299.

22. J.O'M.Bockris, J.D.Mackenzie and J.A.Kitchener,
ibid., 1955, 51, 1734.

23. J.O'M.Bockris and N.E.Richards,
Proc.Roy.Soc., 1957, A241, 44.

24. J.O'M.Bockris, E.H.Crook, H.Bloom and N.E.Richards,
ibid., 1960, A225, 558.

25. R.Furth,
Proc.Camb.Phil.Soc., 1941, 37, 281.

26. D.W. McCall, D.C.Douglass and E.W.Anderson,
Phys. Fluids, 1959, 2, 87.

27. S.Takeuchi and O.Watanabe,
Nippon Kinzoku.Gakkaishi, 1964, 28, 627, 633, 728.

28. A.D.Graves and D.Inman,
Electroplating and Metal Finishing, 1966, 19, 314.

29. M.M.Benarie,
J.Inorg.Nucl.Chem., 1961, 18, 32.

30. J.Perie, M.Chemla and M.Gignoux,
Bull.Soc.Chim.France, 1961, 1249.

31. F.Menes, G.Derian and E.Roth,
Kernenergie, 1962, 5, 295.

32. S.G.Meibuhr,
Electrochim. Acta, 1966, 11, 1301, 1325.

33. R.P.Tischer,
ibid., 1966, 11, 1309.

34. H.Bloom,
Rev. Pure and Appl.Chem., 1959, 9, 139.

35. H.W.Vornhusen,
Ber.Kernforschanlage Juelich, 1965, 268.

36. R.Lorenz,
Die Elekrolyse Geschmolzener Saltze, Halle, 1905.

37. N.Biltz and A.Klemm,
Z.anorg.u.allgem.Chem., 1926, 152, 267.

38. P.Drossbach,
Elektrochemie Geschmolzener Saltze, Berlin, 1938.

39. P.Camescasse,
J.Chim.Phys., 1957, 54, 792.

40. G.J.Janz, C.Solomons and H.J.Gardner,
Chem.Rev., 1958, 58, 461.

41. N.K.Voskresenskaya,
Itogi Nauki Khim., Nauki, 1959, 4, 160.

42. M.G.Watelle-Marion,
J.Chim.Phys., 1959, 56, 302.

43. G.E.Blomgren and E.R.Van Artsdalen,
Ann.Rev.Phys.Chem., 1960, 11, 273.

44. E.F.Johnson and F.W.Pardee,
U.S.At.Energy Comm., MAT-99, 58, 1961.

45. G.J.Janz,
J.Chem.Educ., 1962, 39, 59.

46. R.W.Laity,
ibid., 1962, 39, 67.

47. G.J.Janz,
Bibliography of Molten Salts, 2nd edit.,
Rensselaer Polytechnic Institute, Technical Publications,
Troy, N.Y., U.S.A., 1960.

48. A.G.Morachevskii,
Zhur.prikl.Khim., 1960, 33, 1434; 1961, 34, 1398;
1962, 35, 1390.

49. E.R.Buckle,
Physical Properties of Molten Salts,
Metals Reference Book, edit. Smithells, 4th edition,
Butterworths, London, 1967.

50. Yu.K.Delimarskii and B.F.Markov,
Electrochemistry of Fused Salts,
Transl. A.Peiperi and R.E.Wood, Sigma Press,
Washington, D.C. 1961.

51. Molten Salt Chemistry, edit. Blander, Interscience,
New York, 1964.

52. Fused Salts, edit. Sundheim, McGraw-Hill, New York, 1964.

53. Modern Aspects of Electrochemistry, edit. Bockris,
Butterworths, London, 1959.

54. Physico Chemical Measurements at High Temperatures, edit. Bockris, White and Mackenzie, Butterworths, London, 1959.

55. Disc.Faraday Soc., 1961, 37.

56. L.D.Landau and E.M.Lifshitz, Electrodynamics of Continuous Media, Transl. J.B.Sykes and J.S.Bell, Pergamon Press, Oxford, 1960, pp.36-40.

57. E.A.Guggenheim, Thermodynamics, North Holland Publishing Co., Amsterdam, 1949, pp. 361-365.

58. K.G.Denbigh, Chemical Equilibrium, Cambridge University Press, 1961, p.88.

59. C.P.Smythe, Dielectric Behaviour and Structure, Maple Press, New York, 1955, p.88.

60. L.D.Landau and E.M.Lifshitz, see ref. 56, pp.186-193.

61. E.R.Buckle and P.E.Tsaoussoglou, Trans.Faraday Soc., 1964, 60, 2144.

62. E.R.Van Artsdalen and I.S.Yaffe, J.Phys.Chem., 1955, 59, 118.

63. E.R.Buckle and P.E.Tsaoussoglou, J.Chem.Soc., 1964, 667.

64. J.D.Edwards, C.S.Taylor, A.S.Russel and L.F.Maranville, J.Electrochem.Soc., 1952, 99, 527.

65. E.W.Yim and M.Feinleib, ibid., 1957, 104, 622.

66. J.W.Tomlinson,
see ref. 54, p.247.

67. G.Jones and R.C.Josephs,
J.Amer.Chem.Soc., 1928, 50, 1049.

68. T.Shedlovsky,
ibid., 1930, 52, 1793.

69. F.S.Feates, D.J.G.Ives and J.H.Pryor,
J.Electrochem.Soc., 1956, 103, 580.

70. H.E.Gunning and A.R.Gordon,
J.Amer.Chem.Soc., 1959, 81, 3207.

71. L.A.King and F.R.Duke,
U.S.At.Energy Comm., Rept. I.S-667, 1963.

72. idem.,
J.Electrochem.Soc., 1964, 111, 712.

73. F.R.Duke and L.Bissel,
ibid., 1964, 111, 717.

74. S.J.Yosim, L.F.Grantham, E.B.Luchsinger and R.Wike,
Rev.Sci.Instr., 1963, 34, 994.

75. L.F.Grantham and S.J.Yosim,
J.Chem.Phys., 1963, 38, 1671.

76. J.Frenkel,
Acta Physiochim. U.R.S.S., 1935, 3, 633, 913.

77. H.Eyring,
J.Chem.Phys., 1936, 4, 283.

78. R.A.Swalin,
Acta Met., 1959, 7, 736.

79. M.H.Cohen and D.Turnbull,
J.Chem.Phys., 1959, 31, 1164.

80. J.O.Hirschfelder, C.F.Curtis, and R.B.Bird,
Molecular Theory of Gases and Liquids,
Wiley, New York, 1954, pp. 661-667.

81. E.R.Van Artsdalen and I.S.Yaffe,
J.Phys.Chem., 1955, 59, 118.

82. R.C.Spooner and F.E.W.Wetmore,
Can.J.Chem., 1951, 29, 777.

83. J.Bryne, H.Fleming and F.E.W.Wetmore,
ibid., 1952, 30, 922.

84. H.C.Cowen and H.J.Axon,
Trans.Faraday Soc., 1956, 52, 242.

85. W.H.Davies, S.E.Rogers and A.R.Ubbelohde,
Proc.Roy.Soc., 1947, A188, 392.

86. J.L.Copeland and W.C.Zybko,
J.Amer.Chem.Soc., 1964, 86, 4734.

87. D.J.Fray,
Ph.D.Thesis, London, 1965.

88. A.Klemm,
see ref. 51, p.543.

89. S.Karpachev and S.Pal'guev,
Zh.Fiz.Khim., 1949, 23, 942.

90. Yu.K.Delimarskii, P.P.Turov and E.B.Gitman,
Ukrain.Khim.Zh., 1955, 21, 314.

91. G.Harrington and B.R.Sundheim,
J.Phys.Chem., 1958, 62, 1454.

92. H.H.Kellogg and P.Duby,
ibid., 1962, 66, 191.

93. W.B.Frank and L.M.Foster,
ibid., 1957, 61, 1531.

94. F.R.Duke and R.A.Fleming,
J.Electrochem.Soc., 1959, 106, 130.

95. F.R.Duke and A.L.Bowman,
ibid., 1959, 106, 626.

96. E.D.Wolf,
ibid., 1961, 108, 811.

97. A.Lunden,
ibid., 1962, 109, 260.

98. H.H.Kellogg and P.Duby,
ibid., 1963, 110, 349.

99. H.Bloom and N.J.Doull,
J.Phys.Chem., 1956, 60, 620.

100. M.R.Lorenz and G.J.Janz,
ibid., 1957, 61, 1683.

101. F.R.Duke and R.Laity,
ibid., 1955, 59, 549.

102. R.W.Laity and F.R.Duke,
J.Electrochem.Soc., 1958, 105, 97.

103. J.W.Tomlinson,
see ref. 54, p.258.

104. A.Klemm and E.U.Monse,
Z.Naturforsch., 1957, 12a, 319.

105. F.R.Duke and J.P.Cook,
J.Phys.Chem., 1958, 62, 1593.

106. M.Chemla and A.Bonnin,
Compt. rend., 1955, 241, 1288.

107. J.A.A.Ketelaar and E.P.Honig,
J.Phys.Chem., 1964, 68, 1596.

108. A.Klemm,
see ref. 51, p.541.

109. J.R.Sundheim,
J.Phys.Chem., 1956, 60, 1381.

110. C.Sinistri,
ibid., 1962, 66, 1600.

111. A.Klemm,
Z.Naturforsch., 1960, 15a, 173.

112. B.R.Sundheim,
J.Phys.Chem., 1956, 60, 1381.

113. H.Bloom and E.Heymann,
Proc.Roy.Soc., 1947, A188, 392.

114. J.Frenkel,
Kinetic Theory of Liquids,
Oxford Univ.Press, London, 1946.

115. A.Klemm,
Z.Naturforsch., 1958, 13a, 1039.

116. W.K.Behl and J.J.Egan,
J.Phys.Chem., 1967, 71, 1764.

117. L.Yang and M.T.Simnad,
see ref. 54, p.295.

118. J.Szekely,
Trans.Faraday Soc., 1965, 61, 2679.

119. W.Jost,
Diffusion in Solids, Liquids and Gases.
Academic Press, New York, 1952.

120. A.R.Ubbelohde,
Melting and Crystal Structure,
Clarendon Press, Oxford, 1965, p.136.

121. H.Towers, P.Paris and J.Chipman,
Trans.A.I.M.E., 1953, 197, 1455.

122. H.Towers and J.Chipman,
ibid., 1957, 209, 769.

123. C.A.Angell and J.O'M.Bockris,
J.Sci.Instr., 1958, 35, 458.

124. R.E.Grace and G.Derge,
Trans.Amer.Inst.Min.(Metall.) Engrs., 1955, 203, 839.

125. A.Z.Borucka, J.O'M.Bockris and J.A.Kitchener,
J.Chem.Phys., 1955, 23, 1295.

126. J.O'M.Bockris and G.W.Hooper,
see ref. 55, p.218.

127. L.Yang, M.T.Simnad and G.Derge,
Trans.A.I.M.E., 1953, 197, 1455.

128. S.J.Rothman and L.D.Hall,
ibid., 1953, 197, 1580.

129. E.P.Honig and J.A.A.Ketelaar,
Trans.Faraday Soc., 1966, 62, 190.

130. R.B.Stein,
J.Electrochem.Soc., 1959, 106, 528.

131. S.Djordjevic and G.J.Hills,
Trans.Faraday Soc., 1960, 56, 269.

132. J.O'M.Bockris and G.W.Hooper,
see ref.55, p.218

133. S.B.Tricklebank, L.Nanis and J.O'M.Bockris,
J.Phys.Chem., 1964, 68, 58.

134. J.O'M.Bockris, S.Yoshikawa and S.R.Richards,
ibid., 1964, 68, 1841.

135. J.O'M.Bockris, S.R.Richards and L.Nanis,
ibid., 1965, 69, 1627.

136. H.Bloom and J.O'M.Bockris,
see ref. 52, p.15.

137. A.Berlin, F.Menes, S.Forcheri and C.Monfrini,
J.Phys.Chem., 1963, 67, 2505.

138. J.A.Ketelaar and J.C.Th.Kwak,
ibid., 1967, 71, 1149.

139. A.Z.Borucka, J.O'M.Bockris and J.A.Kitchener,
Proc.Roy.Soc., 1957, A241, 554.

140. M.K.Nagarajan and J.O'M.Bockris,
J.Phys.Chem., 1966, 70, 1854.

141. J.D.Mackenzie,
see ref. 54, p.313.

142. H.M.Goodwin and R.D.Mailey,
Phys.Rev., 1908, 26, 28.

143. H.Bloom, B.S.Harrap and E.Heymann,
Proc.Roy.Soc.,1948 , A194, 237.

144. B.S.Harrap and E.Heymann,
Trans.Faraday Soc., 1955, 51, 259.

145. R.Lorenz and H.T.Kalmus,
Z.Physik.Chem.(Leipzig), 1907, 59, 244.

146. K.E.Spells,
Proc.Phys.Soc., 1936, 48, 299.

147. I.G.Murgulescu and St.Zuca,
J.Physik.Chem(Leipzig), 1961, 218, 379; 1963,222,300.

148. idem.,
Rev.Roumaine. Chim., 1965, 10, 123.

149. I.G.Murgulescu and St.Zuca,
ibid., 1965, 10, 129.

150. R.D.Reeves and G.J.Janz,
Trans.Faraday Soc., 1965, 61, 2300, 2305.

151. G.J.Janz and F.Saegusa,
J.Electrochem.Soc., 1963, 110, 452.

152. C.B.Oliver,
ibid., 1965, 112, 629.

153. A.Jobling and A.S.C.Lawrence,
Proc.Roy.Soc., 1951, A206, 257.

154. C.F.Lucks and H.W.Dean,
A.S.M.E.Rept., 56-5A-31, 1956.

155. J.A.Lane, H.G.McPherson and F.Maslan,
Fluid Fuel Reactors, Addison-Wesley, Reading, Mass., 1958.

156. A.G.Turnbull,
Australian J.Appl.Sci., 1961, 12, 30.

157. H.Bloom, A.Doroszkowski and S.B.Tricklebank,
Australian J.Chem., 1965, 18, 1171.

158. A.G.Turnbull,
Australian J.Appl.Sci., 1961, 12, 324.

# CHAPTER 2.

## FREQUENCY DISPERSION OF THE IMPEDANCE OF ELECTROLYTIC SYSTEMS.

### INTRODUCTION.

The accuracy attainable in electrolytic conductance measurements, and in properties such as energies and volumes of activation[1] derived from these measurements is limited by the dispersion observed in the resistance of a capillary cell, particularly in molten salts[2]. Spurious dispersion can originate in the measuring apparatus, such as the Wheatstone bridge and its auxiliary equipment, especially at high frequencies. When these effects are corrected for, or when the equipment is operated under conditions in which they are negligible, dispersion that is an intrinsic property of the electrolyte is revealed[2].

Modern theories of electrode phenomena postulate that current is carried across the electrode-electrolyte interface by at least two kinds of process, each possessing its own impedance. The first to be discussed occurs when current is carried across the interface by means of an electrochemical reaction, (e.g. electrolysis), and is termed a Faradaic process. This occurs if the p.d. applied across the electrolyte exceeds the decomposition voltage, and

charge is transferred. In the second kind of process, known as a non-Faradaic process, current is carried across the interface by the charging and discharging of an electrical double layer. Layers of this sort, which act as capacitors, can result from the specific adsorption of ions at the electrode surface, but, in general, a double layer will exist due to the effects first described by Gouy [3]. Briefly, the tendency for the ions to concentrate near the electrodes in an attempt to neutralize the applied potential is opposed by their thermal motion. Further discussion of this effect is given below, (page 63).

The cause of intrinsic dispersion in conductance measurements on simple ionic melts is not clear [4] at present. It is even uncertain whether it results from a Faradaic or a non-Faradaic process, or from a combination of the two.

## DISPERSION IN ELECTRICAL CONDUCTANCE MEASUREMENTS.

### BRIDGE DISPERSION.

In order to study dispersion in electrolytes at audio and radio frequencies, equipment of the highest precision is required, since the change in the resistance is normally less than 1% over the whole frequency range. ($10^2$ - $10^5$ Hz ). It is therefore essential to check whether the components of the bridge network give rise to any appreciable spurious dispersion. In practice, the precision of most impedance bridges falls off at frequencies below 500 Hz , where the reactive component is small, while above 100 KHz the measurements become unreliable due to the onset of a number of unavoidable high frequency effects, including induction and dissipation in the components of the bridge itself. These will be discussed further in Chapter 4, for the particular bridge used in this research.

Dispersion of the measured impedance may also result from induction in the leads and connecting cables in the circuit. If the cell impedance is observed as a parallel resistance-capacitance circuit in series with the lead inductance, L, then the measured resistance and capacitance, $R_N$ and $C_N$, are related to the cell values, $R_p$ and $C_p$, by the equations [5]:

$$R_p = R_N (1 - \omega^2 L C_N)^2 + \omega^2 L^2/R_N \qquad (2.1)$$

$$C_p = [R_N^2 C_N(1 - \omega^2 L C_N) - L]/[R_N^2 C_N(1 - \omega^2 L C_N) - \omega^2 L^2] , \qquad (2.2)$$

obtained from standard a.c. network analysis. In the above equations, $\omega$ is the angular frequency of the applied alternating voltage. Thus, at high enough frequencies, the errors introduced by this effect, which are frequency dependent and can be of the same order of magnitude as the electrolytic dispersion, could lead to erroneous conclusions being drawn from experimental data. Such effects were recognized by Van Artsdalen and Yaffe [6,7], who plotted their resistance values to the base of $\omega^{-2}$ and extrapolated to infinite frequency. They claimed that this procedure eliminated inductance effects caused by the close proximity of the electrode leads. They did not justify the use of this extrapolation, however, and the theoretical basis for it is obscure.

Dissipation in co-axial connecting cables can also occur if the dielectric separating the core and the screen is of poor quality or has been damaged in some way. This gives rise to a frequency effect in the impedance, governed solely by the characteristics of the dielectric in question. Dissipation can also occur, with the same consequences, in imperfectly soldered or dirty connectors

and switches. The skin effect, which also gives rise to dispersion, may become important at high frequencies if the cables have an insufficient number of conducting strands.

It is important to distinguish these effects from the dispersion observed when a series resistance-capacitance circuit is measured on a bridge as its parallel analogue. The relations between the series and parallel values are given by the equations [5],

$$R_s = R_p / (1 + \omega^2 C_p^2 R_p^2) , \qquad (2.3)$$

and

$$C_s = C_p + 1 / (1 + \omega^2 C_p^2 R_p^2) , \qquad (2.4)$$

where the subscripts s and p refer to the series and parallel values respectively. Unless stated to the contrary, the components of the impedance discussed in the following sections of this chapter are series values.

These effects illustrate the difficulties involved in measuring conductances at high frequencies, and the consequent need for a reliable extrapolation formula. Most workers, while recognizing the experimental difficulties involved, do not stress their importance in making accurate electrical conductance measurements.

FARADAIC DISPERSION.

The Early Work.

Dispersion was first investigated in detail by Kohlrausch [8], who believed that an electrolytic cell could be represented by a series combination of a resistance and a capacitance, both of which were frequency independent. If this were true, total bridge balance could be obtained by the insertion of a suitable capacitor in an adjacent arm of the bridge. Wien [9], however, found that there was a 'polarization resistance', $R_W$, which could not be eliminated by the use of a capacitor as described above. His measurements over the frequency range 64 - 256 Hz indicated that $R_W$ was independent of frequency. Warburg [10] first suggested that dispersion resulted from the retardation of diffusion controlled electrode reactions, (concentration polarization). He showed, by integrating Fick's equation, that the impedance of a cell polarized in this way could be represented by a series combination of a resistance $R_W$ and a capacitance $C_W$, where $R_W$ and $C_W$ jointly comprise what is nowadays called the Warburg Impedance. In contrast to Wien, he showed that $R_W$ and $1/C_W$ should vary linearly with $\omega^{-\frac{1}{2}}$, that the phase angle at the electrodes should be $45^\circ$, and consequently that $R_W\ C_W\ \omega = 1$.

The fact that the apparent values of the resistance and capacitance of a polarized cell are functions

of the frequency is of fundamental importance, since it shows that the cell cannot be represented physically by the conventional circuit components of linear networks.

Randles' Theory.

Randles [11] derived a theory to explain dispersion in dilute aqueous solutions during reversible cationic discharge at a liquid metal(mercury)cathode. By integrating Fick's second law and applying appropriate boundary conditions he obtained, with the aid of a Tafel equation [12], the following relations :

$$R_W = (RT/n^2F^2Ac)\,[(2/\omega D)^{\frac{1}{2}} + (1/r)]\,, \qquad (2.5)$$

$$C_W = [n^2F^2Ac\,/\,RT]\;(D/2\omega)^{\frac{1}{2}}\,, \qquad (2.6)$$

$$R_W - 1/\omega C_W = [RT/n^2F^2Ac\,]\;(1/r)\,, \qquad (2.7)$$

where n is the number of electrons involved in the electrode reaction, F is the Faraday constant, c is the electrolyte concentration, D is the diffusion coefficient of the solute in the solution and the metal in the mercury electrode (assumed equal), and r is the rate constant of the electrode reaction. The remaining symbols have been defined earlier.

The analogous circuit due to Randles is shown in Fig.9(a). There are several assumptions made in the derivation of Randles' theory which are not justifiable. One is that the electric field is uniform over the electrode

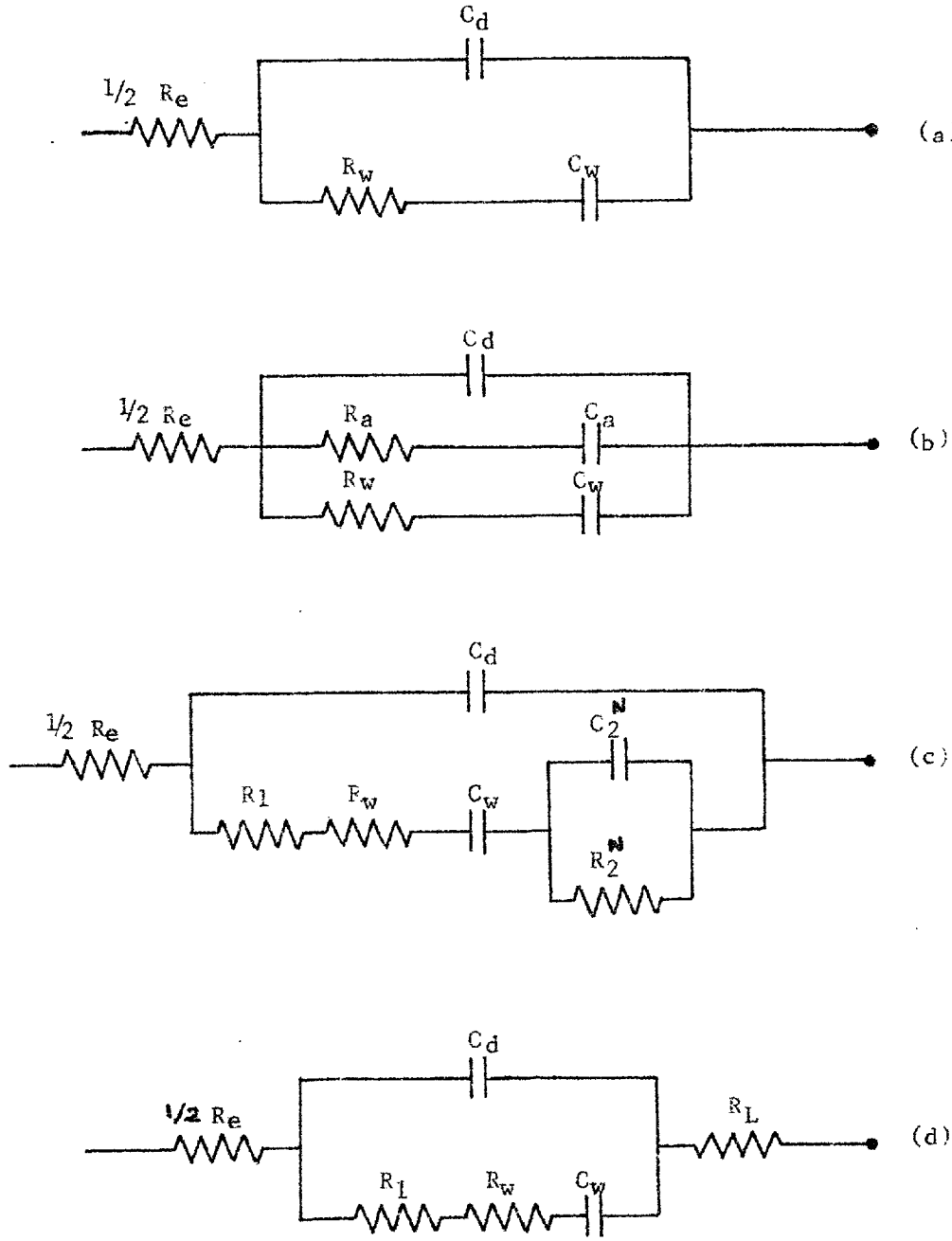


Figure 9: ~~Analogous~~ Analogues Circuits for Single Electrodes at which Electroysis is Occurring.

(a) After Randles [11] (b) After Laitinen and Randles [18]

(c) After Grahame [21] (d) After Remick and McCormick [22]

surface. Concerning the assumption that the diffusion coefficients of the ions in the water, and the metal in the mercury are equal, Randles himself [11] found that, for cadmium, they differed by 20%. Although this difference would result in an error in the measured rate constant, the predicted frequency dependence of the impedance would not be affected. A further assumption concerns the validity of the Tafel equation, which is essentially empirical, and is justifiable theoretically only for the simplest electrode reactions, (e.g. the evolution of hydrogen [12]). The weaknesses of this equation in molten salt systems are clearly shown in, e.g., the current-voltage curves of Laitinen and Gaur [13].

Randles' theory has been extended by Gerischer[14] and Hillson [15] to cover the case of a solid electrode where diffusing cations are reduced to the metal, which is then deposited upon it. Essentially identical equations to those of Randles were obtained.

Experimental Evidence in Support of Randles' Theory.

In spite of the reservations expressed above, the frequency dependence of the impedance in aqueous solutions and ionic melts has, in a number of cases, actually conformed to the $\omega^{-\frac{1}{2}}$ predictions of Randles. In order to test his theory, Randles [11] studied the behaviour of the Faradaic impedance in a number of aqueous solutions. The

theory, [Eqns. (2.5) - (2.7)], predicts that plots of $R_W$ and $1/\omega C_W$ against $\omega^{-\frac{1}{2}}$ should be linear and parallel, and that their vertical separation should be inversely proportional to the rate constant r. He obtained linear plots, which were approximately parallel, for systems having slow electrode reactions (e.g., $Zn^{++} + 2e \rightleftharpoons Zn$), and was able to determine values for the rate constants.

Hillson[15] studied dispersion in the aqueous system $Cu^{++} + 2e \rightleftharpoons Cu$, using copper electrodes. At high frequencies he obtained plots of the resistive and reactive components of the impedance which were linear in $\omega^{-\frac{1}{2}}$ and parallel. However, at low frequencies (2500 Hz and below), marked deviations from linearity occurred, which were attributed to incomplete reversibility of the electrode reaction [16]. The addition of surface active materials such as gelatin to the solution resulted in the blocking of active sites on the electrode surface, and considerably reduced these deviations.

Ukshe and Bukun [17] studied the Faradaic impedance of $PbCl_2$ in KCl-NaCl melts, using liquid lead electrodes. They showed that Randles' equations were obeyed, except at low concentrations of $PbCl_2$. They considered that secondary reactions of the type,

$$2Na^+ + X\,Pb \rightleftharpoons Pb^{++} + Na_2Pb_{X-1} \quad ,$$

and

$$4Na^+ + Pb \rightleftharpoons Pb^{++} + 2Na_2^+ \quad ,$$

occurred under these conditions and caused the observed deviations from Randles' equations, which were derived only for the case of a single electrode reaction.

The Effect on Dispersion of Adsorption at the Electrodes.

Laitinen and Randles [18] studied the Faradaic impedance to a.c. of a dropping mercury electrode in a solution containing tris(ethylenediamine)-cobaltous and cobaltic ions. They obtained plots for $R_W$ and $1/\omega C_W$ against $\omega^{-\frac{1}{2}}$ which were not only non-linear, but also inverted in the Randles sense, (i.e. for a given value of $\omega^{-\frac{1}{2}}$, $1/\omega C_W > R_W$). In addition, they obtained values of the phase angle at the electrodes greater than $45^\circ$. This is contrary to Randles' theory, which predicts a limiting value of $45^\circ$ as $\omega \to 0$. This anomalous behaviour was attributed to the adsorption of ions on the electrode surface. A mathematical analysis of this effect showed that a correction could be made by the insertion of a resistance and a capacitance, $R_a$ and $C_a$, both independent of frequency, into Randles' original circuit analogue, as shown in Fig. 9(b). In order to apply their correction, Laitinen and Randles chose a series combination of $R_a$ and $C_a$ so that the conditions set out below were obeyed as closely as possible. These conditions were that : (1) the reactance line was straight and passed through the origin; (2) the resistance line was straight and parallel to the reactance line. It was found that this

procedure worked for high and low concentrations, but at intermediate values it was less satisfactory. However, the authors considered that their correction was valid because the corrected plots obeyed Randles' equations, and also the product $R_a C_a$ was approximately constant, as predicted by their analysis.

Laitinen and Gaur [13], using solid platinum electrodes, similarly obtained non-linear and inverted plots for the reduction of $CdCl_2$ in molten LiCl-KCl mixtures at 450°C. These authors were also successful in correcting their plots for supposed adsorption at the electrode surface, using the method of Laitinen and Randles. They also made a study of the rates of the electrode reactions, and found that the values obtained by Randles' equation, [Eqn.(2.7)], were incompatible with those obtained from current-voltage curves in conjunction with a Tafel equation [12].

Hills and Johnson [19] studied the dispersion of Faradaic impedance for the reactions $Pt \rightleftharpoons PtCl_2$, and $Ni \rightleftharpoons NiCl_2$ in the LiCl-KCl eutectic melt. In the case of platinum, dispersion plots were obtained over a rather narrow frequency range (1 - 16 KHz.), which were approximately linear in $\omega^{-\frac{1}{2}}$, but not parallel, (cf. Laitinen and Osteryoung [20]). Their plots for the nickel reaction, however, were both non-linear and inverted, and no correction of the type used by Laitinen and Randles could correct the inversion.

Grahame's Theory.

Grahame [21] also produced a theory of the Faradaic impedance at an electrode-electrolyte interface. Like Randles' [11] this theory applies only to systems having perfectly smooth electrodes, which consequently have a uniform current density. This condition is only strictly realized in practice for liquid metal electrodes. The effect on the Faradaic impedance of a d.c. bias potential superimposed on the normal a.c. signal is also considered in this theory. Grahame obtained from his analysis the analogous circuit shown in Fig. 9(c) for a single electrode. Here $R_1$, (Grahame's $\theta$), is defined by the equation,

$$R_1 = RT / nF \vec{I}_{eq} \qquad (2.8)$$

where $\vec{I}_{eq}$ is the current due to the forward electrochemical reaction at equilibrium, and the other symbols are as defined earlier. The components $R_2^N$ and $C_2^N$, (Grahame's $R_p^N$ and $C_p^N$), depend on the nature of the substance taking part in the electrochemical reaction.

Remick and McCormick [22] used Grahame's model as a basis for their studies on the ferro-ferricyanide redox reaction. They used an a.c. polarized cell in which the interelectrode distance was variable. It follows from Grahame's circuit that the resistance of the cell may be written,

$$R_c = R_E + 2R_G$$
$$= L/A\kappa + 2R_G \qquad (2.9)$$

where $R_E = L/A\kappa$ is the electrolyte resistance, and $R_G$ is the sum of the ohmic components comprising the Faradaic resistance at one electrode. Thus a plot of $R_c$ against L should be linear, and have a zero separation intercept of $2R_G$. The authors found that the values of $R_G$ obtained in this manner were smaller than those they obtained by extrapolation to infinite frequency assuming an $\omega^{-\frac{1}{2}}$ dispersion law. They attributed this difference to an 'electrode layer resistance', $R_L$, first postulated by Vetter[23]. This resistance was assumed to be frequency-independent, and should also have been accompanied by a capacitance, but this was too small to be detectable. The final circuit diagram of Remick and McCormick is shown in Fig.9(d). These authors found that their results were only in accord with the prediction of Grahame if $R_1 = 0$, and the rate of electron transfer were much faster than had previously been expected. In their approach, however, these authors are, like many before them, confusing the theoretical picture by trying to correct for the limitations of theory by the introduction of further circuit components, (cf. Llopis and Vázquez [24]).

Transmission Line Models.

Other workers [25,26] have developed a simpler method of obtaining network analogues by comparing the differential equations for the system, (i.e., reaction and diffusion equations and boundary conditions) with those for a pair of infinite transmission lines or for other combinations of electrical components. The problem of solving the differential equations is thus avoided. All the components obtained by this method are independent of frequency, (see Fig. 10(a), p. 73).

NON-FARADAIC DISPERSION.

The Electrical Double Layer.

In non-Faradaic processes, current is carried across the electrode-electrolyte interface by the charging and discharging of the electrical double layer [27-31], which exists even in the absence of specific adsorption. This concept was first described by Helmholtz [32], who believed that, at the electrode surface, there existed a layer of ions, across which there was sharp fall in potential. This layer was considered to act as a capacitor, whose plates were one ionic diameter apart. Later, Gouy [3] and Chapman [33] postulated that, as a result of thermal agitation, the double layer extended some way into the electrolyte, and consequently that there was a gradual drop in potential across it. However, neither of these theories was adequate in explaining the experimental results of Frumkin [34], and consequently, Stern [35] proposed that the true structure of the double layer was a combination of these two layers. In Stern's model, there is thus an inner, compact layer, (the Helmholtz layer), at the electrode surface, and a diffuse layer, (the Gouy layer) adjacent to it, which extends into the electrolyte [36]. The validity of this model has been supported experimentally by Grahame [27]. The double layer capacitance is generally considered to provide a current path across the electrode - electrolyte interface, in parallel with that of the Faradaic process [37], as shown in Fig.9, (p.55).

Space Charge Polarization.

The effect giving rise to non-Faradaic impedance is usually known as space charge polarization. This effect is due to the instantaneous relaxation of structure across the diffuse double layer. This must be distinguished from the progressive decay of the complete layer as the frequency of the applied a.c. potential is increased. Space charge polarization, which occurs not only in liquid electrolytes, but also in semiconductors and semiconducting electrodes [38], is only detectable if the ions have sufficient time to accumulate near the electrodes during the course of one half cycle. At sufficiently high frequencies the ions are unable to follow the applied field, and such polarization is absent. Space charge theories generally include the possibility of discharge at one or both of the electrodes. The non-Faradaic component may be determined from the general expression for the impedance by applying the condition that both electrodes are blocking to all ions; (this means that no ion can cross the electrode-electrolyte boundaries).

Ferry's Theory of Diffuse Double Layer Relaxation.

Ferry [39] followed the method of Falkenhagen [40] for the relaxation of the ionic atmosphere in aqueous solutions of uni-univalent salts. Assuming equal ionic mobilities, he obtained an expression for the a.c. capacitance, $C_d$, of the diffuse double layer at a planar electrode, which may be

written,

$$C_d/C_o = [1/(1 + \theta^2)] + [[(\theta^2 + 1)^{\frac{1}{2}} + 1]/2(\theta^2 + 1)]^{\frac{1}{2}} \qquad (2.10)$$

In the above equation, $C_o$ is the Gouy capacitance, and $\theta$ the dimensionless product of the angular frequency, $\omega$, and a relaxation time $\theta$. Ferry showed, using Eqn.(2.10), that, at high frequencies, ($\theta \gg 1$), $C_d$ is proportional to $\omega^{-\frac{1}{2}}$ while at low frequencies, ($\theta \ll 1$), it is constant and equal to $C_o$.

Ferry compared his predictions with some results of Oncley[41], and Ferry and Oncley[42] on the parallel a.c. impedance of $10^{-4}$M. KCl solution, at frequencies above 25KHz. Anomalous dispersion of the capacitance was observed in these measurements at frequencies below 500 KHz, and was attributed to polarization. A correction was made for this by assuming that there was a 'polarization capacitance', in series with the cell, which was proportional to $\omega^{-\frac{1}{2}}$, as predicted by Warburg[9] for discharge processes. That these authors obtained dispersion in this region is surprising, since previous experience in this laboratory[2] has shown that, even in molar KCl solutions, the dispersion was extremely small. Also, the occurrence of the Warburg capacitance was unlikely, considering the low p.d. (0.1 volt) applied across the cell in these measurements. It is possible that the observed dispersion originated in the measuring equipment, and that

the $\omega^{-\frac{1}{2}}$ dependence was therefore spurious.

Ferry compared his predicted value for $C_d$ at 25 KHz , which was essentially equal to $C_o$, with those of Ferry and Oncley for $10^{-4}$M. KCl solution. The experimental values were 2-20 times too low, suggesting that dispersion set in two decades too low in frequency. Ferry supposed that this comparison was of doubtful value, due to the difference between the true and geometrical areas of the electrode. Since, however, the true area is not likely to be smaller than the geometrical area, the observed capacitance should be larger, not smaller, than the predicted value. The observation would, in fact, seem to indicate that dispersion was already underway at 25KHz.

There is an intermediate frequency region, apparently overlooked by Ferry, for which his formula (2.10) reduces to a Debye expression. Thus, when $\theta \ll 1$, $\theta^2 \ll 1$,

$$C_d/C_o = 1/ (1 + 11\ \theta^2/16), \qquad (2.11)$$

which describes the early stages in the dispersion of $C_d$ before the point where the $\omega^{-\frac{1}{2}}$ law is reached. Some of the dispersion observed experimentally below 1MHz would be explained on this basis if Ferry's estimate of $\theta$ was in error, (see below, p. 97, for further discussion).

One of Ferry's more important theoretical conclusions was that the $\omega^{-\frac{1}{2}}$ law would hold at frequencies of 1 MHz and above. This led him to suggest, and others [29,31]

to accept, that diffuse layer relaxation would not be observable at lower frequencies. This ignores the region covered by Eqn.(2.11), and is not upheld by the experimental evidence.

Jaffé's Theories of Space Charge Polarization.

Jaffé[43] developed a space charge theory to explain polarization in semiconductors. The treatment was later extended by Chang and Jaffé[44] to include electrolytic solutions. In these theories, the authors solved the transport equations, originally derived by Wagner [45], for the motion of mobile ions under the influence of a small alternating voltage. Using the Poisson space charge equation and other boundary conditions, they obtained expressions for the complex a.c. impedance.

Chang and Jaffé first considered the case in which discharge occurred at identical electrodes. In order to solve their equations, however, they made a number of assumptions which rather limit the usefulness of their results. These assumptions were : (1) that the field was homogeneous; (2) that the diffusion coefficients of the mobile ionic species were equal, as were their mobilities; and (3) that the rate constants for the anionic and cationic discharge reactions were equal. They obtained expressions for the parallel resistance and capacitance of the space charge layer in terms of a reduced rate constant and hyperbolic functions

of a reduced frequency variable, which was proportional to $\omega^{\frac{1}{2}}$. In order to examine the variation of the thickness of the space charge layer with frequency, the authors reverted to the case of completely blocked electrodes. They assumed that the field was hyperbolic, and obtained expressions in which the series polarization resistance and capacitance were approximately proportional to $\omega^{-\frac{1}{2}}$.

In order to test this theory, Jaffe and Rider [46] studied the dispersion in aqueous solutions of KCl and $MgSO_4$, and in conductance water, in the frequency range 18 - 18,000 Hz. They obtained plots for the resistance and capacitance which were linear in $\omega^{\frac{1}{2}}$ over a rather narrow frequency range, but these showed marked curvature at frequencies below 100 Hz. The authors therefore concluded that ions were being discharged at the electrodes, even though the signal applied across the cell was only 0.12 volts r.m.s. Resistance and capacitance measurements for a series of conductance water samples showed a random variation, and the authors postulated that the ions causing the observed capacitance were not necessarily the same as those carrying the current. Their inability to make their experimental curves coincide with the theoretical ones was attributed to the existence of a group of slow moving ions, which were most probably the normal ions surrounded by an atmosphere of water molecules. However, they were unable to confirm this experimentally, and it would seem more probable that the authors' inability to match theoretical

predictions with experimental data results from the limitations imposed in the formulation of the theory. Nevertheless, the authors considered that the theory was adequate for the inert metallic electrodes, (Al, Ni, Au), used in their research, but doubted whether it would apply to systems having reversible electrodes.

The Space Charge Theories of Friauf and Macdonald.

The approach of Chang and Jaffe[44] was succeeded by the basically similar treatments of Friauf [47] and Macdonald [48] for ionic crystals. These represented a considerable advance over earlier theories, since solutions of the basic equations were obtained without the need to assume a homogeneous field. This was, however, assumed to be anti-symmetrical about the centre of the electrode system, and the Nernst-Einstein relation, [Eqn.(1.32)], was used. For the case of both charge carriers blocked at the electrodes, Friauf obtained the equation,

$$(G_\infty - G)/G_\infty = C/C_0 = 1/(1 + \omega^2\tau^2), \qquad (2.12)$$

where $G_\infty$ is the high frequency limit of the conductance G, and $\tau$ is the Debye relaxation time.

Friauf [47] measured the parallel a.c. impedance of silver bromide crystals, using gold and silver electrodes. He found that his results were qualitatively explained if the positive carriers were free and the negative carriers blocked.

Although the slopes of his experimental curves were in reasonable accord with the theoretical predictions for this case, the calculated magnitudes of the polarization resistance and capacitance were somewhat smaller than the observed values. The author attributed this to the apparent electrode area being larger than the geometrical area, (cf. Ferry [43] above), and to an excess concentration of vacancies near the electrodes, even in the absence of an applied p.d., both of which would result in enhanced polarization.

Allnatt and Jacobs [49] studied the parallel impedance to a.c. of potassium chloride crystals, both in the pure state and doped with strontium chloride, in the frequency range 300 - 50,000 Hz. They obtained dispersion of the resistance only in the most heavily doped crystals. The dependence of the capacitance of the pure crystals on frequency, temperature, and interelectrode distance were held to be in good accord with Friauf's predictions for the case of free anion vacancies and completely blocked cation vacancies, while in the doped crystals the results indicated that the reverse was true. However, these workers obtained, and were unable to explain, values of the capacitance greater by a factor of $10^3$ to $10^4$ than those calculated from the theory. In a later paper, Jacobs and Maycock [50] described further measurements made on these crystals, and found that, by now considering both charge carriers to be blocked at the

electrodes, good quantitative agreement with Friauf's theory was obtained for capacitance.

Further Dispersion Studies on Aqueous and Molten Salt Electrolytes.

Jones and Christian [51] studied dispersion in aqueous silver nitrate solutions in a cell having silver electrodes, the separation of which was variable. Like Remick and McCormick's (see above), their values for the polarization resistance, $R_W$, obtained by extrapolation to infinite frequency were slightly higher than those obtained by extrapolation to zero inter-electrode distance. Slight curvature, concave to the frequency axis, was obtained in the resistance versus $\omega^{-\frac{1}{2}}$ plots, and the authors considered the latter method, which gave linear and parallel plots at given frequencies, to be the more reliable. They also found that the resistance and capacitance were very sensitive to the type of electrodes used, and, to a lesser extent, to the electrolyte and temperature.

Ukshe and Bukun [52] also obtained resistance plots which were linear in $\omega^{-\frac{1}{2}}$ for equimolar KCl-NaCl melts, using liquid lead electrodes up to 700°C. However, their measurements were in the range 2 - 200 KHz., and consequently omitted the low frequency region where the resistance changes are reported by some workers [2] to be more rapid.

Winterhager and Werner [53] measured the electrical

conductance of a number of molten alkali- and heavy metal halides. They found that simple series or parallel analogues were not satisfactory in describing the polarization in alkali halide melts, and suggested an analogue resembling a filter network and consisting of an infinite series of differential resistive and capacitative components. The network, Fig.10(b), may be viewed as representing the various microscopic paths taken by the current at the irregular electrode-electrolyte interface. At high frequencies, this circuit reduces to a simple resistance-capacitance series circuit.

In the heavy metal halide melts, the resistance measurements showed relatively little variation with frequency. The authors claimed that the linear dependence of conductance on temperature, also obtained for these salts, resulted from the absence of polarization errors. They also suggested that there was a possible connection between dispersion and the apparent temperature dependence of conductance.

Buckle and Tsaoussoglou [2] agreed with this conclusion, and confirmed for molten thallous halides [54] the low dispersion in heavy metal halides. These authors obtained dispersion curves of excess resistance against frequency, which exhibited plateaux in the range 10-100 KHz, where the parallel resistance was constant to within the limits of the experimental error of 0.05%. They evaluated the electrical conductance from the resistance in this plateau region, as they considered this procedure to be more reliable

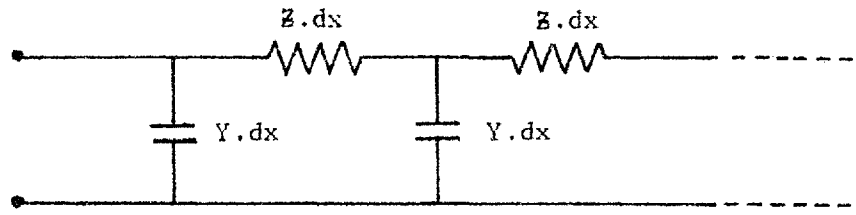


(a)

$Z$ = $(\xi/C_a D_a)$ is the Resistive Component / Unit Length,

$Y$ = $(C_a/\xi)$ is the Capacitative Component / Unit Length,

$C_a$ is the Concentration of a,

$D_a$ is the Diffusion Coefficient of a,

$\xi$ = $\nu a^2 RT/N^2F^2A$,

A is the Area,

$\nu a$ is the Stoichiometric Coefficient in the Electrode Reaction.

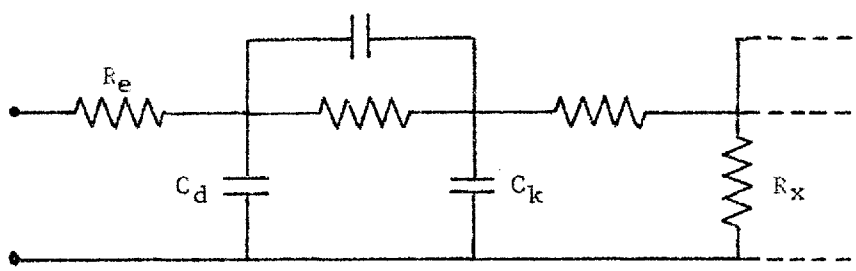


(b)

$R_x$ is the Exchange Resistance

$C_k$ is the Capacitative Component of the Concentration Polarization.

Figure 10: Analogous Circuits for non-Faradaic Processes.

(a) After Chao-Wu [25] (b) After Winterhager and Werner [53]

than the use of any recommended dispersion formula.

Laitinen and Roe [55] measured the double layer capacities at platinum and bismuth electrodes in the LiCl-KCl eutectic melt by a voltage step method. They assumed that their cell, in the absence of any discharge process, could be represented by the cell resistance, $R_c$, in series with the double layer capacitance, $C_d$, and consequently that the charging current, I, was given by the equation,

$$I = (V/R_c) \exp(-t/R_c C_d) \quad (2.13)$$

where V is the magnitude of the voltage pulse, and t is time. Plots of $\log_{10} I$ against t were obtained by the authors for values of t down to 2 $\mu$ sec., and were linear as predicted. They were able to determine $C_d$ as a function of the applied bias potential. The results would have been more conclusive, however, had they investigated the effect of rise-time on the values of $R_c$ and $C_d$, so as to prove that their results were free from dispersion.

OTHER CAUSES OF DISPERSION.

Apart from the three major causes of dispersion described above, other possible explanations for this effect have been put forward. These are described briefly below.

Geometrical Effects.

Inhomogeneity of the current density at the electrodes, (the Wenner effect), may give rise to dispersion.

Jones and Bradshaw[56] discovered a small, but constant, error in their measurements of the conductance of standard potassium chloride solutions, which they attributed to this effect.

Polarography[57-59] is commonly used for the measurement of double layer capacities. The mercury electrode[60] has been widely employed in aqueous solutions, and in melts of salts with low melting points[61]. Grahame[62] investigated the effect on non-Faradaic dispersion, of the geometry of the capillary on which his stationary mercury drop electrode was suspended. He found that any dispersion observed could be eliminated by sufficiently reducing the wall thickness. The dispersion obtained with thick wall capillaries was attributed to partial shielding of the drop, which resulted in an inhomogeneous current density at the electrode surface. He also suggested that this effect was enhanced by gas bubble formation at the tip of the capillary. The same conclusions about shielding were reached by Melik-Gaikazyan [63].

Discharge of Impurities.

The possibility of preferential discharge of impurities at low applied voltages has been suggested [4,19] as a possible cause of dispersion in molten salts. For this to occur, the discharge reaction must be essentially reversible. The suggestion[19] that decomposition of the solvent occurs at large underpotentials, and so causes Faradaic dispersion, would seem to contradict the laws of Thermodynamics.

Adsorption of Solvent or Impurities at the Electrodes.

The effect of electrode adsorption on the a.c. impedance has been discussed by Laitinen and Randles [18] for Faradaic processes, (see above, p.58). Adsorption was also considered by Hills and Johnson [19] to be a possible cause of dispersion in low-voltage impedance measurements on molten salts. Bockris and Conway [64] attributed the differences in dispersion behaviour observed using different metallic electrodes to variations in the relaxation times of solvent molecules adsorbed on the electrode. These authors obtained the theoretical expressions,

$$R_A = (1/\Delta\varepsilon\, C_o)\,[(\tau'^{1-\beta'}/\omega^{\beta'}) + (\tau'^{\beta'-1}/\omega^{2-\beta'})] \quad (2.14)$$

$$\Delta C_A = [C_o \Delta\varepsilon (\omega\tau')^{2-\beta'}]/[1 + (\omega\tau')^{2-2\beta'}] \quad (2.15)$$

for the resistance $R_A$ and the excess capacitance, $\Delta C_A$, due to this effect. In the above equations, $\Delta\varepsilon$ is the difference between the low and high frequency dielectric constants, and $0 < \beta' \leq 1$, according to whether the relaxation time $\tau$ has one or an infinite range of values, the mean of which is $\tau'$. The authors calculated the relaxation times for water absorbed on a number of electrode surfaces, and suggested that the absence of this effect at high temperatures could explain the lack of dispersion in measurements of the series a.c. impedance in molten salts.

## SUMMARY.

Intrinsic dispersion in electrolytic cells can be divided into Faradaic and non-Faradaic categories.

Faradaic dispersion occurs when the p.d. applied across the cell exceeds the decomposition potential, and is observed at audio and radio frequencies.

Of the non-Faradaic effects, one which is always present, in solutions at least, is diffuse double layer relaxation, which should also be observable at these frequencies.

Other causes of non-Faradaic dispersion include adsorption of solvent and impurities at the electrodes, and inhomogeneity of the current distribution, due to cell geometry and electrode surface texture.

It is very difficult to resolve these various effects, particularly diffuse double layer relaxation, in experiments. A popular method is to devise a.c. networks to describe the separate processes occurring. This is an empirical procedure, and has led to much confusion in the literature.

## REFERENCES.


1. S.B.Brummer and G.J.Hills,
   Trans.Faraday Soc., 1961, 57, 1816, 1823.

2. E.R.Buckle and P.E.Tsaoussoglou,
   J.Chem.Soc., 1964, 667.

3. G.Gouy,
   J.Phys.radium, 1910, 9, 457; Compt.rend., 1910, 149, 654.

4. K.E.Johnson,
   Elecktrochim.Acta, 1964, 9, 653.

5. L.T.Agger,
   Alternating Currents, Macmillan, London, 1950.

6. E.R.Van Artsdalen and I.S.Yaffe,
   J.Phys.Chem., 1955, 59, 118.

7. I.S.Yaffe and E.R.Van Artsdalen,
   J.Phys.Chem., 1956, 60, 1125.

8. F.Kohlrausch,
   Pogg.Ann., 1873, 148, 143.

9. M.Wien,
   Ann.Physik.u.Chem., 1896, 58, 37.

10. S.Warburg,
    Ann.Physik, (Leipzig), 1899, 67, 493; 1901, 6, 125.

11. J.E.B.Randles,
    Disc.Faraday Soc., 1947, 1, 11.

12. G.Kortüm and J.O'M.Bockris,
    Electrochemistry, Vol.II, Elsevier, Amsterdam, 1951, p.425.

13. H.A.Laitinen and H.C.Gaur,
    J.Electrochem.Soc., 1957, 104, 730.

14. H.Gerischer,
    Z.Physik.Chem. (Leipzig), 1951, 198, 286.

15. P.Hillson,
Trans.Faraday Soc., 1954, 50, 385.

16. M.Leblanc and P.Schick,
Z.Physik.Chem. (Leipzig), 1903, 46, 213.

17. E.A.Ukshe and N.G.Bukun,
Zh.fiz.Khim., 1961, 35, 2689.

18. H.A.Laitinen and J.E.B.Randles,
Trans.Faraday Soc., 1955, 51, 54.

19. G.J.Hills and K.E.Johnson,
J.Electrochem.Soc., 1961, 108, 1012.

20. H.A.Laitinen and R.A.Osteryoung,
ibid., 1955, 102, 598.

21. D.C.Grahame,
ibid., 1952, 99, 370c

22. A.E.Remick and H.W.McCormick,
ibid., 1955, 102, 534.

23. K.Vetter,
Z.Physik.Chem. (Frankfurt), 1952, 99, 285.

24. J.Llopis and M.Vázquez,
Electrochim. Acta, 1963, 8, 163.

25. T.Chao-Wu,
Sci.Sinica, 1964, 13, 1943.

26. D.Elliot and G.S.Buchanan,
Australian J.Chem., 1966, 19, 2083.

27. D.C.Grahame,
Chem.Rev., 1947, 41, 441.

28. J.T.G.Overbeek,
Colloid Science, Vol.1, edit. Kruyt, Elsevier,
Amsterdam, 1952, pp. 115-193.

29. R.Parsons,
Modern Aspects of Electrochemistry, Vol.1,
edit. Bockris, Butterworths, 1954, pp.103-179.

30. H.Gerischer,
Ann.Rev.Phys.Chem., 1961, 12, 227.

31. P.Delahay,
Double Layer and Electrode Kinetics, Interscience,
New York, 1965.

32. H.L.F.Van Helmholtz,
Ann.Physik, 1853, 89, 211; 1879, 7, 337.

33. D.L.Chapman,
Phil.Mag., 1913, 25, 475.

34. A.N.Frumkin,
Phil.Mag., 1920, 40, 375.

35. O.Stern,
Z.Eleckrochem., 1924, 30, 508.

36. S.Glasstone,
A Textbook of Physical Chemistry, 2nd Edit.,
Macmillan, London, 1960, p.1220.

37. F.Krüger,
Z.Physik.Chem., (Leipzig), 1903, 45, 1.

38. R.Memming,
Philips Res.Repts., 1964, 19, 323.

39. J.D.Ferry,
J.Chem.Phys., 1948, 16, 737.

40. H.Falkenhagen,
Electrolytes, Oxord University Press, 1934, p.176.

41. J.L.Oncley,
J.Amer.Chem.Soc., 1938, 60, 1115.

42. J.D.Ferry and J.L.Oncley,
J.Amer.Chem.Soc., 1941, 63, 272.

43. G.Jaffé,
Phys.Rev., 1952, 85, 354.

44. H.Chang and G.Jaffé,
J.Chem.Phys., 1952, 20, 1071.

45. C.Wagner,
Phys.Z., 1931, 32, 641.

46. G.Jaffé and J.A.Rider,
J.Chem.Phys., 1952, 20, 1077.

47. R.J.Friauf,
J.Chem.Phys., 1954, 22, 1329.

48. J.R.Macdonald,
Phys.Rev., 1953, 92, 4.

49. A.R.Allnatt and P.W.M.Jacobs,
J.Phys.Chem.Solids, 1961, 19, 281.

50. P.W.M.Jacobs and J.N.Maycock,
J.Chem.Phys., 1963, 39, 757.

51. G.Jones and S.M.Christian,
J.Amer.Chem.Soc., 1935, 57, 272.

52. E.A.Ukshe and N.G.Bukun,
Zh.Fiz.Khim., 1963, 37, 890.

53. H.Winterhager and L.Werner,
Forschungsber. Wirtschafts-u.Verkehrsministeriums
Nordrhein-Westfalen, 1956, No.341.

54. E.R.Buckle and P.E.Tsaoussoglou,
Trans.Faraday Soc., 1964, 60, 2144.

55. H.A.Laitinen and D.K.Roe,
Coll.Czech.Chem.Commun., 1960, 25, 3065.

56. G.Jones and B.C.Bradshaw,
J.Amer.Chem.Soc., 1933, 55, 1780.

57. Chi-Ming Tseng,
Hua Hsueh Tung Pao, 1963, 419.

58. H.A.Laitinen and R.A.Osteryoung,
Fused Salts, edit. Sundheim, McGraw-Hill,
New York, 1964, pp. 282-300.

59. C.H.Liu, K.E.Johnson and H.A.Laitinen,
Molten Salt Chemistry, edit. Blander,
Butterworths, London, 1964, pp. 683-700.

60. P.Schubert,
Z.Chem., 1964, 4, 11.

61. J.E.B.Randles and W.White,
Z.Elektrochem., 1955, 59, 666.

62. D.C.Grahame,
J.Amer.Chem.Soc., 1946, 68, 301.

63. V.I.Melik-Gaikazyan,
Zhur.Fiz.Khim., 1952, 26, 560.

64. J.O'M.Bockris and B.E.Conway,
J.Chem.Phys., 1958, 28, 707.

# CHAPTER 3.

## THEORY OF SPACE CHARGE POLARIZATION IN LIQUID ELECTROLYTES.*

### INTRODUCTION.

Experiments on solids[1-3], solutions[4,5], and melts[6,7], indicate that, even in the apparent absence of ionic discharge, dispersion of the a.c.conductance and capacitance is common to all electrolytes. The aim of this research was to investigate possible causes of this dispersion in pure molten salts. It is widely accepted that space charge polarization is at least partially responsible for dispersion in solids and aqueous solutions, and it has been suggested[6,8] that this effect may contribute to the frequency dependence in melts. This suggestion is pursued in the present theory.

A molten salt may be viewed as a matrix of ions in a cloud of electrons. The application of a p.d. across the melt gives rise to phased displacement of ions over and above their random thermal motion. Under these conditions the ions might be expected to shift relative to the electron cloud and form diffuse double layers at the electrodes, (cf. Dick and Overhauser[9]). As the a.c. frequency is increased, the amplitude of the ionic displacements decreases until, at sufficiently high frequencies, it disappears altogether. This effect is essentially the relaxation of the diffuse

---

* C.G.J.Baker and E.R.Buckle, Trans.Faraday Soc., In press.

double layer.

In the theoretical treatment which follows, the earlier theories of space charge polarization in solids[1,10,11] and aqueous solutions[12,13] are extended to fully dissociated electrolytes, such as molten salts. The method is based on that of Jaffé[10], as improved by Macdonald[11] and Friauf[1]. Short range ionic displacements, induced by a small alternating voltage applied across the electrolyte are described by the linear phenomenological laws of diffusion and electromigration. It is assumed that no discharge occurs, and that electronic conduction may be neglected.

## THE THEORY.

### THE BASIC EQUATIONS.

The electrolyte consists of the melt, or solution in a non-polar solvent, of the compound $M_{\xi} X_{z\xi}$ completely dissociated into cations $M^{\mu+}$ and anions $M^{\nu-}$ with concentrations $p_e = \xi N/v$, and $n_e = zp_e$ respectively, where $z = \mu/\nu$ , N is the Avogadro number, and v is the molar volume. Subscript e denotes equilibrium conditions in the absence of an external field.

Consider the motion of ions in the electrolyte when contained in a straight insulating tube of narrow bore, (e.g. the capillary of a conductance cell [7]) under the influence of a p.d. applied across identical metal electrodes positioned at each end. The electrodes are clean, inert, perfectly flat, and perpendicular to the bore, slightly overlapping the ends. The distance between them is 2s, and end effects are negligible. The temperature is constant and uniform. The phenomenological equations of motion parallel to the capillary axis (co-ordinate x) during time t lead to the following transport equations, (for derivation see Appendix 3.1, p.105) :

$$\begin{aligned} \partial p/\partial t &= D_p \partial^2 p/\partial x^2 - u_p \partial (pE)/\partial x , \\ \partial n/\partial t &= D_n \partial^2 n/\partial x^2 + u_n \partial (nE)/\partial x , \end{aligned} \qquad (3.1)$$

where $D_p$ and $D_n$ are the Fick's law diffusion coefficients of

the ions, $u_p$ and $u_n$ are their electrical mobilities, and E is the local field intensity. Subscripts p and n refer throughout to cations and anions respectively.

According to the above equations, the field-induced drift causes p and n to vary from their equilibrium values by displacement along x, no account being taken of bulk electrostriction. The motions of the two species are also linearly independent according to (3.1), but this independence is implicitly removed by application [1,11] of the Poisson equation*

$$\begin{aligned} \partial E/\partial x &= \beta(\mu p - \nu n), \\ &= 4\pi e/\varepsilon_o , \end{aligned} \qquad (3.2)$$

where e is the electronic charge and $\varepsilon_o$ is the permittivity of the medium. In the melt, $\varepsilon_o$ will be dependent only on the electronic polarization, whereas, in solutions the solvent will make a contribution to it. In both cases it will be assumed to show no dispersion and to be independent of both the field strength and the ionic concentrations. The p.d. across the cell is given by

$$V = \int_0^{2s} E\,dx , \qquad (3.3)$$

and will be small enough to be consistent with the linear law of migration assumed in (3.1), (E < 0.1 volt/cm say; see

---

* In Eqns. (3.1) and (3.2) the conventional field direction, (i.e., E = -grad V), is reversed. cf. refs. 1, 10, 11.

e.g. Frenkel [14]). Under such conditions the electrocalorific and electrostrictive effects are likely to be exceedingly small, as shown in Appendix 3.2, (p.107). Also, the condition of overall electroneutrality requires that

$$\int_0^{2s} (\mu p - \nu n)\, dx = 0. \qquad (3.4)$$

Since there is no discharge, the ionic fluxes at the electrodes may be equated to zero, giving the boundary conditions,

$$\begin{aligned} u_p\, pE - D_p\, \partial p/\partial x &= 0 \\ u_n\, nE + D_n\, \partial n/\partial x &= 0 \end{aligned} \qquad x = 0,\ 2s. \qquad (3.5)$$

LINEARIZATION OF THE EQUATIONS.

As in a typical conductance experiment let

$$V = V_1 \exp(i\omega t), \qquad (3.6)$$

where $\omega$ is the angular frequency of the applied sinusoidal p.d., and $i = (-1)^{\frac{1}{2}}$. Then, to the first harmonic approximation[1,10,11],

$$\begin{aligned} E &= E_o + E_1 \exp(i\omega t) \\ p &= p_o + p_1 \exp(i\omega t) \\ n &= n_o + n_1 \exp(i\omega t) \end{aligned}, \qquad (3.7)$$

where the static components, (subscript 0) are functions of x, and the dynamic amplitudes, (subscript 1), are functions of x and $t$. However, in a symmetrical cell there can be no static component of the field resulting from the application

of V as given by (3.6). Assuming that the forces of asymmetry at the electrode-electrolyte interface have a very short range, it is therefore permissible to put $E_o = 0$. It follows from (3.2) that another boundary condition is

$$p_o / n_o = p_e / n_e , \qquad (3.8)$$

and that the static components of the concentrations do not depart from local electroneutrality.

Substitution of (3.7) into (3.1) shows that $(dp_o/dx)$ and $(dn_o/dx)$ are constants, and in (3.5) it gives, for $x = 0, 2s$, $(dp_o/dx)_{0,2s} = (dn_o/dx)_{0,2s} = 0$. Therefore, $p_o$ and $n_o$ are homogeneous, (i.e. independent of x), in the first harmonic approximation. Ionic space charge polarization will therefore arise through the inhomogeneous amplitudes $p_1$ and $n_1$.

Eqns. (3.1) - (3.5) are linearized by the elimination of t using (3.7). Recalling that $E_o = 0$ and that $p_o$ and $n_o$ are homogeneous, the results, to the first harmonic approximation, are

$$i\omega p_1 = D_p d^2p_1/dx^2 - u_p\, p_o dE_1/dx , \qquad (3.9)$$

$$i\omega n_1 = D_n d^2n_1/dx^2 + u_n\, n_o dE_1/dx , \qquad (3.10)$$

$$dE_1/dx = \beta(\mu\, p_1 - \nu\, n_1) , \qquad (3.11)$$

$$V_1 = \int_0^{2s} E_1\, dx , \qquad (3.12)$$

$$\int_0^{2s} (\mu\, p_1 - \nu\, n_1)\, dx = 0 , \qquad (3.13)$$

$$u_p\, p_o\, E_1 - D_p\, dp_1/dx = 0 \qquad (3.14)$$

$$x = 0, 2s\ .$$

$$u_n\, n_o\, E_1 + D_n\, dn_1/dx = 0 \qquad (3.15)$$

THE CURRENT DENSITY.

Ionic motion in the electrolyte results in a net current density which is a function of the co-ordinate x. It is given at any location by the sum of four terms representing the diffusion and migration of cations and anions:

$$j_1(x) = e\,[\mu(u_p\, p_o E_1 - D_p dp_1/dx) + \nu(u_n n_o E_1 + D_n dn_1/dx)]$$

$$= e[u_p p_o E_1\, \mu(1+\phi) - D_p(d/dx)\,(\mu p_1 - \nu\psi\, n_1)], \qquad (3.16)$$

where

$$\phi = u_n/u_p\ , \qquad \psi = D_n/D_p\ . \qquad (3.17)$$

In view of Eqns. (3.14) and (3.15), this local current vanishes at the electrodes, but its space average corresponds to part of the current in the external circuit. The amplitude of this current per $cm^2$ is, by (3.12) and (3.16),

$$J_1 = (1/2s) \int_0^{2s} j_1\,(x)\, dx$$

$$= (e/2s)[u_p p_o \mu(1+\phi)\, V_1 - \mu D_p\, [p_1(2s) - p_1(0)]$$

$$+ \nu\psi D_p\, [n_1(2s) - n_1(0)\ ]\ ]\ . \qquad (3.18)$$

The first term on the r.h.s. of Eqn. (3.18) gives the current when the ionic concentrations are homogeneous, and consequently,

$$p_o = p_e \ , \quad n_o = n_e \ , \text{ and } n_o/p_o = z \ . \tag{3.19}$$

In the melt, electronic polarization contributes the current $I = (\varepsilon_o/8\pi s)dV/dt$ per $cm^2$, which may be regarded as flowing through a parallel circuit comprising the geometrical capacitance $C_g = \varepsilon_o/4\pi\mathbb{K}$, where $\mathbb{K}$ is the cell constant of the apparatus. In solutions, $\varepsilon_o$ and I contain terms due to the solvent.

It now remains to solve for the functional forms of $p_1$ and $n_1$, in order to evaluate the remaining terms on the r.h.s. of Eqn. (3.18).

SOLUTION OF THE TRANSPORT EQUATIONS.

Elimination of $E_1$ from (3.9) and (3.10), using (3.11) gives,

$$d^2p_1/dx^2 - (i/\lambda^2)p_1 - (1/\lambda_o^2)(\mu p_1 - \nu n_1) = 0 \ , \tag{3.20}$$

$$d^2n_1/dx^2 - (i/\psi\lambda^2)n_1 + (z\phi/\psi\lambda_o^2)(\mu p_1 - \nu n_1) = 0 \ , \tag{3.21}$$

where

$$\begin{aligned} \omega_o &= u_p p_e \beta \\ \lambda_o &= (D_p/\omega_o)^{\frac{1}{2}} \\ \lambda &= (D_p/\omega)^{\frac{1}{2}} \end{aligned} \ . \tag{3.22}$$

The simultaneous solutions of (3.20) and (3.21) are

$$\begin{aligned} p_1 &= \sum_{\substack{q=1 \\ r=1}}^{4} A_q \exp(a_r x) \ , \\ n_1 &= \sum_{\substack{q=1 \\ r=1}}^{4} B_q \exp(a_r x) \ . \end{aligned} \tag{3.23}$$

The four eigenvalues $a_{\pm} = \pm (b_{\pm})^{\frac{1}{2}}$ are given by the roots $b_+$, $b_-$ of the characteristic equations,

$$b^2 - [(\mu/\lambda_0^2)(\psi + \phi) + (i/\lambda^2)(1 + \psi)]\, b = (1/\lambda^4) - (i\mu/\lambda^2\lambda_0^2)(1 + \phi), \qquad (3.24)$$

obtained by the elimination of either $p_1$ or $n_1$ between (3.20) and (3.21).

In order to evaluate the coefficients $A_q$, $B_q$, in Eqn. (3.23), it is necessary to make a further assumption, namely that $p_1$ and $n_1$ are antisymmetrical about $x = s$. Integrating (3.11) over $0 \leq x \leq 2s$, and using (3.13), gives

$$\beta \int_0^{2s} (\mu p_1 - \nu n_1)\, dx = E_1(2s) - E_1(0) = 0. \qquad (3.25)$$

This result permits, although it does not establish, symmetry in $E_1$ about $x = s$, (cf. refs. 1, 11). Multiplication of (3.20) and (3.21) by $\mu$ and $\nu\psi$ respectively, subtraction, integration of the result over $0 \leq x \leq 2s$, and use of (3.13) gives

$$z\,(d/dx)\,[p_1(2s) - p_1(0)] = \psi\,(d/dx)\,[n_1(2s) - n_1(0)]. \qquad (3.26)$$

Multiplication of (3.14) and (3.15) by $\mu\phi$ and $\nu$ respectively, subtraction, and use of (3.17) and (3.19) gives

$$z\phi\, dp_1/dx = -\psi\, dn_1/dx, \quad x = 0, 2s, \qquad (3.27)$$

whence,

$$z\phi\,(d/dx)\,[p_1(2s) - p_1(0)] = -\psi\,(d/dx)\,[n_1(2s) - n_1(0)]. \qquad (3.28)$$

In liquids $\phi > 0$, and comparison of (3.26) and (3.28) yields

$$\begin{aligned} (d/dx)\,[p_1(2s) - p_1(0)\,] &= 0\,, \\ (d/dx)\,[n_1(2s) - n_1(0)\,] &= 0\,, \end{aligned} \tag{3.29}$$

which fulfils one requirement for antisymmetry in $p_1$ and $n_1$. It may now be supposed that in weak fields these amplitudes are small enough to warrant the assumption of antisymmetry. This reduces to two the number of eigenvalues in (3.23), and these functions may now be written ,

$$\begin{aligned} p_1 &= A_+ \sinh\,[a_+(x-s)] + A_- \sinh\,[a_-(x-s)\,]\,, \\ n_1 &= B_+ \sinh\,[a_+(x-s)] + B_- \sinh\,[a_-(x-s)\,]\,, \end{aligned} \tag{3.30}$$

where $a_\pm = +\,(b_\pm)^{\frac{1}{2}}$.

From (3.18), (3.19), (3.22) and (3.30), the current density is

$$J_1 = [e\omega_0\mu(1+\phi)\,V_1/2s\beta\,] - (eD_p A_+/s)[(\mu - \nu\psi k_1^+)\sinh\eta_+ + k_2(\mu - \nu\psi k_1^-)\sinh\eta_-\,]\,, \tag{3.31}$$

where $\eta_\pm = s\,a_\pm$, $k_1^\pm = B_\pm/A_\pm$ , and $k_2 = A_-/A_+$ . (3.32)

The coefficients of (3.30) are now found from the eigenvalues and the constants $\mu, \nu, \psi, \phi, s$, and $V_1$.

Substitution of (3.30) into (3.20), and comparison of the coefficients of $\sinh\,[a_+(x-s)]$ gives ,

$$k_1^\pm = (1/\nu)\,[\mu + i\theta^2 - \lambda_0^2\, a_\pm^{\,2}]\,, \tag{3.33}$$

where $$\theta^2 = \lambda_0^2/\lambda^2 = \omega/\omega_0\,, \tag{3.34}$$

is a reduced frequency.

From (3.27) and (3.30) ,

$$k_2 = -a_+(z\,\phi + \psi k_1^+)\cosh\eta_+ / a_-(z\,\phi + \psi k_1^-)\cosh\eta_- \quad (3.35)$$

Now, from (3.14) and (3.30) ,

$$(1/\beta)\,E_1(2s) = \lambda_o^2\,[a_+A_+\cosh\eta_+ + a_-A_-\cosh\eta_-\,], \quad (3.36)$$

and from (3.11) and (3.30) ,

$$(1/\beta)\,E_1(2s) = (1/a_+)\,(\mu A_+ - \nu B_+)\cosh\eta_+ + (1/a_-)\,(\mu A_- - \nu B_-)\cosh\eta_- + C\,. \quad (3.37)$$

Elimination of the integration constant C between (3.36) and (3.37), and use of (3.12) yields,

$$V_1/2\beta A_+ = (\mu - \nu k_1^+)\,(\sinh\eta_+ - \eta_+\cosh\eta_+)/a_+^2 + k_2(\mu - \nu k_1^-)\,(\sinh\eta_- - \eta_-\cosh\eta_-)/a_-^2 + \lambda_o^2\,(\eta_+\cosh\eta_+ + k_2\,\eta_-\cosh\eta_-). \quad (3.38)$$

Combination of (3.31) and (3.38) gives an expression for the admittance per unit area, Y', of the electrolyte :

$$Y' = (J_1/V_1) = [e\omega_o\mu(1+\phi)/2s\beta\,] - (eD_p/2s\beta)f_1/f_2 \quad (3.39)$$

where,

$$f_1 = (\mu - \nu\psi k_1^+)\sinh\eta_+ + k_2(\mu - \nu\psi k_1^-)\sinh\eta_-\,, \quad (3.40)$$

$$f_2 = (\mu - \nu k_1^+)\,(\sinh\eta_+ - \eta_+\cosh\eta_+)/a_+^2 + k_2\,(\mu - \nu k_1^-)\,(\sinh\eta_- - \eta_-\cosh\eta_-)/a_-^2 + \lambda_o^2\,(\eta_+\cosh\eta_+ + k_2\eta_-\cosh\eta_-)\,. \quad (3.41)$$

SIMPLIFICATION OF THE ADMITTANCE EQUATION.

Since $\omega_o$ is an optical frequency, $\theta \ll 1$ in the present problem, and the solution of the characteristic equation (3.24) to the second order in $\theta$ is therefore,

$$[2\psi \lambda_o^2/\mu(\psi + \phi)]\, b_{\pm} = 1 + [i\,\theta^2\,(1+\psi)/\mu\,(\psi+\phi)] \pm [1 - i\theta^2(1-\psi)(\psi-\phi)/\mu(\psi+\phi)^2], \quad (3.42)$$

and, to the same order of approximation, the eigenvalues are :

$$a_+ = (1/\lambda_o)[\mu(\psi + \phi)/\psi]^{\frac{1}{2}} \cdot [1 + i\theta^2(\psi^2+\phi)/2\mu(\psi+\phi)^2], \quad (3.43)$$

$$a_- = (1/\lambda)\,[(1+\phi)/(\psi+\phi)]^{\frac{1}{2}} \exp(i\pi/4). \quad (3.44)$$

It may be shown using Eqns. (3.31), (3.33), and (3.35), that the current will be independent of frequency when these eigenvalues are equal. However, as can be seen from the above equations, this possibility is excluded in the present frequency range ($\theta \ll 1$) since $\lambda \gg \lambda_o$. These equations also show that $\lambda$ and $\lambda_o$ are lengths characteristic of the attenuation along the cell of the space charge polarization.

If mod $(\eta_{\pm}) \gg 1$, the problem is considerably simplified, since the approximations,

$$\sinh \eta_{\pm} \simeq \cosh \eta_{\pm} \simeq (1/2) \exp(\eta_{\pm}), \quad (3.45)$$

may be made. Since $s \sim 1$ in conductance cells, and $\phi \sim \psi \sim 1$, it follows from (3.43) that mod $(\eta_+) \gg 1$ for all $\omega \ll \omega_o$, and from (3.44) that mod $(\eta_-) \gg 1$, if $1/\lambda = (\omega/D_p)^{\frac{1}{2}} \gg 1$. This is realized for molten salts if $\omega \gg 10^{-4}$, taking $10^{-4}$ $cm^2 sec^{-1}$

as maximum value of $D_p$. Consequently, (3.45) and the solution given below are valid in the frequency range $10^{-4} \ll \omega \ll \omega_o$. Therefore, from (3.35), (3.39)-(3.41) and (3.45),

$$Y' = [e\omega_o\mu(1+\phi)/2s\beta] - (eD_p/2s\beta) \cdot f_1^*/f_2^* , \quad (3.46)$$

where $f_1^* = a_-(\mu - \nu\psi k_1^+)(z\phi + \psi k_1^-) - a_+(\mu - \nu\psi k_1^-)(z\phi + \psi k_1^+)$, (3.47)

$$f_2^* = [a_+(\mu - \nu k_1^-)(z\phi + \psi k_1^+)(\eta_- - 1)/a_-^2]$$
$$-[a_-(\mu - \nu k_1^+)(z\phi + \psi k_1^-)(\eta_+ - 1)/a_+^2] - a_+a_-(k_1^+ - k_1^-)\psi\lambda_o^2 s. \quad (3.48)$$

Substitution for $k_1^{\pm}$ in (3.47) and (3.48) using (3.33), and retention of terms consistent with the second order of approximation in $a_{\pm}$ yields :

$$f_1^* = [\mu z(1-\psi)(\psi+\phi)(a_- - a_+) + z\psi(\psi+\phi)\lambda_o^2 a_+a_-(a_+ - a_-)$$
$$+ z\psi(1-\psi)\lambda_o^2 a_+^3 + (\psi^2/\nu)\lambda_o^4 a_+^3 a_-^2]$$
$$- i[z\psi(1-2\psi-\phi)\theta^2 a_+ + (\psi^2/\nu)\lambda_o^2\theta^2 a_+^3] , \quad (3.49)$$

$$f_2^* = [z(\psi+\phi)\lambda_o^2 (a_- - a_+) + (\psi/\nu)\lambda_o^4 a_+^3 - (\psi/\nu)\theta^4(a_+/a_-^2)$$
$$+ (\psi/\nu)s\theta^4(a_+/a_-)] + i[sz(\psi+\phi)\theta^2((a_-/a_+) - (a_+/a_-))$$
$$- (\psi/\nu)\lambda_o^2\theta^2 a_+ + z(\psi+\phi)\theta^2(a_+/a_-^2) - (\psi/\nu)\lambda_o^2\theta^2(a_+^3/a_-^2)$$
$$+ (\psi/\nu)s\lambda_o^2\theta^2(a_+^3/a_-)] . \quad (3.50)$$

Substitution for $a_{\pm}$ in (3.49) and (3.50) using (3.43) and (3.44), and retention of terms consistent with the above approximation, gives :

$$f_1^* = (\theta/\lambda_o)\,\mu z(\psi+\phi)^{\frac{1}{2}}(1+\phi)^{3/2}\exp(i\pi/4)\,, \qquad (3.51)$$

$$f_2^* = \lambda_o\theta z\,(\psi+\phi)^{\frac{1}{2}}(1+\phi)^{\frac{1}{2}}\exp(i\pi/4)$$

$$-[\theta^3 sz(\psi+\phi)/(\mu\psi)^{\frac{1}{2}}(1+\phi)^{\frac{1}{2}}]\exp(-i\pi/4)\,. \qquad (3.52)$$

Substitution of (3.51) and (3.52) into (3.46), and use of (3.22) gives a Debye type relaxation equation :

$$Y' = (e\omega_o\mu(1+\phi)/2s\beta)\,[1-(1-i\omega\tau)/(1+\omega^2\tau^2)]\,, \qquad (3.53)$$

where $\tau = s(1+\phi/\psi)^{\frac{1}{2}}/(\mu\omega_o D_p)^{\frac{1}{2}}(1+\phi)\,, \qquad (3.54)$

is the relaxation time.

PARALLEL AND SERIES ANALOGUES.

Following conventional procedure, the admittance may now be depicted as a combination of a resistance and a capacitance, either in parallel or in series. This procedure is merely an experimental convenience, as neither of these analogues describes literally the physical behaviour in the diffuse double layer.

<u>The Parallel Network</u>.

Let $G_p'$ and $C_p'$ be respectively the parallel conductance and the capacitance of the diffuse double layer,

the primes denoting unit area. Then, $Y' = G_p' + i\omega C_p'$, and it follows from (3.17), (3.22), (3.53), and (3.54) that,

$$(G_{p\infty} - G_p)/G_{p\infty} = C_p/C_{p_o} = (1 + \omega^2\tau^2)^{-1}, \quad (3.55)$$

$$G_p/G_{p\infty} = (C_{p_o} - C_p)/C_{p_o} = 1 - (1 + \omega^2\tau^2)^{-1}, \quad (3.56)$$

$$\kappa_\infty = K G_{p\infty} = e\mu p_e (u_p + u_n), \quad (3.57)$$

$$C_{p_o}' = [(e\mu p_e \varepsilon_o/16\pi)(u_p/D_p) + (u_n/D_n))]^{\frac{1}{2}}, \quad (3.58)$$

$$\tau^2 = (C_{p_o}/G_{p\infty})^2 = \varepsilon_o s^2[(u_p/D_p) + (u_n/D_n)]/4\pi e\mu p_e \cdot (u_p+u_n)^2, \quad (3.59)$$

where $G_{p\infty}$ is the high frequency limiting conductance, and $C_{p_o}$ is the low frequency limiting capacitance. In the Nernst-Eistein approximation $u/D = e/kT$, $C_{p_o}$ reduces to,

$$C_{p_o} = [e^2 \mu p_e \varepsilon_o/8\pi kT]^{\frac{1}{2}}, \quad (3.60)$$

which is the low potential limit of the Gouy capacitance [15]. The total permittivity $\varepsilon = 8\pi s C_p'$ relaxes from the static value of $8\pi s C_{p_o}'$ to the high frequency value of $8\pi s C_g' = \varepsilon_o$.

Equation (3.55) predicts that the parallel capacitance, and the relative dispersion of the conductance, should follow a simple Debye curve with a relaxation time given by (3.59). A result of this form was first given by Friauf[1]. In the Nernst-Einstein approximation, the present value of $\tau$ reduces to that of Friauf, except for a factor $\mu^{\frac{1}{2}}$ arising through the variable valencies permitted in the present theory. Ferry's[12] relaxation time $\theta = (\varepsilon_o/8\pi e u_p p_e)$ is

apparently inconsistent with the present result, and the origin of the factor 11/16 in (2.11) is obscure.

The Series Network.

The series values, (subscript s), calculated from (3.55) and (3.56), using the relations (2.3) and (2.4) are :

$$G_s = G_{p\infty} , \tag{3.61}$$

$$C_s = C_{p_o} , \tag{3.62}$$

$$C_s/G_s = \tau . \tag{3.63}$$

APPLICATION OF THE THEORY TO EXPERIMENTS.

According to the relations (3.55) to (3.63), the following deductions from experiment are possible when other dispersion effects are absent or negligible. Measurements on a series resistance - capacitance bridge are independent of frequency, and $G_{p\infty}$, $C_{p_o}$ and $\tau$ may be obtained from them. Alternatively, the plot of $1/C_p$ against $\omega^2$ is linear with a slope $\tau^2/C_{p_o}$ and zero frequency intercept of $1/C_{p_o}$. This gives $C_{p_o}$ and $\tau$, and the polarization-free specific conductance $\kappa_\infty = K\, C_{p_o}/\tau$, without the need to assume values of the constants. The plot of $G_p$ against $C_p$ is also linear, with a slope $-G_{p\infty}/C_{p_o}$, $G_p$-axis intercept $G_{p\infty}$, and $C_p$-axis intercept $C_{p_o}$. Also, from (3.54) and (3.55),

$$K\, C_{p_o} \tau = (s^2 \varepsilon_o/4\pi D_p)\, (1 + \phi/\psi) \,/\, (1 + \phi), \tag{3.64}$$

giving an order of magnitude calculation of $\varepsilon_o/D_p$, assuming that $\phi \simeq \psi \simeq 1$ and that s is known approximately. Finally, from (3.54), (3.56) and (3.57),

$$\kappa_\infty \tau^2 = (e \mu p_e s^2/4\pi) (\varepsilon_o/D_p) (1 + \phi/\psi) u_p \tag{3.65}$$

yields $u_p$, and $D_p$ follows if $\varepsilon_o$ is known.

The presence of other effects which are equivalent to frequency independent components in series with the diffuse double layer are not detectable in either series or parallel measurements. However, if these components exhibit dispersion, or if a parallel current path exists across the diffuse double layer [11], then deviations from the above predictions will be observed.

## DISCUSSION.

Relaxation of the diffuse double layer in melts and solutions is illustrated in Fig.11. The reduced parallel capacitance and relative dispersion of the parallel conductance were calculated from (3.55) assuming $\phi = \psi = 1$, $2s = 5$ cm., and various values of the parameter $\mu\omega_o D_p$ ($cm^2 sec^{-2}$). A considerable range of $\tau$ is allowed by the frequency range of the present theory, but for $\omega \gg 10^6$, radiation losses might affect experiments, and in solutions the Debye-Falkenhagen relaxation [16] would appear.

It is assumed in (3.1) that the diffusion and electromigration of ions may be treated as independent macroscopic motions. This assumption is supported by calculations of Rice [17], who showed that the Coulombic forces in a simple ionic melt are too weak to explain the observed value of D, the macroscopic self-diffusion coefficient. Better agreement was obtained using the short range terms of the interionic pair potential. The phased drift of anions and cations is ignored in (3.1), but use of the Poisson equation, (3.2), with constant $\varepsilon_o$ as a boundary condition for the internal field removes this independence of motion. This equation requires that the electrolyte be considered as consisting of point charges in a structureless medium of permittivity $\varepsilon_o$. This is only an approximation because of

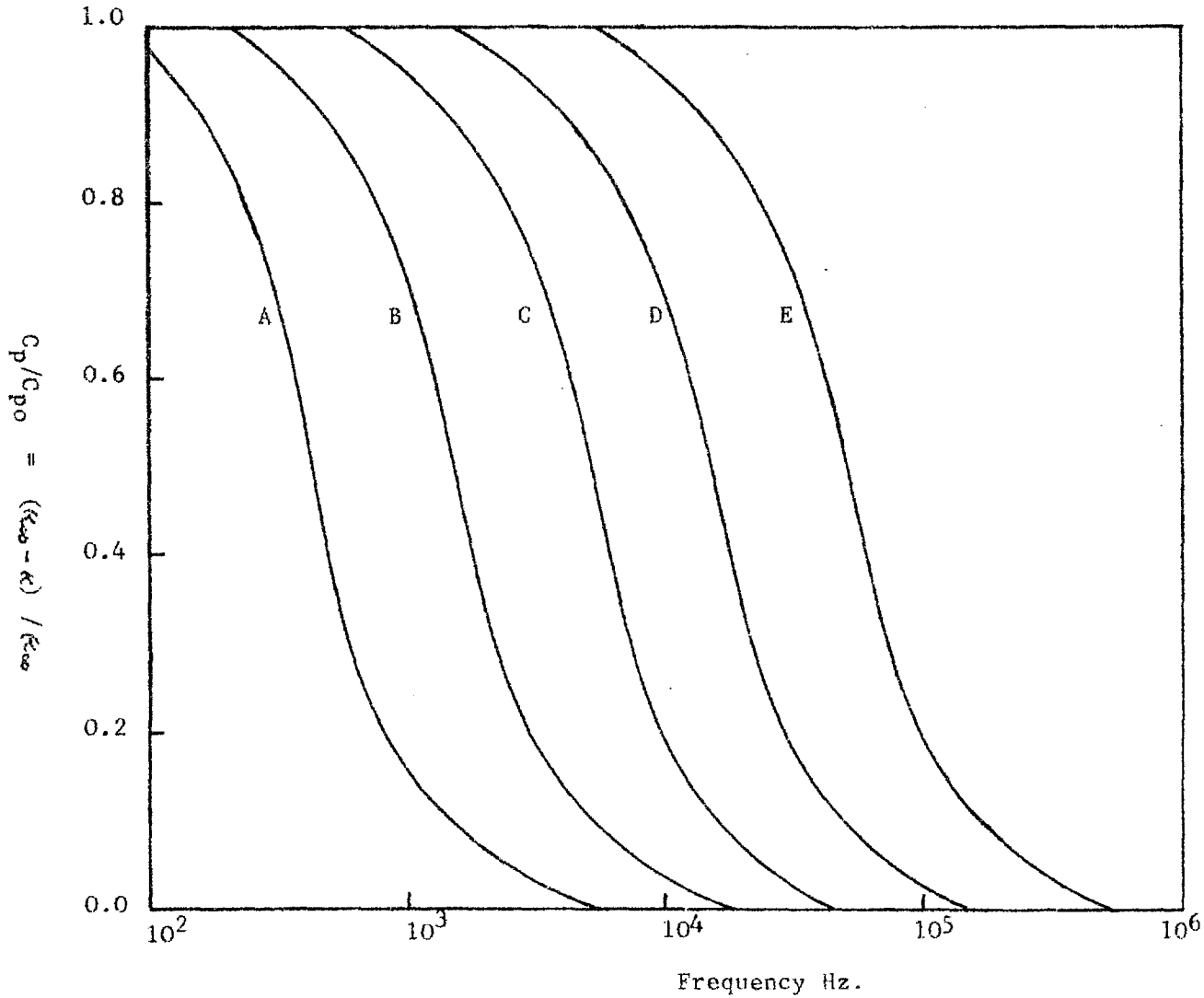


Values of $\mu\omega_o D_p$

Curve A, $10^6$

B, $10^7$

C, $10^8$

D, $10^9$

E, $10^{10}$

Figure 11: Reduced Capacitance and Relative Dispersion of the Conductance as Functions of the Parameter $\mu\omega_o D_p$

the finite size of the ions, and the distortion of the electron cloud near the electrodes. In solutions, non-polar solvent molecules are dispersed randomly in this cloud, and may be assumed to affect the calculation only by altering the constants of the theory. However, a more exact analysis, which would test the validity of the assumption of the constancy of D, $\mu$ and $\varepsilon_0$, would require a microscopic theory. This is not forthcoming at present, and in view of the limitations of Poisson's equation, it seems inappropriate to introduce a further boundary condition for linked motion. The assumption of antisymmetry as an ad hoc boundary condition is therefore made in order to solve the problem.

The solution given above does not hold if $E_0 \neq 0$. The presence of a Helmholtz or adsorption layer at the electrodes will cause inhomogeneity of the field close to the boundaries, and may give rise to an appreciable static field $E_0$. These layers will also cause a departure from the antisymmetrical profiles assumed for the ionic concentrations. The problem is more complicated in the presence of a discharge process, since this is invariably accompanied by Faradaic rectification of the applied a.c. signal [18,19], (cf. refs. 1, 10, 11). Experimental tests are necessary to show whether these effects are significant.

The predictions of the theory could have been expressed in terms of the more basic quantities current,

voltage, and phase angle instead of an RC circuit. The use of series and parallel analogues is simply an experimental convenience, and in no way implies a physical interpretation of the mechanisms in the cell. The results given above, (3.55) - (3.60), (3.64), and (3.65), could also have been obtained by identifying the cell with a circuit consisting of the low potential limit of the Gouy capacitance in series with the Ohm's law resistance of the electrolyte. This purely empirical approach should not lead one to suppose that the RC circuit is physically analogous to an electrolytic cell, (cf. ref. 20). Considering one half of an electrolytic cell, this analogue views the bulk of the electrolyte as the Ohmic resistor, and the double layer at the electrode as the capacitor. Charge would therefore flow through the bulk of the electrolyte, and accumulate at the boundary with the capacitor, which would periodically charge and discharge. This picture is inconsistent with the idea of charge carriers flowing right up to the electrode -electrolyte interface, [see Eqns. (3.16), (3.30)]. Further complications are introduced if the capacitor is identified with the Gouy capacitance. This is derived under static field conditions where the ions are stationary, whereas under the influence of an alternating p.d., the charge carriers are in motion. The first harmonic approximation in (3.7) is valid if $V_1 \ll kT/e$. This approximation is consistent with the use of the Nernst-Einstein relation, which applies if the ionic

concentrations obey the Maxwell-Boltzmann equation [14]. This condition is realized in (3.A.1) and (3.A.3) below if the ionic fluxes, and hence the current, are equated to zero.

The theory confirms that, to a certain approximation, the diffuse double layer in an electrolytic cell may be represented, in the audio and radio frequency ranges, by a series resistance-capacitance network. The relations given above apply only for $10^{-4} \ll \omega \ll \omega_0$; at frequencies outside this range different dispersion behaviour is to be expected. The very high and very low frequency solutions have not been calculated, as, besides the mathematical complications involved, the results are not applicable to present experimental techniques. On physical grounds, however, it may be assumed that, as in the Debye region, the very low frequency solution will converge asymptotically as $\omega \to 0$ to the Gouy capacitance, and the very high frequency solution to the Ohm's law resistance as $\omega \to \infty$.

## APPENDIX 3.1.

### DERIVATION OF THE TRANSPORT EQUATIONS.

The transport equations (3.1) may be derived by assuming that (1) for each ionic species, diffusion opposes migration; (2) Fick's law describes diffusion, and Ohm's law describes migration; and (3) the net flow of cations is in the opposite direction to the net flow of anions.

Consider the application of a field, as defined on p. 86, in the direction of increasing x. Let us assume that the net flow of cations is also in this direction, i.e. that $v_m^+ > v_d^+$, where $v_m^+$ and $v_d^+$ are respectively the components of the velocity due to migration and diffusion. Now, the migration flux is $p\, v_m^+ = u_p pE$, the diffusion flux is $p\, v_d^+ = -D_p \partial p/\partial x$, and consequently, the net flux in the direction of increasing x is

$$pv^+ = u_p\, pE - D_p \partial p/\partial x \,. \qquad (3.A.1)$$

Consider now a volume element of unit area between x and x + dx. Let the cation concentrations at x and x + dx be respectively $p_x$ and $p_{x+dx}$, and the field strengths at these points be $E_x$ and $E_{x+dx}$.

The net accumulation of cations into the element is

$$(pv^+)_x - (pv^+)_{x+dx}$$

$$= [U_p(pE)_x - D_p(\partial p/\partial x)_x] - [U_p(pE)_{x+dx} - D_p(\partial p/\partial x)_{x+dx}]$$

$$= D_p(\partial^2 p_1/\partial x^2)dx - U_p\,[\partial(pE)/\partial x]\,dx\ , \qquad (3.A.2)$$

from (3.A.1). The net accumulation into the element may also be written $(\partial p/\partial t)dx$, and from (3.A.2) ,

$$\underline{\partial p/\partial t = D_p(\partial^2 p/\partial x^2) - U_p \partial(pE)/\partial x}\ . \qquad (3.1)$$

The net flow of anions is in the direction of decreasing x. Consequently, the migration flux along the positive x co-ordinate is $n\nu_m^- = U_n\, nE$. The diffusion flux is $n\nu_d^- = -D_n\,\partial n/\partial x$ and the net flux is, therefore,

$$n\nu^- = -U_n\, nE - D_n\,\partial n/\partial x\ . \qquad (3.A.3)$$

The net accumulation into the element is,

$$(n\nu^-)_x - (n\nu^-)_{x+dx}$$

$$= [-U_n(nE)_x - D_n(\partial n/\partial x)_x] - [-U_n(nE)_{x+dx} - D_n(\partial n/\partial x)_{x+dx}]$$

$$= D_n(\partial^2 n/\partial x^2)dx + U_n[\partial(nE)/\partial x]\,dx\ . \qquad (3.A.4)$$

Since the rate of accumulation of anions into the element is $(\partial n/\partial t)\,dx$, it follows from (3.A.4) that

$$\underline{\partial n/\partial t = D_n\,\partial^2 n/\partial x^2 + U_n\,\partial(nE)/\partial x}\ . \qquad (3.1)$$

## APPENDIX 3.2.

## THE ELECTROSTRICTIVE AND ELECTROCALORIFIC EFFECTS IN MOLTEN SALTS.

In order to calculate the electrostrictive and electrocalorific coefficients from (1.14b) and (1.18), a knowledge of $\varepsilon_o$, $(\partial\varepsilon_o/\partial T)_{P,E}$, and $(\partial\varepsilon_o/\partial P)_{T,E}$ is required. Such data for molten salts is lacking. However Bosman and Havinga [21] have published data for the refractive index N, and for $(\partial N/\partial T)_P$ and $\rho(\partial N/\partial\rho)_T$ of a number of solid salts.

Since $N = \varepsilon_o^{\frac{1}{2}}$,

$$(\partial\varepsilon_o/\partial T)_{P,E} = 2N\varepsilon^o(\partial N/\partial T)_{P,E} , \qquad (3.A.5)$$

$$(\partial\varepsilon_o/\partial P)_{T,E} = 2N\gamma\varepsilon^o[\rho(\partial N/\partial\rho)_{T,E}], \qquad (3.A.6)$$

where $\rho$ is the density, $\gamma = -(1/v)(\partial v/\partial P)_{T,E}$ is the isothermal compressibility, and $\varepsilon^o = 8.854 \times 10^{-12}$ $Fm^{-1}$, (ref.22), is the permittivity of free space.

The calculations will now be carried through using Bosman and Havinga's data for solid NaCl. These authors give $N = 1.54$, $(\partial N/\partial T)_P = -3.7 \times 10^{-5}$ $^oK^{-1}$, and $\rho(\partial N/\partial\rho)_{T,E} = 0.24$. Also, for molten NaCl [23], $\gamma = 2.87 \times 10^{-11}$ $cm^2$ $dyne^{-1} = 2.87 \times 10^{-10} m^2.N^{-1}$.

Hence, from (3.A.5) and (3.A.6),

$$(\partial\varepsilon_o/\partial T)_{P,E} \simeq -10^{-15} \text{ F.m}^{-1} {}^oK^{-1}$$

and $$(\partial \varepsilon_o / \partial P)_{T,E} \simeq 2 \times 10^{-21} \text{ F.m.N}^{-1}.$$

Eqn. (1.14a) gives :

$$(1/v)\,(\partial v/\partial E)_{T,P} = -(Ev_c/4\pi v)\,(\partial \varepsilon_o/\partial P)_{T,E}\,.$$

Assuming an average field of 10 $Vm^{-1}$, a molar volume of 40 $cm^3$ ($4 \times 10^{-5}$ $m^3$), and a capillary of length 5 cm ($5 \times 10^{-2}$ m) and diameter 0.05 cm ($5 \times 10^{-4}$m), $(Ev_c/4\pi v) \simeq 2 \times 10^{-4}$ $V.m^{-1}$, and therefore,

$$(1/v)(\partial v/\partial E)_{T,P} = -4 \times 10^{-25} \text{ V.F.N}^{-1}$$
$$= \underline{-4 \times 10^{-25} \text{ m V}^{-1}}.$$

Eqn. (1.18) gives :

$$(\partial H/\partial E)_{T,P} = (v_c E/4\pi)\,[\varepsilon_o + T(\partial \varepsilon_o/\partial T)_{P,E}\,].$$

Under the same conditions as above, $(v_c E/4\pi) \simeq 8 \times 10^{-9}$ $Vm^2$. Also, $\varepsilon_o = N^2 \varepsilon^o \simeq 2 \times 10^{-11}$ $F.m^{-1}$, and if T = 1200°K., $T(\partial \varepsilon_o/\partial T)_{P,E} \simeq 1 \times 10^{-12}$ F $m^{-1}$, and therefore

$$(\partial H/\partial E)_{T,P} = 1 \times 10^{-12} \text{ VmF}$$
$$= \underline{1 \times 10^{-12} \text{ JmV}^{-1}}.$$

Now, $(\partial T/\partial E)_{T,P} = (\partial H/\partial E)_{T,P} \cdot (\partial T/\partial H)_{T,P}$

$$= (1/\sigma)\,(\partial H/\partial E)_{T,P} \text{ mole } ^\circ\text{K mV}^{-1}$$
$$= (v/\sigma v_c)\,(\partial H/\partial E)_{T,P} \,^\circ\text{K mV}^{-1},$$

where $\sigma$ is the specific heat (J $mole^{-1}$ $^\circ K^{-1}$).

For molten NaCl[24], $\sigma$ = 16 cal $mole^{-1}$ $^\circ K^{-1}$ = 62 J $mole^{-1}$ $^\circ K^{-1}$.

Also, $v/v_c \simeq 4 \times 10^3$, and therefore,

$$(\partial T/\partial E)_{T,P} \simeq 6 \times 10^{-11} \ {}^{o}K \ mV^{-1}.$$

The magnitude of these results indicates that the electronic contribution to the electrostrictive and electrocalorific effects for molten salts and solutions in conductance cells are completely negligible. Moreover, if $\varepsilon$ is given its maximum value of $8\pi sC'_{p_o}$ (p.97), and the same temperature and pressure coefficients assumed, the effects, although much larger than those due to electronic polarization, are still negligible.

## REFERENCES.


1. R.J.Friauf,
   J.Chem.Phys., 1954, 22, 1329.

2. A.R.Allnatt and P.W.M.Jacobs,
   J.Phys.Chem.Solids, 1961, 19, 281.

3. P.W.M.Jacobs and J.N.Maycock,
   J.Chem.Phys., 1963, 39, 757.

4. G.Jones and S.M.Christian,
   J.Amer.Chem.Soc., 1935, 57, 272.

5. G.Jaffé and J.A.Rider,
   J.Chem.Phys., 1952, 20, 1077.

6. G.J.Hills and K.E.Johnson,
   J.Electrochem.Soc., 1955, 102, 598.

7. E.R.Buckle and P.E.Tsaoussoglou,
   J.Chem.Soc., 1964, 667.

8. K.E.Johnson,
   Electrochim.Acta, 1964, 9, 653.

9. B.G.Dick, Jr., and A.W.Overhauser,
   Phys.Rev., 1958, 112, 90.

10. G.Jaffé,
    ibid., 1952, 85, 384.

11. J.R.Macdonald,
    ibid., 1953, 92, 4.

12. J.D.Ferry,
    J.Chem.Phys., 1948, 16, 737.

13. H.Chang and G.Jaffé,
    J.Chem.Phys., 1952, 20, 1071.

14. J.Frenkel,
    Kinetic Theory of Liquids, Oxford University Press,
    1946, p.40.

15. E.C.Potter,
Electrochemistry, Cleaver-Hume, London, 1961, p.155.

16. H.Falkenhagen,
Electrolytes, Oxford University Press, 1934.

17. S.A.Rice,
Trans.Faraday Soc., 1962, 58, 499.

18. G.C.Barker,
Anal.Chim.Acta, 1958, 18, 118.

19. K.B.Oldham,
J.Electrochem.Soc., 1960, 107, 766.

20. H.A.Laitinen and D.K.Roe,
Coll.Czech.Chem.Commun., 1960, 25, 3065.

21. A.J.Bosman and E.E.Havinga,
Phys.Rev., 1963, 129, 1593; 1965, 140, A.292.

22. C.P.Smyth,
Dielectric Behaviour and Structure, McGraw-Hill,
New York, 1955, p.1.

23. H.Bloom and J.O'M.Bockris,
Fused Salts, edit. Sundheim, McGraw-Hill,
New York, 1964, p.28.

24. O.Kubachewski and E.Ll.Evans,
Metallurgical Thermochemistry, Pergamon, London,
1955, p.306.

# CHAPTER 4.

# THE MEASUREMENT OF DISPERSION IN PURE MOLTEN SALTS.

## EXPERIMENTAL.

### MATERIALS.

The materials used in this research were :

KCl : "Analar" grade, Hopkin and Williams,
Batch Nos. 200902W60085 and 78769B210384.
Purity not less than 99.8% after drying.

AgBr : Johnson Matthey, Batch No. 8A.
Purity not less than 99.99% after drying.

$CdCl_2$: "Analar grade", Hopkin and Williams,
Batch No. 80518B210649.
Purity not less than 99.5% after drying.

The main impurity in the potassium chloride was sodium ($< 0.2\%$), present predominantly as the chloride. Impurities in cadmium chloride were the sulphates of alkali and other metals, ($< 0.1\%$).

Prior to use, all materials were ground in a mortar, dried in an oven at 200°C for 24 hours, and stored in a desiccator.

In certain experiments, the salts were dried further by bubbling through the melt a mixture of argon and hydrogen chloride gases [1,2], produced in the apparatus shown in Fig.12.

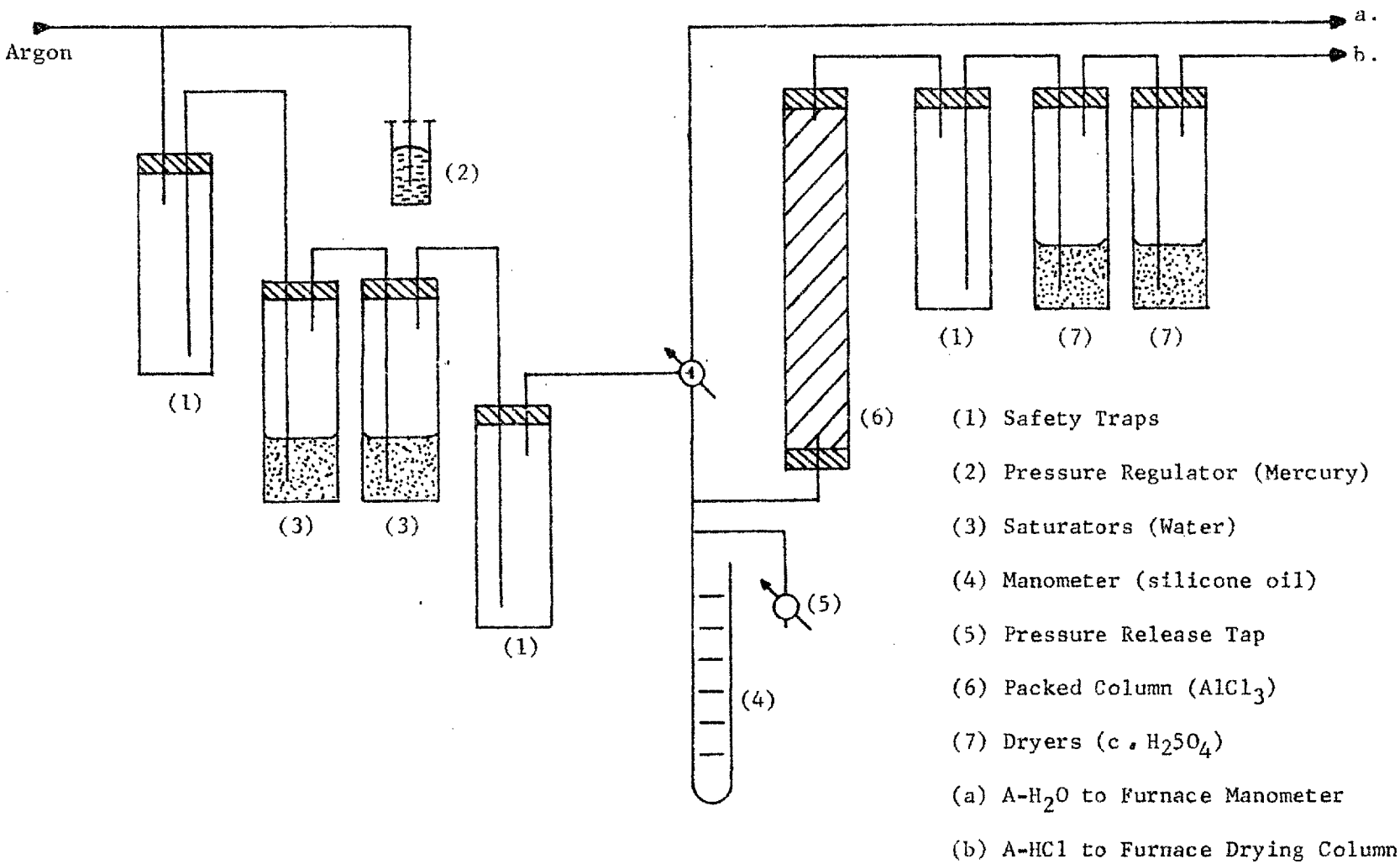


Figure 12: Apparatus for the Production of A-HCl and A-$H_2O$ Gas Mixtures.

Argon, saturated with water in the first series of wash bottles, was fed into a column containing aluminium chloride, where hydrogen chloride was produced by the reaction

$$AlCl_3 + 3H_2O = Al(OH)_3 + 3HCl .$$

The gas mixture was then dried by passing it through a further series of wash bottles containing concentrated sulphuric acid. The water-saturated argon used in studies on wet melts, (see below), was produced by cutting out the latter two stages of this apparatus.

THE CONDUCTANCE CELL.

Description of the Conductance Cell.

The cells, (Fig.13(a)), were similar in construction to those used in previous conductance work in this laboratory [3]. They were constructed from transparent vitreosil silica, (Thermal Syndicate Ltd.), which was able to withstand attack in the potassium chloride and silver bromide melts for about two weeks. However, the silica was more readily attacked in cadmium chloride melts, and the useful life of a cell was only a few days.

One end of a silica capillary, 5-6 cm. in length, was fused onto a silica supporting tube, 45 cm. long, 6 mm bore and the other end expanded into a bell. This assembly was enclosed in a further silica tube, 45 cm long and 10 mm bore, the end of which was sealed to the rim of

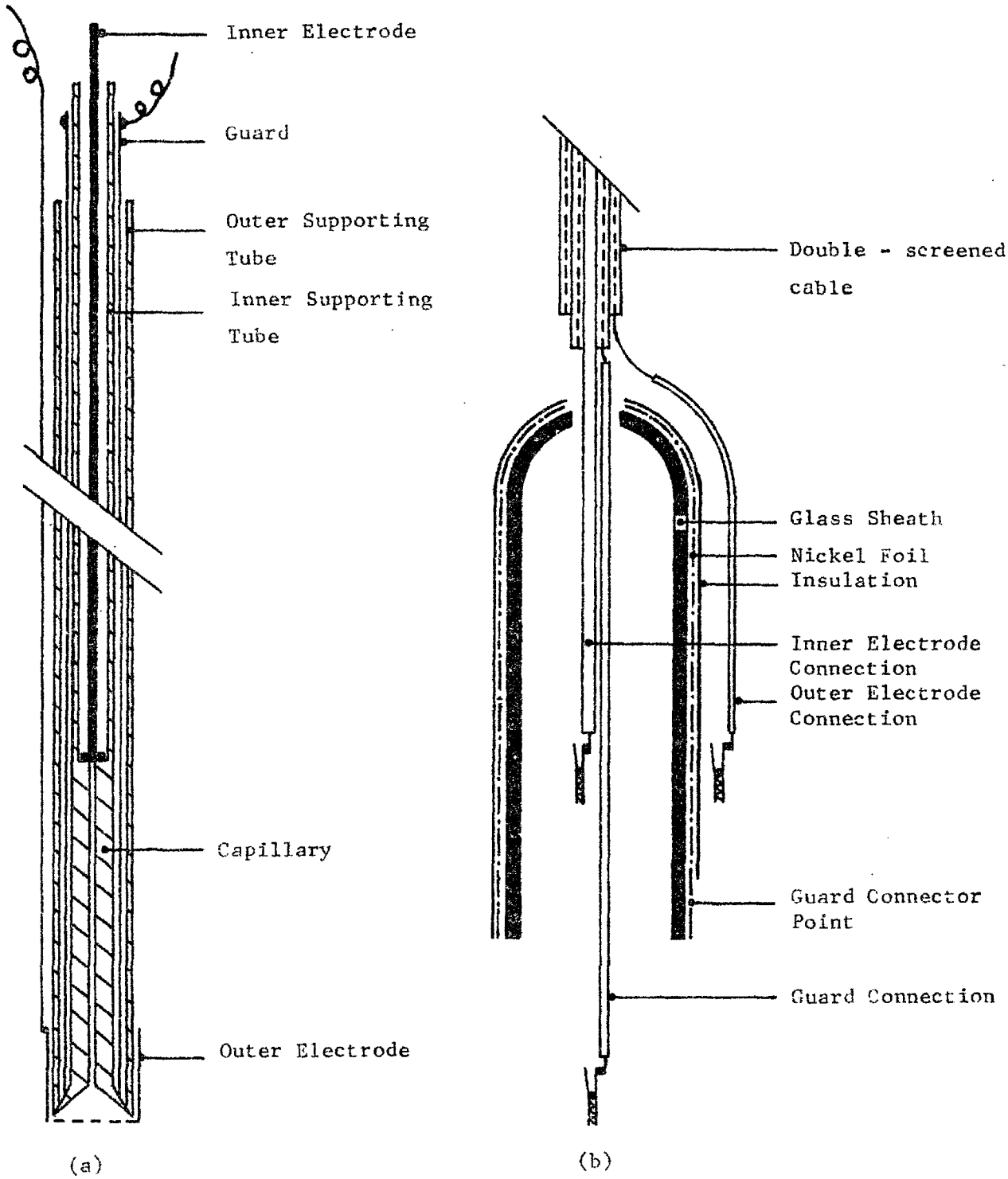


Figure 13: Sectional Drawings of (a) the Cell, and (b) the Cable Connector.

the capillary bell. A tubular guard sheath of 0.002" nickel foil, 48 cm high, was inserted between the inner and outer tubes over the bell to ensure complete electrical screening of the capillary.

The inner electrode consisted of a 16 S.W.G. platinum rod, (Johnson Matthey) with one end hammered into a perpendicular disc of about 5 mm diameter. The electrode was lowered into the inner supporting tube until the disc rested on top of the capillary.

The outer electrode consisted of a piece of platinum foil, (Johnson Matthey), fashioned into a thimble 1.5 cm long, which was perforated in the base and fitted over the end of the sheathed capillary. The inside of the thimble was lined with a piece of platinum gauze, welded to it at the top. This allowed free access of melt, but prevented the capillary getting blocked by any solid matter. A length of 20 S.W.G. platinum wire, which ran outside the silica tubes, formed the electrode lead.

The cell was connected to the bridge with double-screened co-axial cable, the multi-stranded core and the two mesh screens being mutually insulated. The core was connected to the inner electrode, the inner screen to the guard, and the outer screen, which was earthed, to the outer electrode. All connections were made with crocodile clips soldered to the cable. These were periodically inspected

to ensure good electrical contact. A glass sleeve, covered with insulated nickel foil, (Fig.13(b)), provided continuity of the guard at this junction.

Initial measurements were made using cells having capillaries with a nominal bore of 0.8 mm , and cell constants of about 1000 $cm^{-1}$. The measured resistance of molten potassium chloride was therefore of the order of 500 ohms. Later tests, (see below, p.145), showed that capacitance measurements were affected by a stray capacitance if the resistance was less than 1000 ohms. To avoid this, cells having 0.5 mm bore capillaries were used eventually, which had resistances exceeding 1000 ohms in the melt.

Platinization of the Electrodes.

The electrodes were platinized in a solution containing 2 g chloroplatinic acid, (Johnson Matthey) and 0.02 g lead acetate per 100 ml of water [4]. A rheostat was used to regulate the current from a pair of accumulators, so that only a moderate evolution of gas occurred at the electrodes. The direction of the current was reversed about every half-minute, and the process was continued until a moderately thick coating of platinum black was deposited on the electrodes. This operation normally took 10-15 minutes. The platinizing solution was then replaced by dilute sulphuric acid, and the electrolysis continued for a further

10 minutes in each direction to remove traces of chloroplatinic acid from the electrode surfaces. After washing and drying, the electrodes were heated in a bunsen flame to convert the deposit from black to grey platinum.

Calibration of the Cells.

Cells were calibrated in a molar solution of potassium chloride at about 28°C. This was made up in standard flasks to contain 71.3828 g of salt per 1000.000 g of solution. Distilled water, which had been allowed to equilibrate with the atmosphere, was adequate for this purpose since at the present level of accuracy the carbon dioxide content of the water did not affect its electrical conductance.

The flasks, loosely stoppered to minimize evaporation, were immersed in a water-bath thermostatted to ± 0.005°C. The solution temperature was measured with a micro-Beckmann thermometer sensitive to ± 0.002°C. The thermometer had been calibrated to this precision against a platinum resistance thermometer at about 28°C, using a Smith bridge.

The solution was transferred to a graduated cylinder, and with the cell in position, allowed to equilibrate in temperature for at least half an hour before conductance measurements were commenced. No drift in the measurements was observed with time. Reliable conductance

data could not be obtained above 30 KHz because of the high resistance [3], and the cell constant was calculated from the resistance in the frequency range 20-30 KHz, which was constant to within the limits of the bridge precision.

A regression analysis of Jones and Prendergast's conductance data for molar potassium chloride solution [5] showed that their values of the specific conductance, $\kappa$ ohm$^{-1}$ cm$^{-1}$, in the range $0 \leq T \leq 25^{\circ}C$ could be represented by

$$\kappa = 4.496 \times 10^{-6} T^2 + 1.73973 \times 10^{-3} T + 6.5430 \times 10^{-2} \qquad (4.1)$$

with a standard deviation of $7.06 \times 10^{-7}$ ohm$^{-1}$ cm$^{-1}$. The cell constant was calculated from the relation

$$K = \kappa R , \qquad (4.2)$$

where K is the cell constant (cm$^{-1}$), and R is the cell resistance (ohms). Results showed that dispersion was very small in the usual silica conductance cells, ($< 0.25\%$ over the frequency range 1-30 KHz.).

If the errors in the specific conductance and the resistance are $\pm$ d$\kappa$ and $\pm$ dR respectively, the error in the cell constant is

$$dK = (\partial K/\partial \kappa)_R \, d\kappa + (\partial K/\partial R)_\kappa \, dR,$$

or

$$dK/K = d\kappa/\kappa + dR/R . \qquad (4.3)$$

Error arises in the specific conductance from the uncertainty in the solution temperature. At 28°C, an error of $\pm$ 0.002°C

gives rise to an error of ± 0.003% in $\kappa$. The error in the resistance reading results from the limitations on the absolute accuracy of the bridge, which is known to be ± 0.05% (see below). Consequently, the cell constant is subject to an error of ± 0.053%. In the present work, the potassium chloride was weighed in air, whilst Jones and Prendergast weighed their salt under vacuum. This leads to a weighing error of -0.046%, and assuming a linear relation between conductance and concentration over this small composition range, an error of -0.046% in $\kappa$. A correction for this was made to the values of the cell constants.

THE FURNACE.

Details of Construction.

The molten salts were heated in a heavily lagged electrical resistance furnace, (Figs. 14, 15), designed to operate at temperatures up to 1100°C.

The heating elements, constructed from Kanthal A.1 wire consisted of three coiled-coil windings, and in the final apparatus each had a d.c. resistance of about 20 ohms. Since a sufficient length of winding could not be obtained with a single spiral, a centre-tapped winding of 80 ohms was constructed. By connecting the two halves of the winding in parallel, the effective resistance was reduced to 20 ohms.

The windings were mounted independently on a mullite tube of 55 mm bore and 530 mm length, (Morgan

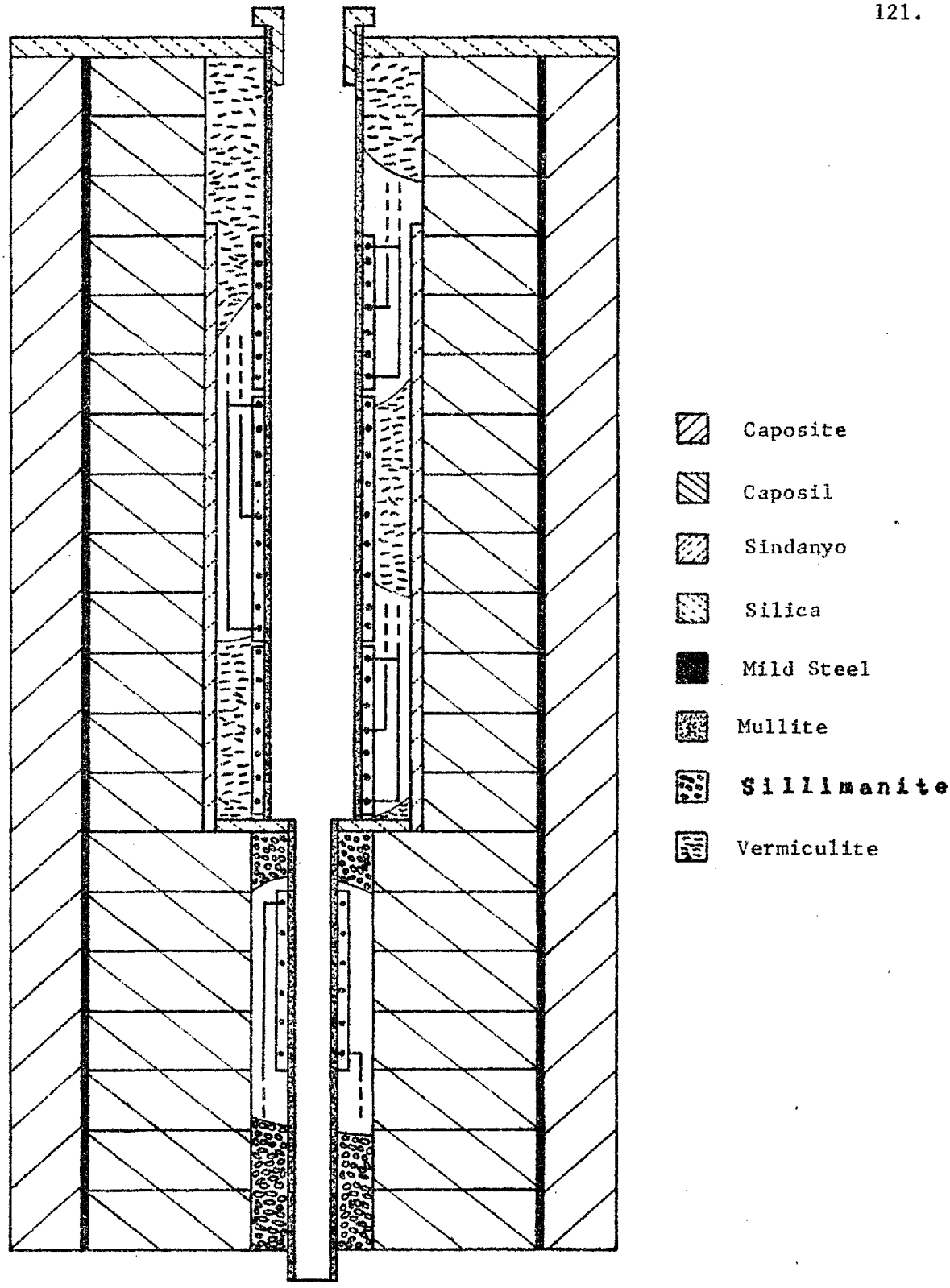


Figure 14: The Furnace

Figure 15. The Equipment.

Refractories). Asbestos rope, held in place with alumina cement, provided insulation between successive turns of the winding. The power leads out of the furnace were insulated with alumina beads. The ends of the windings were secured to the furnace tube with loops of Kanthal wire, so as to be free from undue mechanical strain. In order to obtain a good temperature profile along the furnace tube, care was taken to ensure that the spacing between successive turns was uniform in the central region.

The furnace tube was mounted inside a silica tube of 128 mm bore and 410 mm in length. The space between these tubes was filled with sillimanite powder (100 mesh), and the bottom of the furnace tube rested on a sindanyo disc, 125 mm in diameter and 15 mm thick. A second mullite tube of 55 mm bore and 300 mm in length was mounted immediately below a hole of the same diameter drilled in the centre of this disc. This tube, the bottom of which projected below the base of the furnace, was fitted with a fourth coiled-coil winding of 34 ohms resistance. The purpose of this tube was to assist in the removal of any melt which might accidentally drop to the bottom of the furnace.

The whole of the main furnace tube assembly was surrounded by caposil annuli in a mild steel pipe of 305 mm bore and 770 mm length. This was insulated with a Caposite tube, (Cape Asbestos Co.), of 400 mm o.d. and 770 mm in

length. The furnace was mounted with its axis vertical and was covered with a sheet of sindanyo, the furnace tube projecting through a hole in it. An aluminium hood, mounted on a framework over the furnace, was connected to an exhaust to remove toxic vapours.

The Power Supply.

In the early part of this work, dispersion was studied using a furnace of the design previously employed in this laboratory for conductance [3,6] and density [7] measurements. A.c. power was supplied to three independent windings of 70 ohms resistance through Variac transformers, (Claude Lyons, Type V6H-M). Fluctuations in the mains voltage were compensated by an automatic voltage stabilizer, (Claude Lyons, Type TS-1).

As previously found [3], it was difficult to obtain reproducible dispersion curves, and it was suspected that this was due to the fluctuations in the temperature of the melt observed during the course of a run. Tests were carried out in which the mains voltage, the melt temperature, and the resistance of a conductance cell immersed in molten potassium chloride were recorded over periods of several hours. The results showed correlations between all three. It was found that, provided the fluctuations in temperature were sufficiently slow ($\lesssim 0.2^{\circ}C\ min^{-1}$), a correction to the

resistance values could be made, using the equation

$$dR/dT = -(K/\kappa^2)\, d\kappa/dT \quad . \qquad (4.4)$$

Figure 16 illustrates the effectiveness of this correction. The melt temperature and the resistance of the cell at 20 KHz are plotted simultaneously against time. The resistance values, corrected to the initial temperature using (4.4) are also plotted, and it can be seen that these are constant to within the experimental precision of $\pm$ 0.1 ohms. Typical resistance dispersion data for molten potassium chloride at 740°C are given in Table 4.1, together with the values corrected to a common temperature using (4.4). The results, except for the uncorrected data of Run (1) omitted in the interests of clarity, are illustrated in Fig.17. The agreement between Runs (2) and (3), in which the temperature fluctuations were small, is excellent. In Run (1), the temperature changes were too rapid for (4.4) to be effective.

As a result of these tests, a unit supplying highly stable d.c. power to the furnace windings was designed and built in this department under the supervision of Mr.L.Tyley. It incorporated three independent output channels, each capable of supplying up to 500 watts to a 20 ohm load. The output voltage of each channel (32-100 volts, in three ranges) was stable to about 0.001%. A schematic diagram of this unit is shown in Fig.18. The transformer-rectifier section

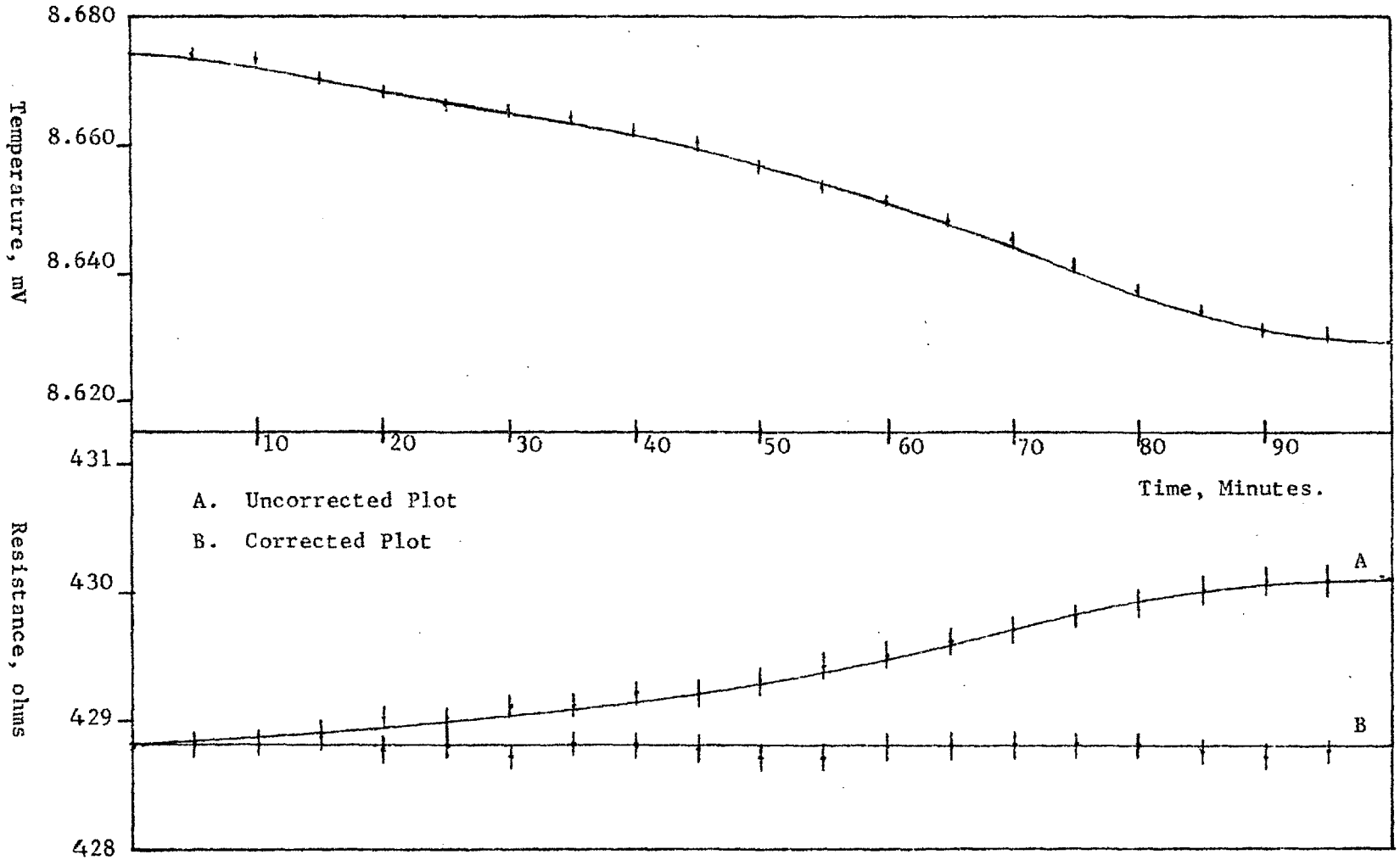


Figure 16: The Influence of Temperature Fluctuations on the Measured Cell Resistance.

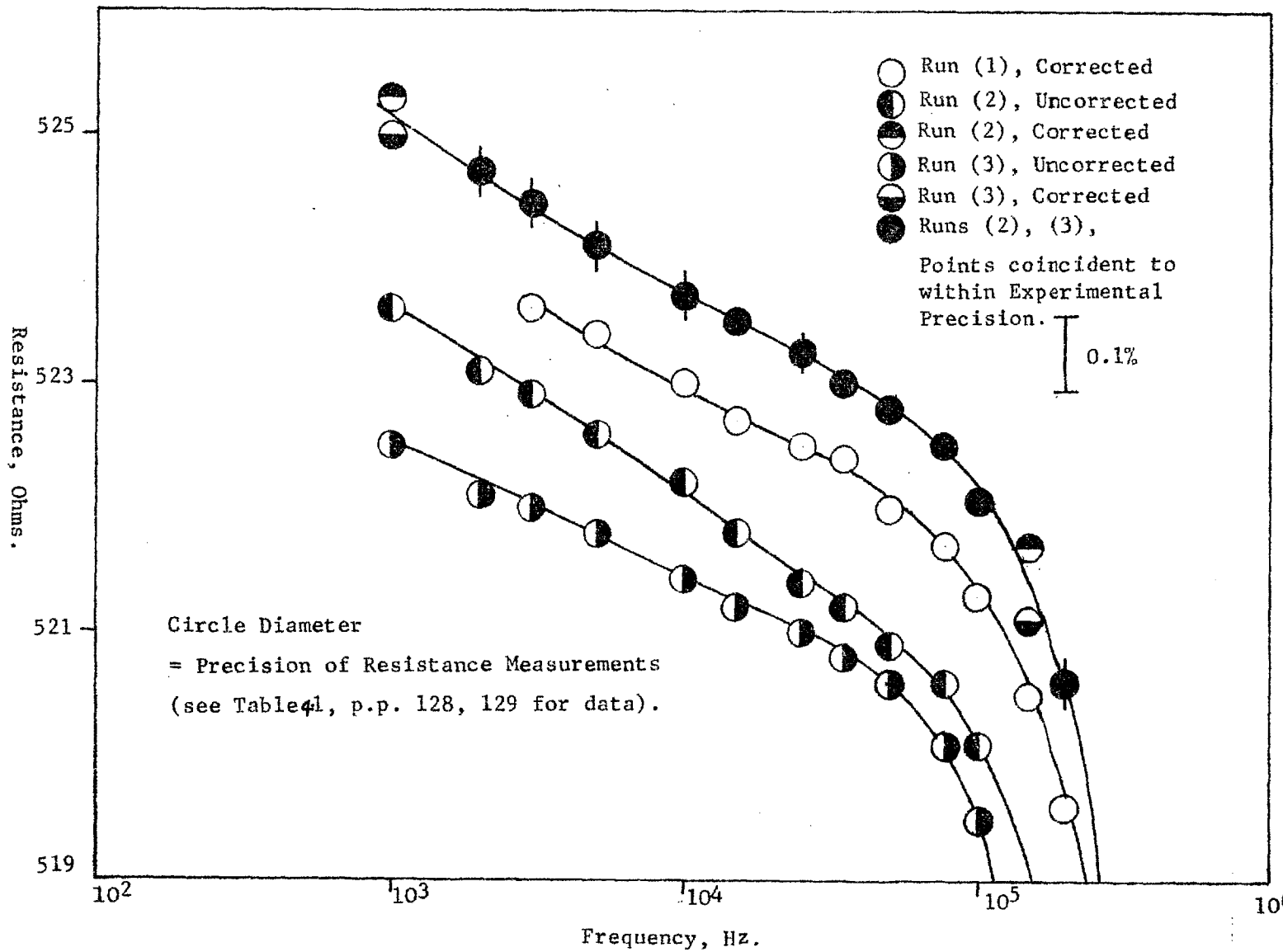


Figure 17: Reproducibility of Results.

Table 4.1.

Reproducibility of Results.

In this table, $R_p$ is the measured cell resistance, and $R_{corr}$ is its value at a temperature of 8.500 mV (844°C).

Run (1).

| Freq.(KHz) | $R_p$ (ohm) | Temp.(mV) | $R_{corr}$(ohm) |
|---|---|---|---|
| 200 | 520.4 ± .1 | 8.476 | 519.6 ± .1 |
| 150 | 521.2 ± .1 | 8.479 | 520.5 ± .1 |
| 100 | 522.0 ± .1 | 8.478 | 521.3 ± .1 |
| 75 | 522.4 ± .1 | 8.478 | 521.7 ± .1 |
| 50 | 522.7 ± .1 | 8.480 | 522.0 ± .1 |
| 35 | 522.9 ± .1 | 8.484 | 522.4 ± .1 |
| 25 | 522.9 ± .1 | 8.488 | 522.5 ± .1 |
| 15 | 523.0 ± .1 | 8.492 | 522.7 ± .1 |
| 10 | 523.1 ± .1 | 8.496 | 523.0 ± .1 |
| 5 | 523.5 ± .1 | 8.498 | 523.4 ± .1 |
| 3 | 523.7 ± .1 | 8.498 | 523.6 ± .1 |

Run (2).

| Freq.(KHz) | $R_p$ (ohm) | Temp.(mV) | $R_{corr}$(ohm) |
|---|---|---|---|
| 200 | 517.8 ± .1 | 8.580 | 520.5 ± .1 |
| 150 | 518.6 ± .1 | 8.576 | 521.1 ± .1 |
| 100 | 519.5 ± .1 | 8.574 | 522.0 ± .1 |
| 75 | 520.1 ± .1 | 8.571 | 522.5 ± .1 |
| 50 | 520.6 ± .1 | 8.566 | 522.8 ± .1 |

(cont.)

| Freq.(KHz) | $R_p$ (ohm) | Temp.(mv) | $R_{corr}$(ohm) |
|---|---|---|---|
| 35 | 520.8 ± .1 | 8.567 | 523.0 ± .1 |
| 25 | 521.0 ± .1 | 8.568 | 523.3 ± .1 |
| 15 | 521.2 ± .1 | 8.568 | 523.5 ± .1 |
| 10 | 521.4 ± .1 | 8.566 | 523.6 ± .1 |
| 5 | 521.8 ± .1 | 8.567 | 524.0 ± .1 |
| 3 | 522.0 ± .1 | 8.573 | 524.4 ± .1 |
| 2 | 522.1 ± .1 | 8.576 | 524.6 ± .1 |
| 1 | 522.5 ± .1 | 8.574 | 525.0 ± .1 |

Run (3).

| Freq.(KHz) | $R_p$ (ohm) | Temp.(mv) | $R_{corr}$(ohm) |
|---|---|---|---|
| 200 | 518.8 ± .1 | 8.556 | 520.7 ± .1 |
| 150 | 519.8 ± .1 | 8.558 | 521.7 ± .1 |
| 100 | 520.1 ± .1 | 8.560 | 522.1 ± .1 |
| 75 | 520.6 ± .1 | 8.558 | 522.5 ± .1 |
| 50 | 520.9 ± .1 | 8.557 | 522.8 ± .1 |
| 35 | 521.2 ± .1 | 8.555 | 523.0 ± .1 |
| 25 | 521.4 ± .1 | 8.554 | 523.2 ± .1 |
| 15 | 521.8 ± .1 | 8.551 | 523.5 ± .1 |
| 10 | 522.2 ± .1 | 8.549 | 523.8 ± .1 |
| 5 | 522.6 ± .1 | 8.548 | 524.2 ± .1 |
| 3 | 522.9 ± .1 | 8.548 | 524.5 ± .1 |
| 2 | 523.1 ± .1 | 8.550 | 524.8 ± .1 |
| 1 | 523.6 ± .1 | 8.552 | 525.3 ± .1 |

N.B. 1 mV ≏ 1/8°C (see below)

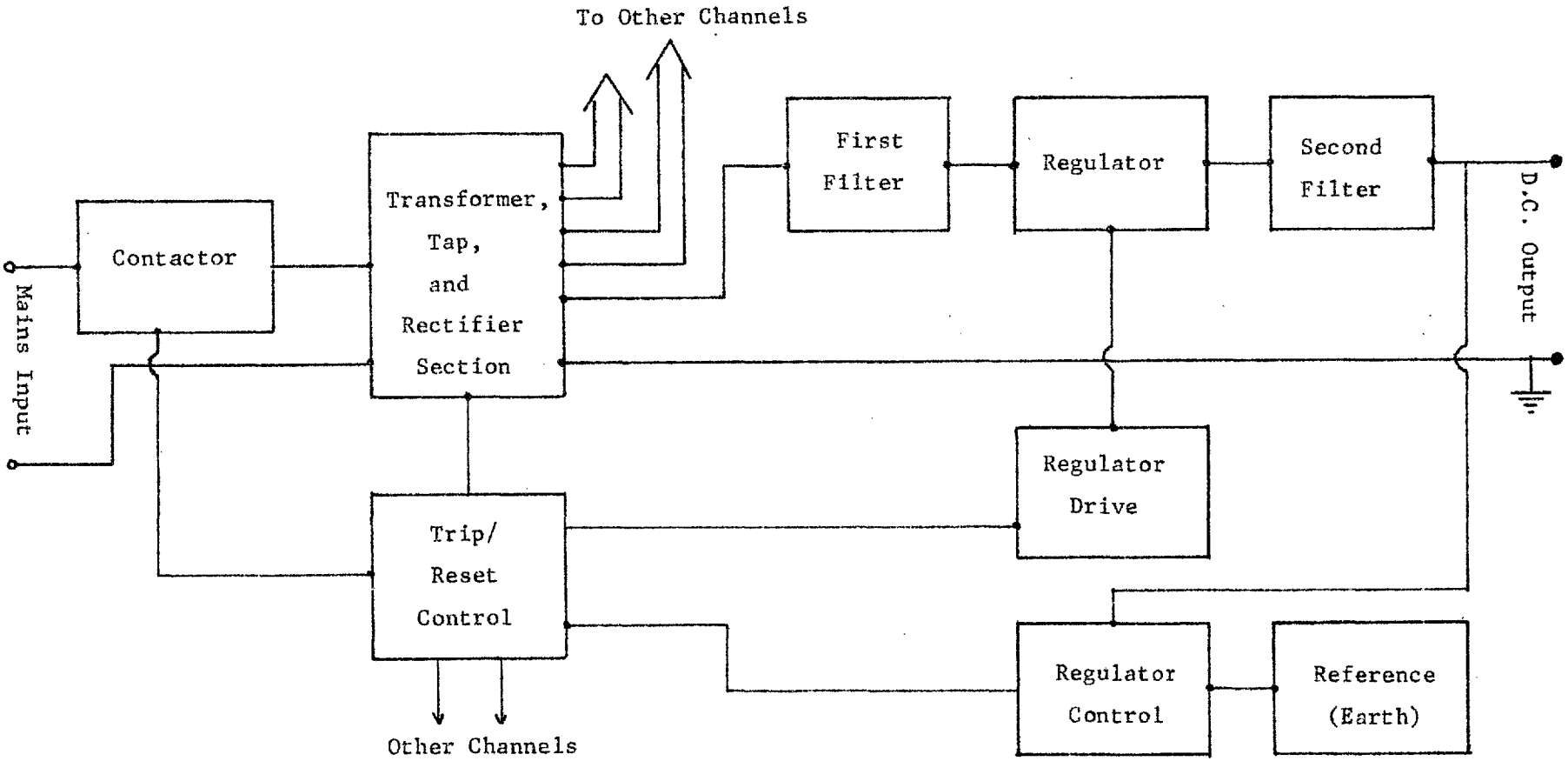


Figure 18: D.C. Furnace Power Supply (Single Channel)

and the trip-reset mechanism are common to all three channels. The control circuit of only one channel is shown, the other two being identical.

Mains power was fed from an automatic voltage stabilizer (Claude Lyons, Type TS-1), into a multi-tapped transformer. A three-way switch, which operated a series of relays, was used to select the transformer secondary tapping appropriate to the required output voltage. The trip-reset mechanism, operating the contactor, protected the switching relays and the fan-cooled power transistors in the regulator from surges while changing range. The output from the transformer was rectified, and then smoothed in the first filter, which consisted of capacitors and current-limiting resistors. The output from this filter was switched on and off at a constant frequency by the regulator. The resulting pulsed waveform was fed into the second filter, which averaged out the pulses into a steady d.c. supply. Stability of the output voltage was achieved by varying the width of the pulses produced by the regulator. This was effected by comparing the output voltage with earth potential in the regulator controller. The output voltage from each channel could be controlled at any desired value in the operating range with the appropriate selector switch, and the coarse and fine adjustment potentiometers on the regulator controller.

Tests showed that, using this power unit, the temperature stability was better than $\pm$ 0.1°C at 900°C over a period of 6 hours. A temperature distribution in the melt, often uniform to $\pm$ 0.1°C over the height of the cell capillary, was achieved by careful adjustment of the power supplies to each winding.

In view of the high precision required for dispersion studies in melts the detection and elimination of temperature drift formed one of the most significant experimental advances of the research.

Temperature Measurement.

The temperature of the melt was measured using Platinum-13% Rhodium/Platinum thermocouples (Johnson Matthey). The certified accuracy of these thermocouples was $\pm$ 1°C at 1000°C. Lengths of twin bore alumina tubing were used to insulate the two thermocouple wires in the furnace. To provide protection against the melt, the hot junction and the insulated wires were enclosed in a thin wall silica tube of 3 mm bore, sealed at the bottom. The cold junctions, enclosed in Pyrex sheaths, were immersed in an ice-water mixture, and allowed to equilibrate for half an hour before measurements were made. Since the mixture was close to the furnace, it was stirred occasionally to ensure uniformity of temperature in the cold junction.

The e.m.f. of the thermocouple was measured to an accuracy of ± 1 μ-volt on a Vernier Potentiometer (Croydon Precision Instrument Co.), using a Pye galvanometer (Cat.No. 11343) and modulator (Cat.No. 11353) as null detector. A temperature-controlled cadmium cell, (Muirhead, Type K-231-A), was used to supply a standard voltage to the potentiometer. The cell, enclosed in an oven at 40 ± 1°C, had an electronically thermostatted jacket which controlled its temperature to ± 0.1°C. The stability of the cell output voltage was better than ± 1 μ-volt, which was essential if changes of 0.1°C in the furnace temperature were to be reliably observed. A 2 volt Potentiometer Supply Unit, (Croydon Precision Instrument Co., Type P10/S), was used in place of an external accumulator, because of its better long term stability.

THE BRIDGE.

Measurements of the cell impedance in melts and solutions were made on a Schering bridge with a guard circuit at frequencies in the range 100 Hz - 200 KHz. The bridge gave direct readings of the parallel resistance and capacitance of the cell. The advantages in making parallel measurements are that these are less sensitive to errors due to shunt admittance and the skin effect at high frequencies. Also, wide variations in the series capacitance are brought

within the scope of a single balancing capacitor. The difference between series and parallel resistances was negligible in the present measurements, (see Eqn. (2.3), p. 52).

General Description of the Bridge Equipment.

A General Radio Type 716-C Capacitance Bridge, (30 Hz - 300 KHz), modified for the measurement of resistance, was used [3]. For this purpose, a General Radio Type 1432 Decade Resistor (0-111,111 ohms in steps of 0.1 ohm), $R_N$, was connected in parallel with the internal balancing capacitor $C_N$ (100 - 1150 pF). Earth admittances in the bridge network and shunt admittances in the cell leads were eliminated with a General Radio Type 716-P4 Guard Circuit, (30 Hz - 300 KHz) using the guard balancing controls $R_G$ and $C_G$. The bridge (B-C-D-A-B) and guard (B-A-G-C-B) networks are illustrated in Fig.19. [3]

The decade resistor $R_N$ was surrounded by two mutually insulated screens. The inner one was connected to the guard point G, and the outer one was earthed. This arrangement ensured that the bridge balance was affected only by the residuals of the decade unit, correction for which could be made using the manufacturer's data (see below).

Resistance and capacitance measurements were made by the direct method. Although this was slightly less accurate than the substitution method, it was far speedier.

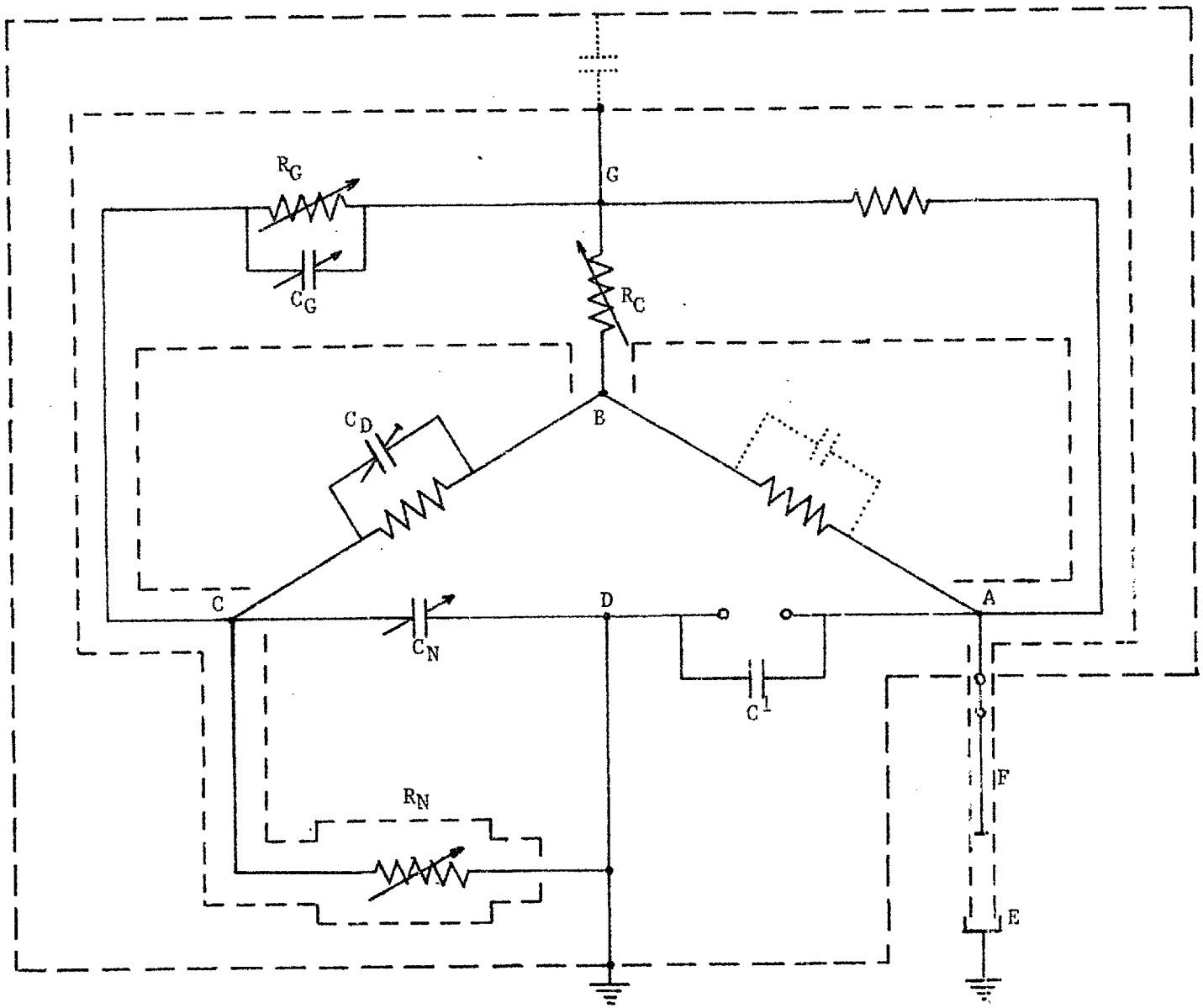


Figure 19: The Bridge.

Capacitance balance was achieved using the internal balancing capacitor $C_N$, the dissipation factor capacitor being permanently set to zero. Balance was obtained when points B and G, (Fig.19), were both brought to earth potential. This was assisted by first partially balancing out the guard-earth capacitance in the coupling network (B-G-D-C-B) using the coupling resistor $R_c$. An accurately measured mica capacitor, C' (208.4 $\pm$ 0.8 pF) was connected across D-A in parallel with the cell. This prevented the measured capacitance falling below the range of the balancing capacitor at high frequencies.

The bridge, guard, and decade resistor were mounted in a closed rack (Imhof's). The air in the enclosure was thermostatically heated, and circulated by a small fan. The temperature was held at 30 $\pm$ 0.1°C to protect the standard resistors and capacitors from changes in atmospheric temperature and humidity.

Sinusoidal a.c. was supplied from a Muirhead Type K-126-A Decade Oscillator (1 Hz - 222 KHz) to points A and C, via the built-in screened transformer (not shown in Fig.19). The rms voltage across the cell was maintained at 0.1 volt, (see below), but it was found that the bridge balance point was unaffected when this was reduced to 1 mV.

A frequency selective detector was connected across the points B and D, as shown in Fig.20. In the early work,

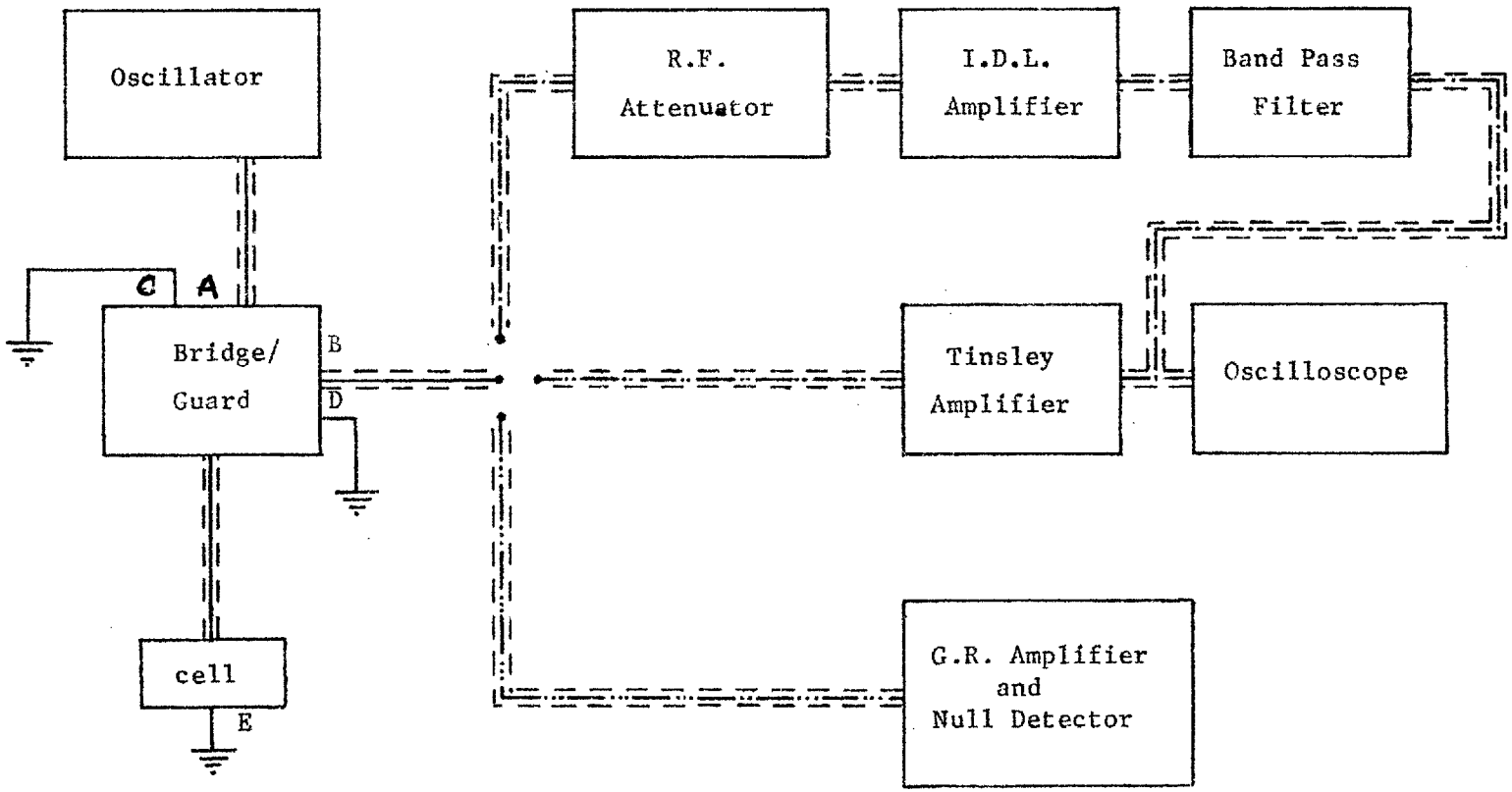


The Return Connections (via Earth) are not Shown.

Figure 20: The Bridge Equipment.

a Tinsley 5212-M Tuned Amplifier was used at frequencies below 10 KHz. Above this, a Dytronics 718 Band Pass Filter was used in conjunction with a Wide Band Amplifier (Isotopes Development, Type 652), and a Marconi Type T.F.1073A Attenuator. The out-of-balance signal was viewed in both cases on an Oscilloscope (Telequipment Type S.43). In the later work, the bridge output was detected by a General Radio Type 1232 A Tuned Amplifier and Null Detector (20 Hz - 20 KHz, 50 KHz, 100 KHz). This instrument greatly improved the precision and reliability of measurements at low frequencies.

Assessment of Bridge Errors:

Resistance.

Effects liable to cause errors of the order of 0.05% in resistance measurements on this bridge have been examined previously [3]. These were : (1) absolute accuracies of resistance windings in $R_N$; (2) temperature coefficient of the resistance windings in $R_N$; (3) skin effects in the windings of $R_N$; (4) resistance of internal connections in $R_N$ (zero resistance); (5) dissipation in the cable insulation; (6) Joule heating in the electrolyte; (7) skin effect in the electrolyte; (8) dissipation in the cell walls; (9) resistance of leads and cables; (10) self induction in leads, cable, and cell; (11) dissipation in $C_N$; (12) dissipation in the stray capacitative residuals of $R_N$;

(13) dissipation in C'; (14) inductance in the bridge components and wiring; (15) dissipation in the stray coupling across the transformer; (16) matching of the ratio arm resistors; (17) sensitivity of detection.

Buckle and Tsaoussoglou [3] found that the absolute accuracy of the bridge was limited by (1), and was therefore $\pm$ 0.05%. In the present work, however, it was the precision that mattered, and as this was potentially better than $\pm$ 0.005%, certain effects liable to cause resistance errors of this order were re-assessed.

Regarding (1), experience showed that for the same resistance setting on the unit using different dial combinations, agreement was generally better than $\pm$ 0.1 ohm. Any chance of resistance variations in $R_N$ and in the bridge components, due to fluctuations in the ambient temperature, was eliminated by thermostatting the units.

In order to determine whether any significant dissipation occurred in the cable insulation, the guard and earth screens were connected together, and used as the guard. A further screen, which was earthed, was provided by twisting aluminium foil round the cable. No apparent difference could be detected between measurements on a carbon resistor using this and the normal cable. It was therefore concluded that (5) could be neglected in the present frequency range.

The effect of (8) was examined by measuring the

resistance of a cell of the usual construction but in which the capillary was replaced by a piece of solid silica rod. Electrical contact between the silica and the electrodes was made with molten potassium chloride. For several days after the cell had been placed in the furnace, it was found impossible to obtain reproducible resistance measurements, and it was suspected that the silica underwent an ageing process. Such an effect has been reported in glass [8-10] and attributed to inter-diffusion of cations between the glass and the melt. No appreciable dispersion of the capacitance of this cell was observed. The reproducible resistance is plotted against frequency in Fig.21. It is shown below that dissipation in the wall of the capillary becomes significant in the measurement of dispersion in molten salts at frequencies above 1.5 KHz.

The effects of (9) and (10) were also re-examined in the present work. A three terminal measurement of the resistance of the cable was made on a Wayne-Kerr Type B-221 Universal Bridge and Type Q.221 Low Impedance Adaptor with the core and the outer screen connected together in series. This was found to be 0.25 ohm, which would cause a cell of resistance 1000 ohms to read high by 0.025%. The combined self inductance of cable and cell was measured on the General Radio bridge by a difference method, and found to be $3.3 \pm 0.2$ μH. This did not affect dispersion measurements

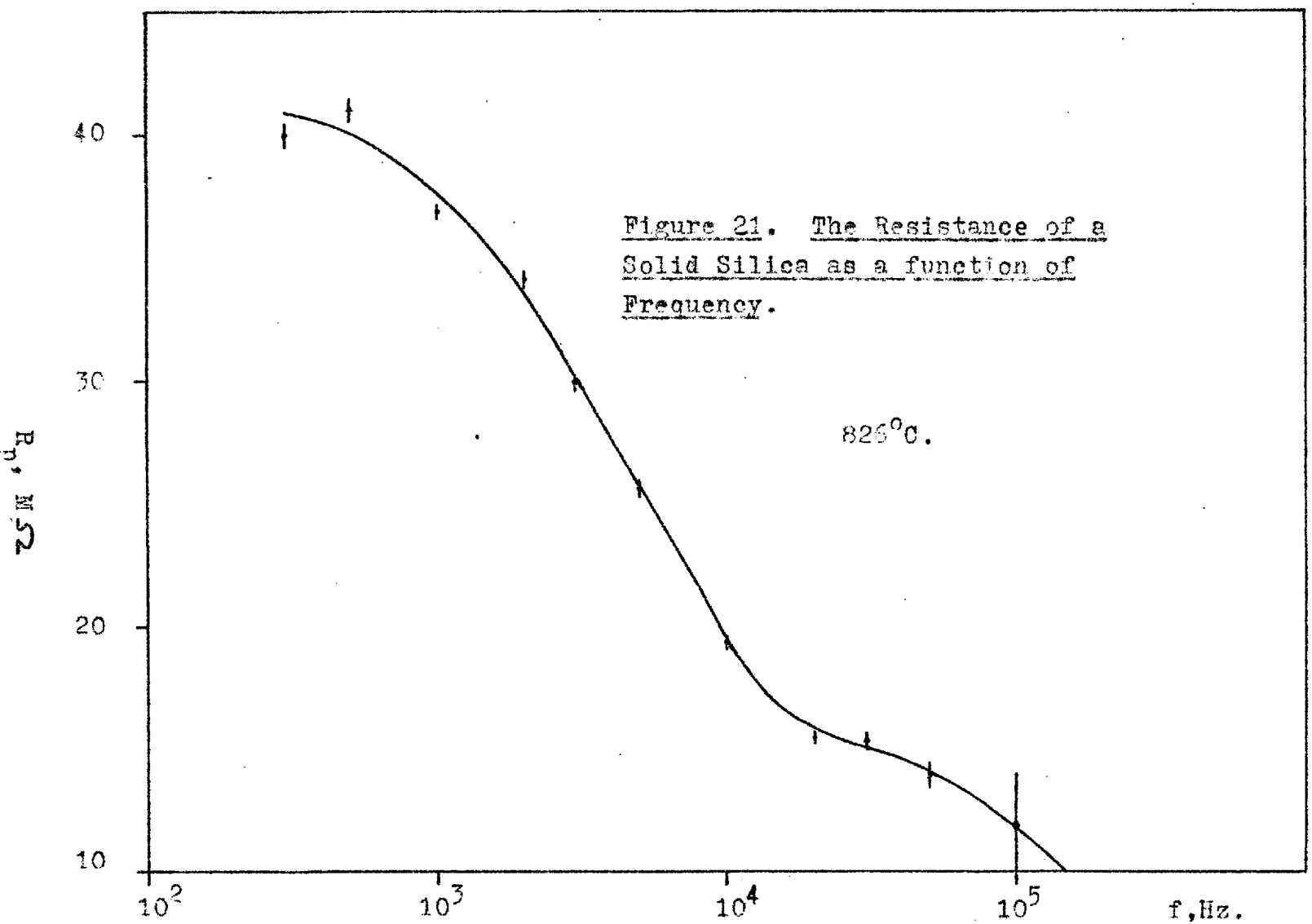


Figure 21. The Resistance of a Solid Silica as a function of Frequency.

in the present frequency range.

The possibility of dissipation in C' was examined by replacing this mica capacitor by a different one, and then by an air-spaced capacitor. No essential difference in dispersion was observed between runs on a carbon resistor at low frequencies. However, at high frequencies, the dispersion with the air-spaced capacitor was unexpectedly greater, presumably due to dissipation in the leads joining it to the bridge. There were, in effect, no leads to the mica capacitor, which was joined directly across the bridge terminals. This drew attention to the likelihood of dispersion troubles caused by all the other leads in the bridge assembly. In order to examine the effect of temperature on dissipation in the mica capacitor, the bridge was balanced and the capacitor heated with a warm air blast. On rebalancing, it was found that the resistance had changed, but not the capacitance. The effect was therefore caused by dielectric leakage. It was concluded that, although dissipation did occur in C', it was unlikely to vary significantly during the course of a run and thereby affect dispersion measurements in cells.

The manufacturer's claim that the ratio arms of the bridge (frequency ranges 10-300 Hz, 100-3000 Hz, 1-30 KHz, and 10-300 KHz) were matched to better than 0.1% was confirmed in the present work. However, when changing

range, measurements at the same frequency on both ranges were made. Any difference between the two values was noted, and by adjusting the readings on the lower range, discontinuity in the dispersion curves resulting from (16) was eliminated. As no information was available on the comparative accuracy of each pair of ratio arms, the choice to adjust the readings on the lower range was purely arbitrary.

A further effect examined in the present work was that of Joule heating in the components of the bridge. With a voltage input of 2 V the resistance of a carbon resistor increased slowly with time at frequencies above 20 KHz. This was attributed to Joule heating in the ratio arms and/or C', and was eliminated by reducing the input voltage to 0.1 V.

There was evidence to suppose that conduction in the vicinity of the capillary wall was influenced by the surface structure of the silica. Following the removal of a cell from the furnace, an increase of at least 0.03% in the melt resistance was observed. This was attributed to a change in the cell constant as a result of cracks developing in the devitrified silica on cooling it to room temperature.

The bridge was judged satisfactory for dispersion measurements on the grounds that the resistance of a carbon resistor, which was mounted in a thermally insulated General Radio Type 874-X Shielded Connector and joined to the bridge with the cable, was constant to within $\pm$ 0.1 ohm at

frequencies below 100 KHz.

Capacitance.

The following factors were considered in the assessment of the capacitance measurements (cf. ref.3): (1) the absolute accuracy of $C_N$; (2) detector sensitivity; (3) the effectiveness of the guard circuit; (4) residuals in the decades of $R_N$; (5) lead inductance; (6) terminal capacitance of the bridge; (7) stray reactance in $R_N$.

The manufacturer's data for (1) indicated that capacitance measurements by the direct method could be made to an accuracy of $\pm$ 0.1% or $\pm$ 0.8 pF. whichever was the greater. Thus, for a measured capacitance of 100 pF, the absolute accuracy was subject to an uncertainty of $\pm$ 0.8 pF, and for 1000 pF, $\pm$ 1 pF. However, in the present adaptation, the sensitivity of the bridge was far higher than this ($\pm$ 0.1 - 0.5 pF) at frequencies above 500 Hz. At lower frequencies, it fell off to about 1% ($\pm$ 10 pF) as the upper limit of $C_N$ was approached. Regarding (3), tests on the equipment showed that the guard circuit was perfectly effective in reducing earth admittances in the bridge network ($\sim$400 pF) to the level of (1).

Correction for the residuals in the decades of $R_N$ could be made using the manufacturer's data. From these, the values of $X_s/\omega$ for the particular dial settings was calculated, where $X_s$ is the series reactance of a dial.

The total series reactance of $R_N$ was then transformed into its equivalent parallel value, from which the effective parallel capacitance was calculated. This was not affected by frequency in the present range. When measuring low resistances, the reactance became inductive due to high settings on low resistance dials. Convergence of the bridge and guard balances under these conditions was slow due to abrupt changes in the parallel reactance of $R_N$.

The inductance of the cable ($L = 3.3 \pm 0.2$ μH) caused $C_N$ to read low by $(L/R_N^2) \times 10^6$ pF. For example, for a resistance of 1000 ohms, $C_N$ read low by 3.3 pF. The terminal capacitance of the bridge added a further 1.1 pF to the reading. It was observed during tests on carbon resistors that the capacitance reading was lower than the measured value of C'. This was attributed to the inductance of the carbon resistors and to capacitive strays in the decade box. These effects caused the capacitance to read low by 3.5 - 4 pF at 500 ohms, and 2 - 2.5 pF at 1000 ohms.

In order to calculate the absolute parallel capacitance of the cell, the value of C' had to be subtracted from the measured capacitance. In view of (7), an 'effective' value of C' equal to the 100 KHz capacitance reading was used for this purpose, since at this frequency the parallel capacitance of cells was essentially zero. The use of this difference method eliminated the error due to (6). The errors due to (5) and (7) were negligible when

high resistance cells (3000 ohms) were used. A correction could easily be made for (4), but in practice this was only significant if a 100, 1000, or 10,000 ohm dial setting was changed.

After making allowance for these factors, the accuracy of the capacitance measurements was limited only by (1). At high frequencies the precision was better than the absolute accuracy, but at low frequencies the reverse was true.

Frequency.

The accuracy of the frequency of the a.c. signal applied to the bridge was determined by the selectivity charactersitics of the oscillator and tuned detectors. Manufacturer's data claimed that the accuracy of the oscillator was $\pm$ 0.4% from 10-222 KHz, and $\pm$ 0.2% in the 50 Hz - 10 KHz range. The harmonic content was 0.1% up to 10 KHz, and still less than 1% at 220 KHz.

The absolute accuracies quoted for the tuned amplifiers and the band pass filter were naturally not as good as the figures given above for the oscillator. The equipment was usually tuned by setting the oscillator to the required frequency, and adjusting the frequency selector controls in the detector circuit for peak output with the guard selector switch at 'coupling'. When the fixed 50 and 100 KHz settings on the General Radio Type 1232A Tuned

Amplifier and Null Detector were used however, the frequency of the oscillator was adjusted for peak response.

EXPERIMENTAL PROCEDURE.

The molten salt was contained in a silica crucible, 100 mm in length and 23 mm i.d., which fitted inside a graphite crucible of the same length and of 2 mm wall thickness. The purpose of the graphite crucible was to aid uniformity of temperature in the melt, and to preserve the test tube (Fig.22). Before use, the graphite crucibles were degassed at a temperature greater than their working temperatures (1000°C), and stored in a desiccator. The melt container rested at the bottom of a silica test tube, 450 mm in length and 34 mm i.d. The top of this tube was covered with a sindanyo cap provided with holes through which the cell and thermocouple could be inserted. In order to blanket the melt and graphite from the atmosphere, argon gas with less than 10 p.p.m. of oxygen, was admitted through a side-arm near the top of the test tube. The flow of gas, regulated with a needle valve, was adjusted to a suitable value using a silicone oil manometer. The gas had been previously dried by passing it through a column packed with silica gel and anhydrone.

At the start of an experiment, the crucible was filled about three-quarters full with dried salt (35 $cm^3$), placed in the test tube, and blanketed with argon. The

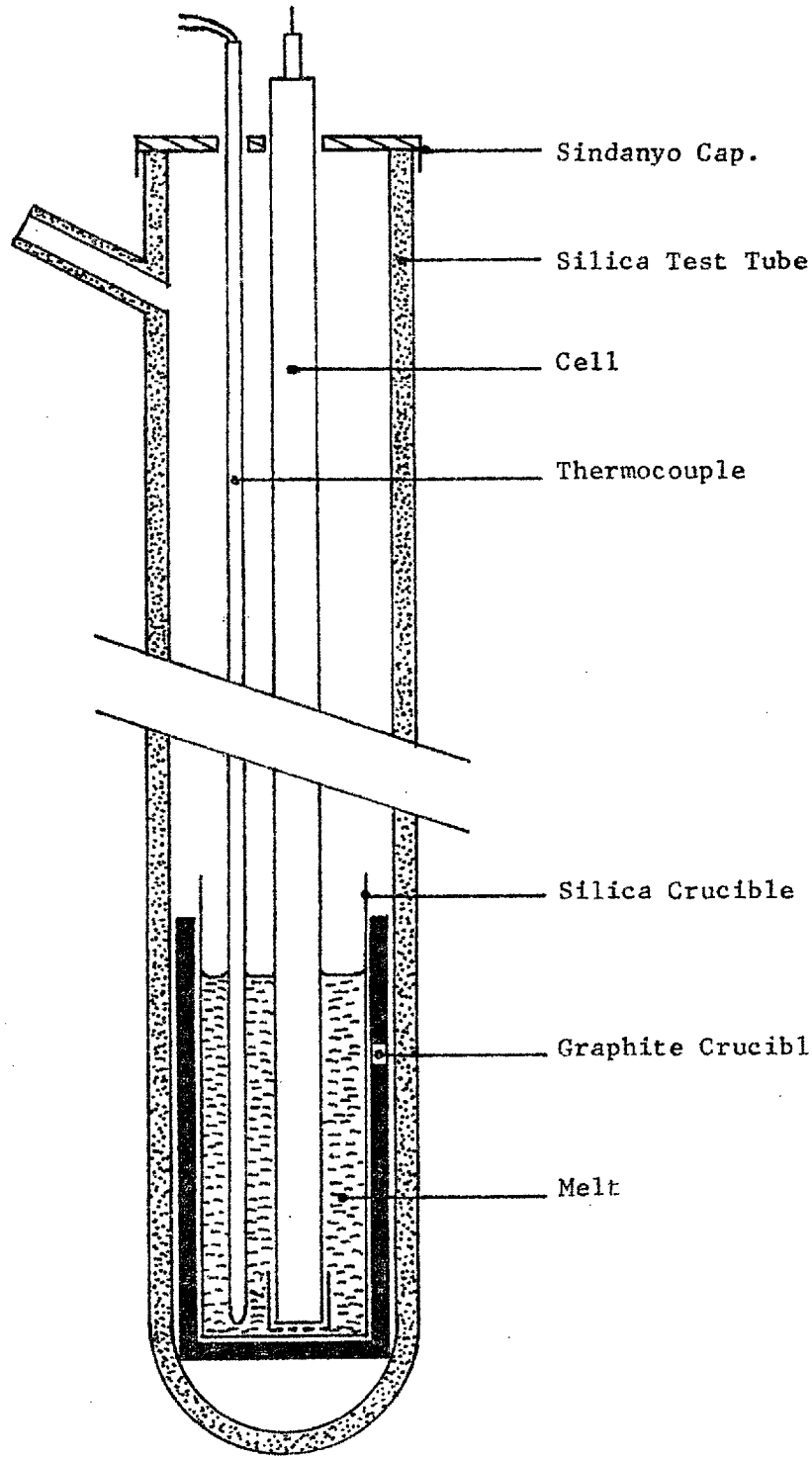


Figure 22: The Test Tube Assembly.

test tube was then gradually lowered into the furnace until the centre of the crucible was about level with the centre of the middle winding. Best uniformity of temperature in the melt could be obtained with the test tube in this position. The apparatus was left to equilibrate for about 12 hours. The cell and thermocouple were then lowered into the test tube and held for about 5 minutes above the crucible to avoid solidifcation of the melt on immersion.

Resistance measurements could not be usefully commenced until the temperature of the apparatus had reached a steady value ($\pm$ 0.1$^{o}$C). This normally took 2-3 days from the time the test tube was placed in the furnace.

At the start of a run, all switches and connectors in the bridge circuit were checked to ensure good electrical contact, and the melt was sucked over the inner electrode with a rubber bulb. During the run, the impedance measurements were repeatedly checked after temporarily displacing the melt in the capillary with dry argon. Agreement was considered satisfactory when successive readings agreed to within the experimental precision. At the end of each run the temperature distribution was checked by measuring the e.m.f. of the thermocouple at a number of levels in the melt. This was considered satisfactory if the uniformity was $\pm$ 0.1$^{o}$C. However, a less uniform distribution ($\pm$ 0.5$^{o}$C) was acceptable if the temperature

rose uniformly up the melt, as this gradient would tend to prevent convection.

On removing the cell from the furnace after a run, the melt was displaced from the capillary with argon. This prevented cracking caused by the salt solidifying in the capillary on cooling.

# RESULTS.

## AQUEOUS M.KCl SOLUTION.

Dispersion in M.KCl aq. is illustrated in Fig.23. Curves I and II [Fig.23(a)] respectively are typical of the dispersion observed in the resistance and capacitance of a silica cell (0.5 mm bore, 6 cm length, 33,000 ohms resistance) during calibration. Here the dispersion is extremely small, that of the capacitance becoming appreciable only at frequencies below 1 KHz. The steep rise in the resistance above 30 KHz is the result of limitations of the bridge in measuring high resistances[3] and may be neglected.

The double layer dispersion theory of Chapter 3 predicts that plots of $1/C_p$ against $\omega^2$ will be linear. It follows from Eqn. (3.55) that, provided $C_{p_o} \gg C_p$, in the frequency range studied plots of $f^2C_p$ against f should be linear and parallel to the frequency axis. This plot (curve V), for the narrow bore silica cell, is shown in Fig.24(a), together with the results for molten salts. Neither of the products $f^2C_p$ nor $f^{3/2}C_p$ are constant, and the trend of the results indicates that the capacitance might be proportional to a negative power of the frequency somewhat lower than 3/2. This behaviour shows that diffuse layer relaxation, if present at all, is masked by some other effect.

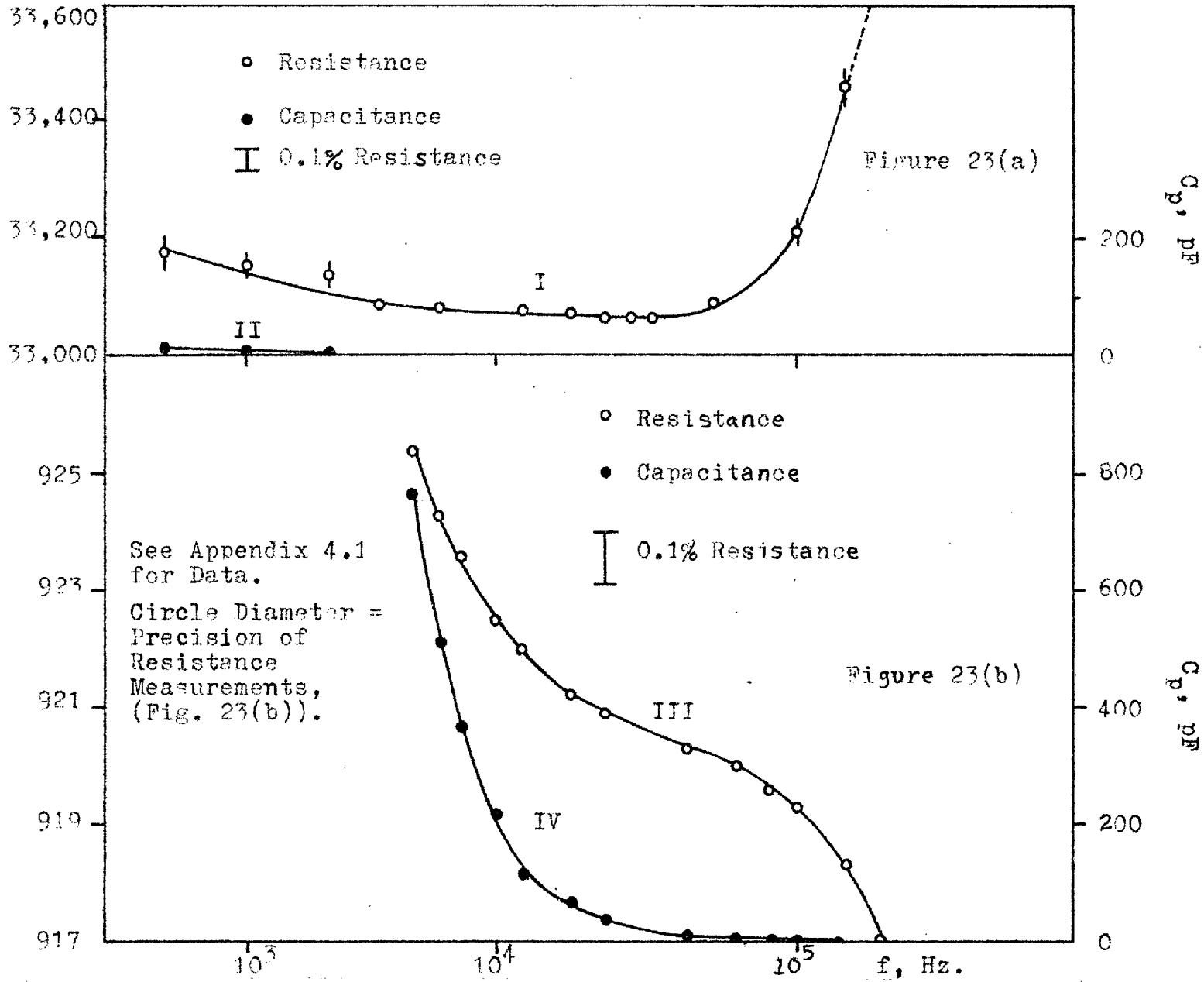


**Figure 23.** **Dispersion of KCl aq. in (a) 0.5 mm Bore Silica Cell and (b) 2.5 mm Bore Glass Cell.**

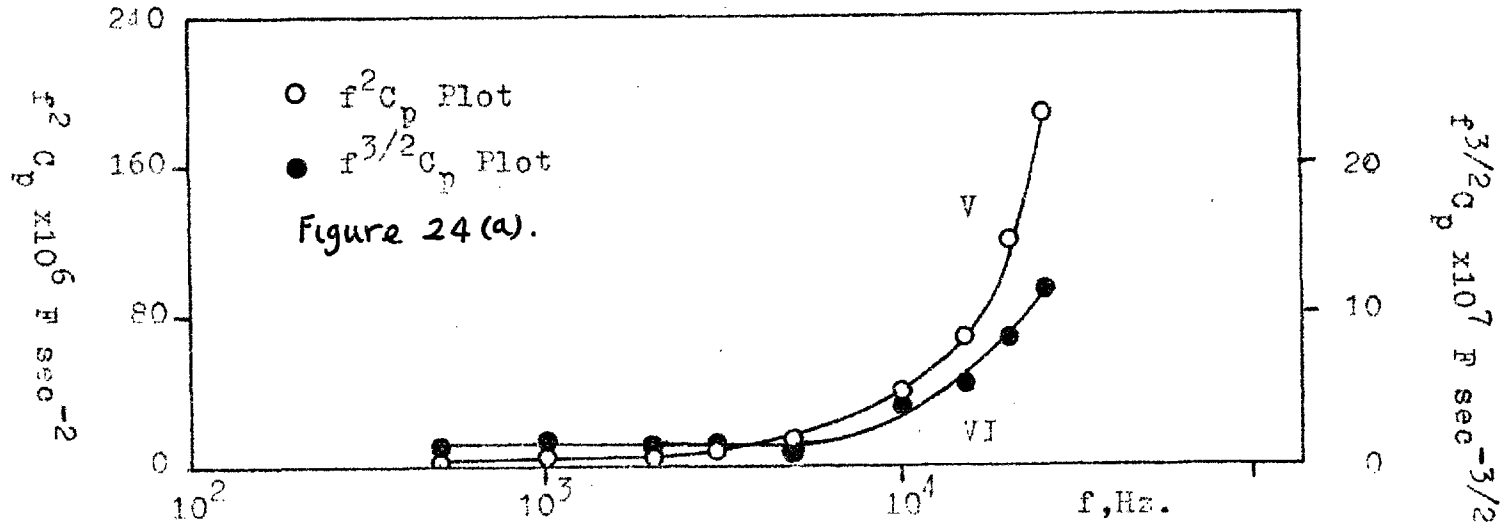


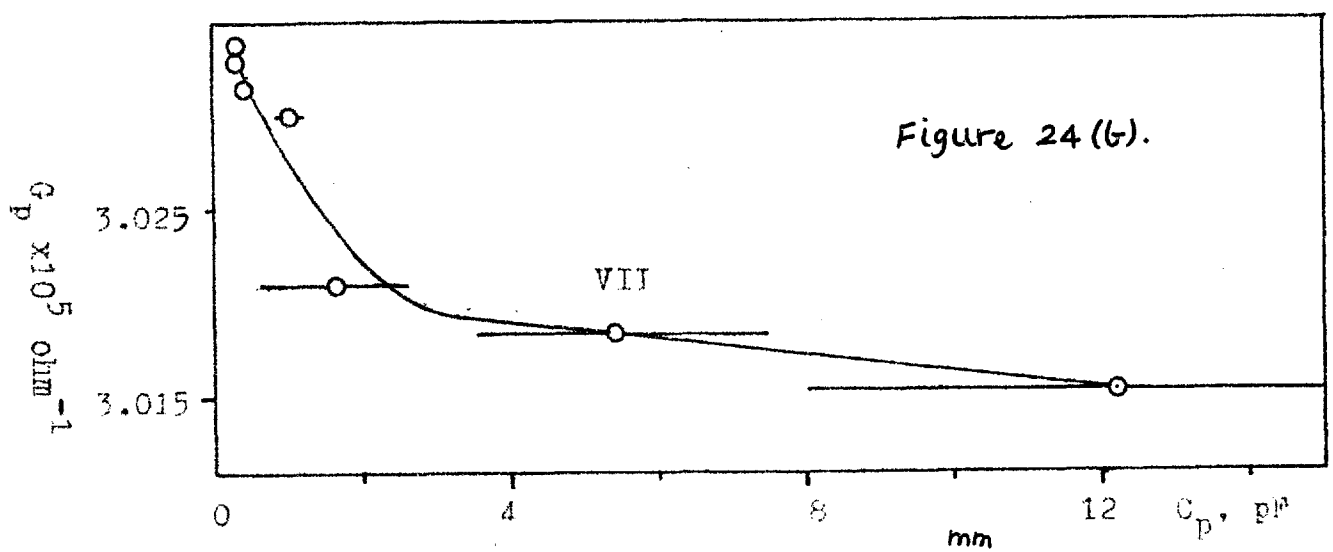


Figure 24. Dispersion in KCl aq. (0.5/Bore Silica Cell)
(a) Capacitance Plots, (b) Conductance-Capacitance Plot.

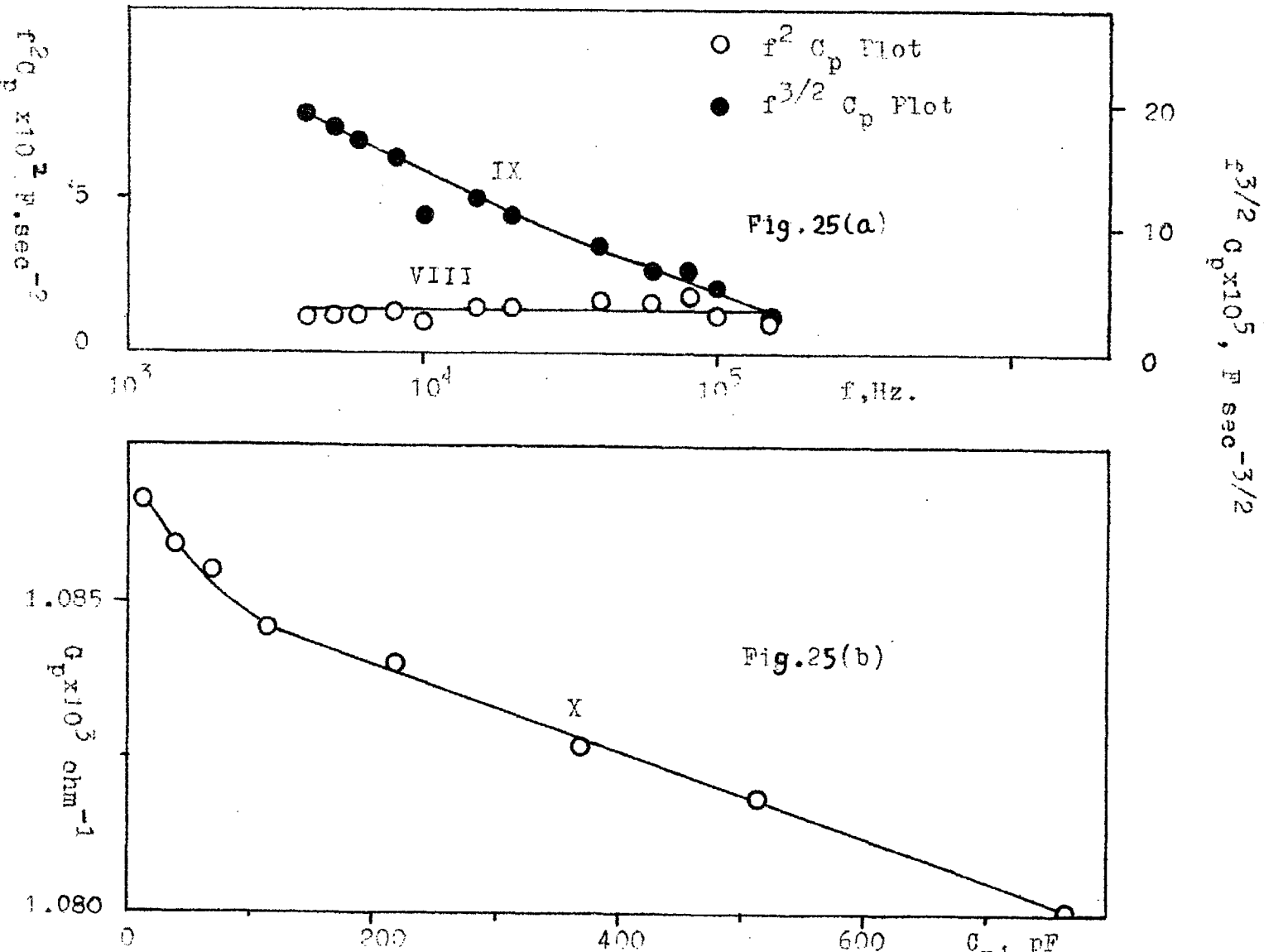


Figure 25. Dispersion in KCl aq. (2.5 mm Bore Glass Cell)
(a) Capacitance Plots, (b) Conductance-Capacitance Plot.

The conductance-capacitance plot for this run is shown in Fig.24(b), curve VII. It is possible that, to within the limits of experimental error, there is linearity between $G_p$ and $C_p$ below 2 KHz. However, calibration data for somewhat wider bore cells[11] showed that there was a curvature in the conductance-capacitance plots which became more marked the narrower the capillary bore. It follows that the linearity in curve VII is therefore spurious, and consequently that the value of any parameter calculated from its apparent slope would have little meaning.

In contrast to the behaviour described above, there is marked dispersion in both the resistance (III) and capacitance (IV), [Fig.23(b)], of a glass cell having a capillary diameter of 2.5 mm, a length of 6 cm, and a resistance of about 920 ohms, filled with the same solution. The $f^2C_p$ and $f^{3/2}C_p$ versus f plots are shown in Fig.25(a), (curves VIII and IX respectively). Here the product $f^2C_p$ is approximately constant and equal to $1.43 \times 10^{-2}$ F $sec^{-2}$. Thus, the product $\omega^2 C_p = C_{p_o}/\tau^2 = 0.565 \pm 0.1$ F $sec^{-2}$. The predicted linearity between $G_p$ and $C_p$ is apparent at frequencies below 1.5 KHz (Fig.25(b), curve X), although above this, curvature is again observed. The parameters derived from the linear region of the conductance-capacitance plot are: $\tau = (1.36 \pm 0.08) \times 10^{-4}$ sec., $C_{p_o} = 0.143 \pm 0.02$ μF, $\omega^2 C_p = C_{p_o}/\tau^2 = 0.80 \pm .18$ F $sec^{-2}$.

The values of $\omega^2 C_p$ obtained from the two plots are therefore in agreement within the limits of experimental error, and there is good agreement between the observed $\tau$ and the value ($\sim 10^{-4}$ sec) calculated from Eqn. (3.54) using typical values for the parameters (e.g., $\psi = \phi = 1$, s = 3 cm, $p_e = 6 \times 10^{20}$ cm$^3$, $U_p = 8 \times 10^{-4}$ cm$^2$volt$^{-1}$ sec$^{-1}$ (ref.12), $D_p = 2 \times 10^{-5}$ cm$^2$ sec$^{-1}$ (ref.12), and $\varepsilon_o = N^2 \varepsilon^o$, where N = 80 is the optical refractive index of water [13], and $\varepsilon^o$ is the permittivity of free space[14]).

It would therefore appear that diffuse layer relaxation was observed in this experiment below 1.5 KHz.

No attempt was made to evaluate the specific conductance of M.KCl aq. in these experiments. However, it is of interest to note that the apparent resistivity of the electrolyte measured in the narrow bore cell is about 31% higher than that measured in the wide bore cell. Since the absence of trapped air bubbles was confirmed by observation, it is probable that the discrepancy can be attributed to irregularity in the geometry at the ends of the capillaries, and to variations in their nominal bores.

## MOLTEN POTASSIUM CHLORIDE.

In the early part of this work, the equipment of Buckle and Tsaoussoglou [3] was to used to measure dispersion in molten KCl. In the light of further experience most of

this dispersion data was considered unreliable as such, due mainly to fluctuations in the furnace temperature.

The values of the specific conductance derived from these measurements are plotted against temperature in Fig.26. The results obtained from the resistance of the melt in the plateau region (see p.72) using newly made conductance cells are indicated by the shaded circles. These points show good agreement with the statistically reduced data of Van Artsdalen and Yaffe [15] (curve XI). Conductances obtained from measurements on cells which had previously been withdrawn from the furnace and then replaced are indicated by crosses, and, for a given temperature are smaller than those obtained with new cells. This difference could perhaps be attributed to a change in the cell constant due to devitrification followed by shattering or crazing of the capillary wall on cooling. Tsaoussoglou [16] obtained results for potassium chloride (curve XII) which were about 0.6% lower than those of Van Artsdalen and Yaffe. Since Tsaoussoglou did not suspect an effect from devitrification, it is possible that his results are too low. Conductance values obtained from the linear portions of conductance-capacitance plots in later experiments are indicated by open circles (curve XIII). These results lie between 1% (800°C) and 2.5% (950°C) below those of Van Artsdalen and Yaffe. A similar discrepancy

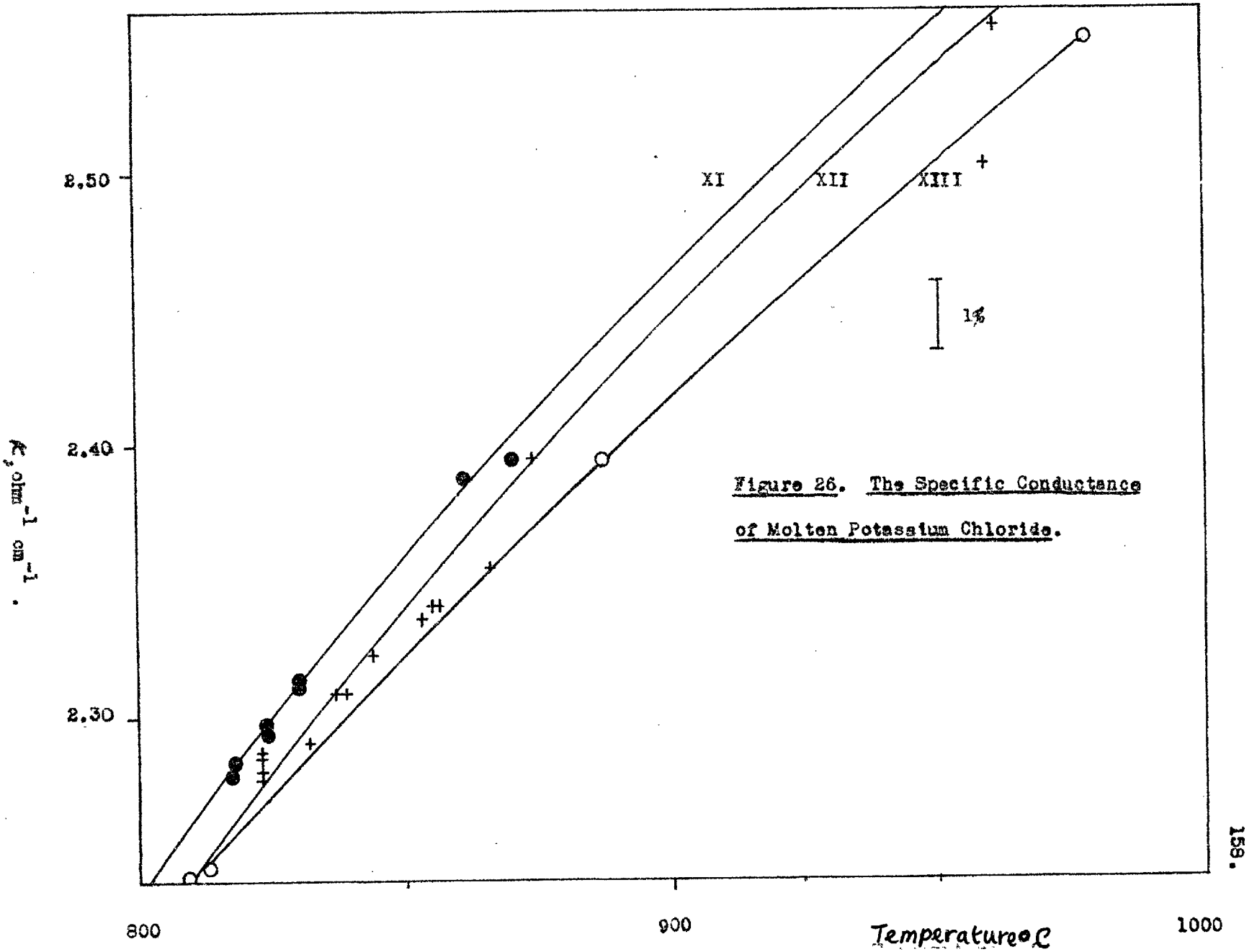


Figure 26. The Specific Conductance of Molten Potassium Chloride.

was reported by Buckle and Tsaoussoglou [3] between their results and those of Van Artsdalen and Yaffe [15] for molten KBr.

Winterhager and Werner [17] obtained values for $\alpha$ in various chloride melts which apparently showed a linear dependence on temperature. They claimed that this behaviour was only disclosed by the successful elimination of polarization from their work. On the other hand, Van Artsdalen and Yaffe attributed the curvature in their own plots to structural changes in the melt and analysed it in terms of the temperature-dependence of the heat of activation for conduction [15,18]. Deductions such as these are futile unless it can be shown that dispersion-free conductance values have been obtained. The curvature (or lack of it) in the specific conductance-temperature plots might be introduced simply through the use of the wrong dispersion formula [3].

DISPERSION.

The Effect of Additives.

A series of experiments was designed to show the effect of hydrolysis products, which may have been present in the untreated melts and possibly contributed to the dispersion [19]. No detectable changes in dispersion followed the addition of 0.05% potassium hydroxide to the

untreated melt. The influence of water content was then studied in a qualitative manner, using the apparatus described on p.112. The results obtained with a cell for which K = 5967 $cm^{-1}$ are shown in Figs. 27-29. Details of the experimental conditions are given in Table 4.2.

Table 4.2.

KCl Runs : Experimental Conditions.

| Run No. | Temp.°C. | A-HCl | A | A-$H_2O$ | Blanketing Gas |
|---|---|---|---|---|---|
| (1) | 809 | - | - | - | Dry Argon |
| (2) | 814 | 6 Hrs. | 1 Hr. | - | " " |
| (3) | 814 | 18 Hrs. | 1½Hrs. | - | " " |
| (4) | 814 | - | - | 16 Hrs. | A-$H_2O$ |
| (5) | 816 | - | - | 24 Hrs. | " |

The same sample of melt was used throughout these experiments, and the cell was removed from the furnace only after Run (1).

Figures 27 and 28(a) show the parallel resistance and capacitance of the cell plotted against frequency. The resistance plot for Run (1), (Fig.27, curve XIV), lies about 0.75% lower than the plots for Runs (2)-(5). This is not explicable by the temperature difference and, in

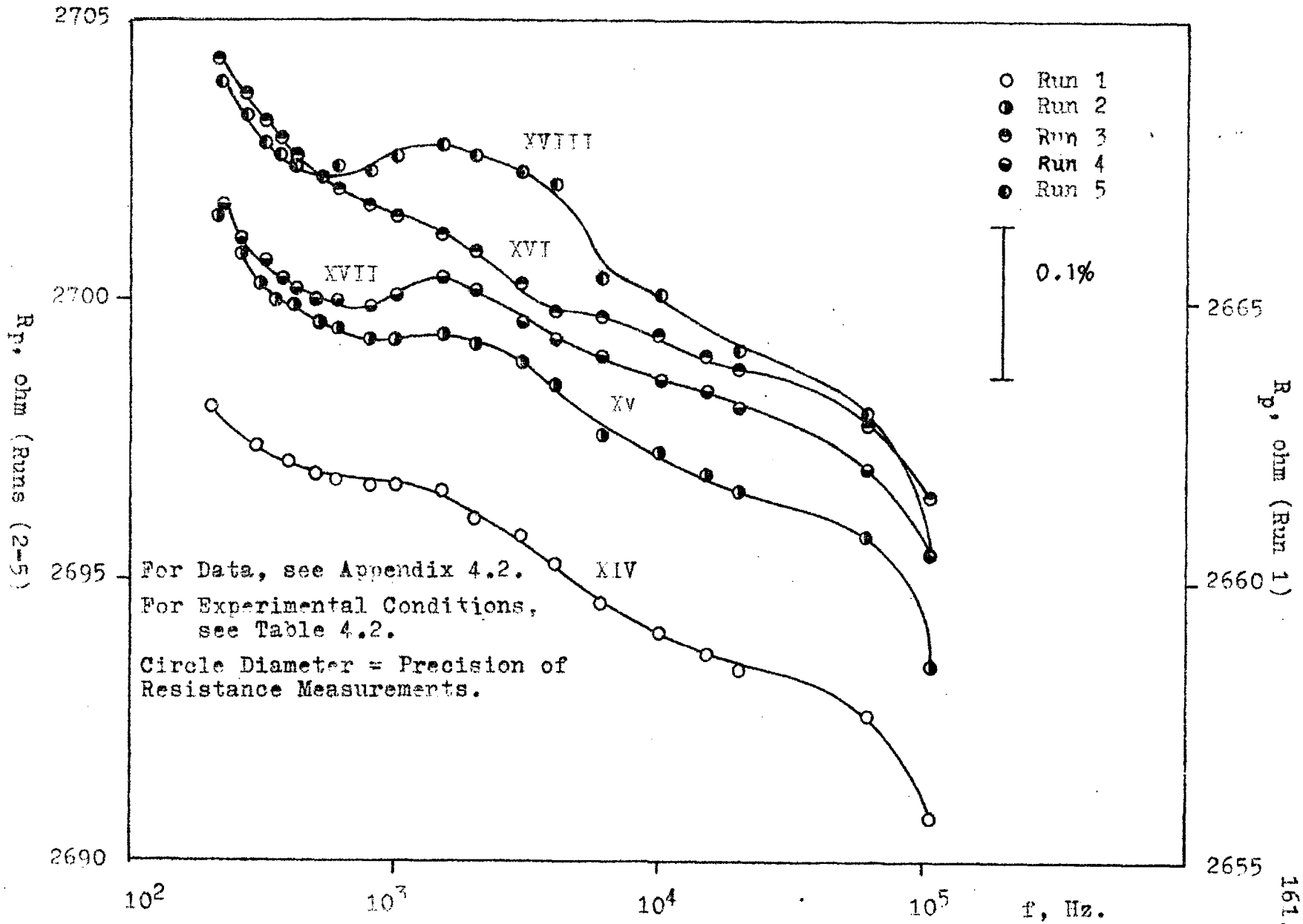


Figure 27. Potassium Chloride, Resistance Plots.

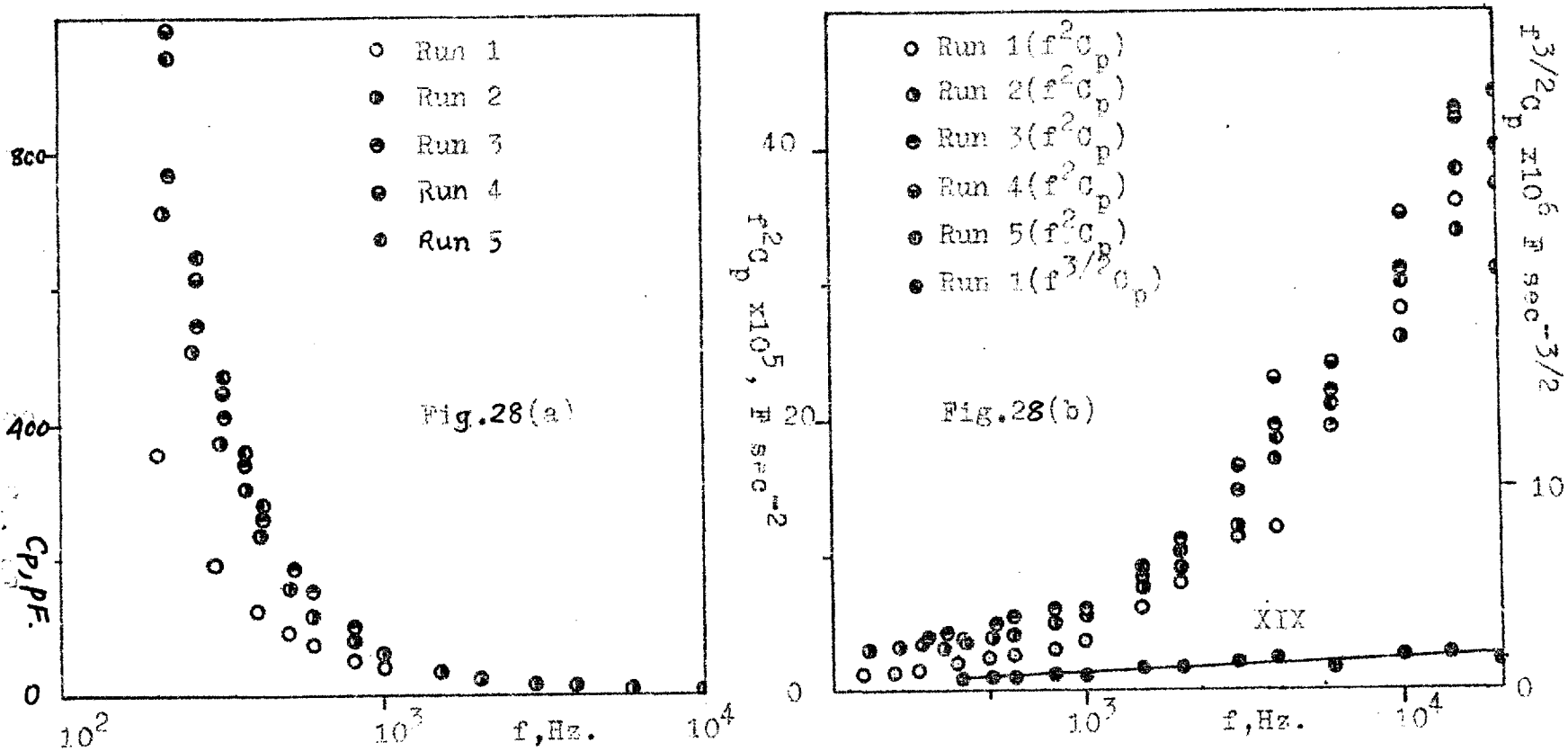


Figure 28. Potassium Chloride, Capacitance Plots.

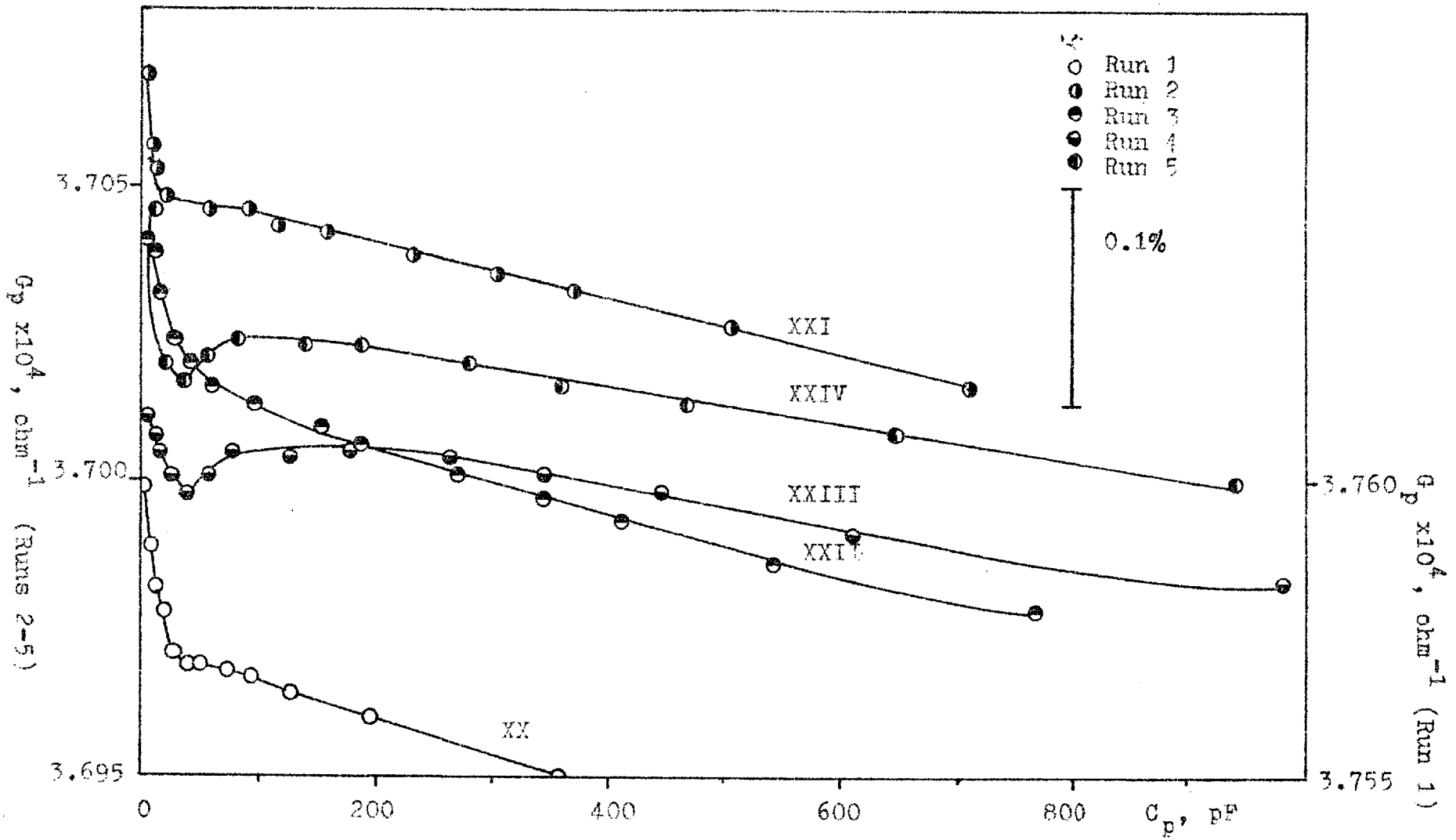


Figure 29. Potassium Chloride, Conductance-Capacitance Plots.

the light of the results for AgBr discussed below, the possibility that reaction of HCl with the melt is responsible for this increase is also discounted. The effect is therefore attributed to a change in the cell constant following the removal of the cell from the furnace after Run (1).

All curves except XVI have a distinct bump extending from 500 - 10,000 Hz. This disappears following the drying of the melt by bubbling the A-HCl gas mixture through it (curves XV and XVI). In curves XVII and XVIII, for melts which had been blanketed by water-saturated argon, the presence of the bump leads to a well-defined maximum at about 1500 Hz and a minimum at about 700 Hz. This behaviour appears to be characteristic of wet melts and it seems that some water was present in the untreated melt. Similar results were also observed in an additional run on water-saturated melt, carried out immediately following Run (1) and omitted from Figures 27-29 in the interests of clarity. Together with the absence of the minimum in curve XV, this indicates that the addition of water to the melt is reversible. If curve XVI is typical of a pure melt it shows that there is no plateau, and that dispersion persists throughout the experimental frequency range.

The capacitance results, [Fig.28(a)], are remarkably insensitive to the gassing conditions of the melt,

and show none of the inflections observable in the resistance plots. The values for Run(1) are, however, somewhat lower than those for Runs (2)-(5). This point is discussed below in the light of the results for AgBr.

As can be seen from Figure 28(b), the constancy of $f^2C_p$ predicted by the diffuse layer relaxation theory is not observed for molten KCl. Logarithmic plots of the parallel capacitance against frequency showed that $C_p$ is approximately proportional to $f^{-3/2}$ below 1 KHz, and that above this point the negative exponent decreases with increasing frequency. The $f^{3/2}C_p$ versus f plot for Run (1) is shown in Fig.28(b), curve XIX, and is approximately parallel to the frequency axis.

The plots of $G_p$ versus $C_p$ which, according to the theory of Chapter 3 should be linear, are shown in Fig.29. As can be seen, there is an excellent linear correlation between these quantities at low frequencies (high capacitances). However, above 1.5 KHz, marked curvature in the plots is observed, which is contributed to by dissipation in the walls of the silica capillary. Evidence for this is provided by the resistance-frequency curve for the solid silica cell shown in Fig.21, (p.141). At 1.5 KHz, the resistance of this cell is approximately 35 MΩ, and is falling rapidly with increasing frequency, presumably as a result of some relaxation process in the

silica. At the level of precision in the present runs, ($\pm$ 0.1 in 2700 ohms), the resistance of the parallel conducting path provided by the silica is sufficiently low to cause deviation from linearity in these plots. The linear region is extended to higher frequencies in the presence of traces of water (Fig.29, curves XXI and XXII). Curves XXIII and XXIV for the humidified melt exhibit minima at 1.5 KHz. The gradients of the linear portions of these curves are smaller than those of the other runs, and it is apparent that the influence of the effect which gives rise to the minimum extends into the low frequency region where the water content is relatively high. The values of the parameters calculated from the slopes and extrapolated intercepts of the linear portions of the curves of Fig.29, and of $k_\infty$ calculated from the "plateau resistances" at 10 KHz (Fig.27) are given in Table 4.3.

Table 4.3.

KCl Runs : Derived Parameters.

| Run No* | $\tau \times 10^3$ (sec.) | $C_{p_o}$ ($\mu$F) | $G_{p_\infty} \times 10^4$ ($ohm^{-1}$) | $\kappa_\infty$ ($ohm^{-1}cm^{-1}$) | $\kappa_{ad}$(plateau) ($ohm^{-1}cm^{-1}$) |
|---|---|---|---|---|---|
| (1) | 1.59±.11 | 0.589±.041 | 3.7572±.0001 | 2.242±.001 | 2.244±.001 |
| (2) | 2.13±.15 | 0.789±.055 | 3.7050±.0001 | 2.211±.001 | 2.212±.001 |
| (3) | 1.85±.13 | 0.685±.048 | 3.7016±.0001 | 2.209±.001 | 2.210±.001 |
| (4) | 2.93±.20 | 1.084±.076 | 3.7014±.0001 | 2.208±.001 | 2.210±.001 |
| (5) | 2.79±.20 | 1.035±.072 | 3.7029±.0001 | 2.209±.001 | 2.210±.001 |

* See Table 4.2 for experimental conditions.

The value of $\tau$ calculated from Eqn. (3.54) using typical macroscopic data for molten salts ($\psi = \phi = 1$, S = 3 cm., $U_p \sim \kappa/e\ p_e = 3 \times 10^{-4}$ $cm^2$ $volt^{-1}$ $sec^{-1}$, $D_p = 1 \times 10^{-4}$ $cm^2$ $sec^{-1}$ (ref.19), and $\varepsilon_o = N^2 \varepsilon^o$ where N = 1.5 (ref.20)) is of the order $10^{-5}$ sec in the present cells. The experimental value of $\tau$ is therefore 50-100 times larger than that calculated from theory. Discussion of this discrepancy is deferred until later.

The Effect of Temperature.

An attempt was made to investigate the temperature dependence of dispersion in untreated KCl melt, using a single cell with K = 1412 $cm^{-1}$ (Runs (6)-(8), Figs. 30-32). The resistance-frequency plots (Fig.30) confirm the expected trend of specific conductance with temperature, and also the observation of Buckle and Tsaoussoglou [3] that the plateau region is flatter at higher temperatures. The capacitance results, which do not trend consistently with temperature, are remarkably similar for the three runs [Fig.31(a)]. The value of $C_p$ at a given frequency is considerably larger than the corresponding value for Runs (1)-(5), even though the same electrodes were used throughout. This increase in capacitance must therefore result from the use of a somewhat larger bore capillary (0.8 mm) in this cell.

Plots of $f^2C_p$ and $f^{3/2}C_p$ against f are shown in Fig.31(b). Neither of these products are constant even at low frequencies [cf. Fig.28(b)] and it would therefore appear that the capacitance depended on a power of frequency f between -3/2 and -2. Curvature in the conductance-capacitance plots (Fig.32) sets in at much lower frequencies than in the corresponding plot for Run (1), (cf. Fig.29, curve XX), but this might have resulted from fluctuations in the temperature of the melt (see Appendix

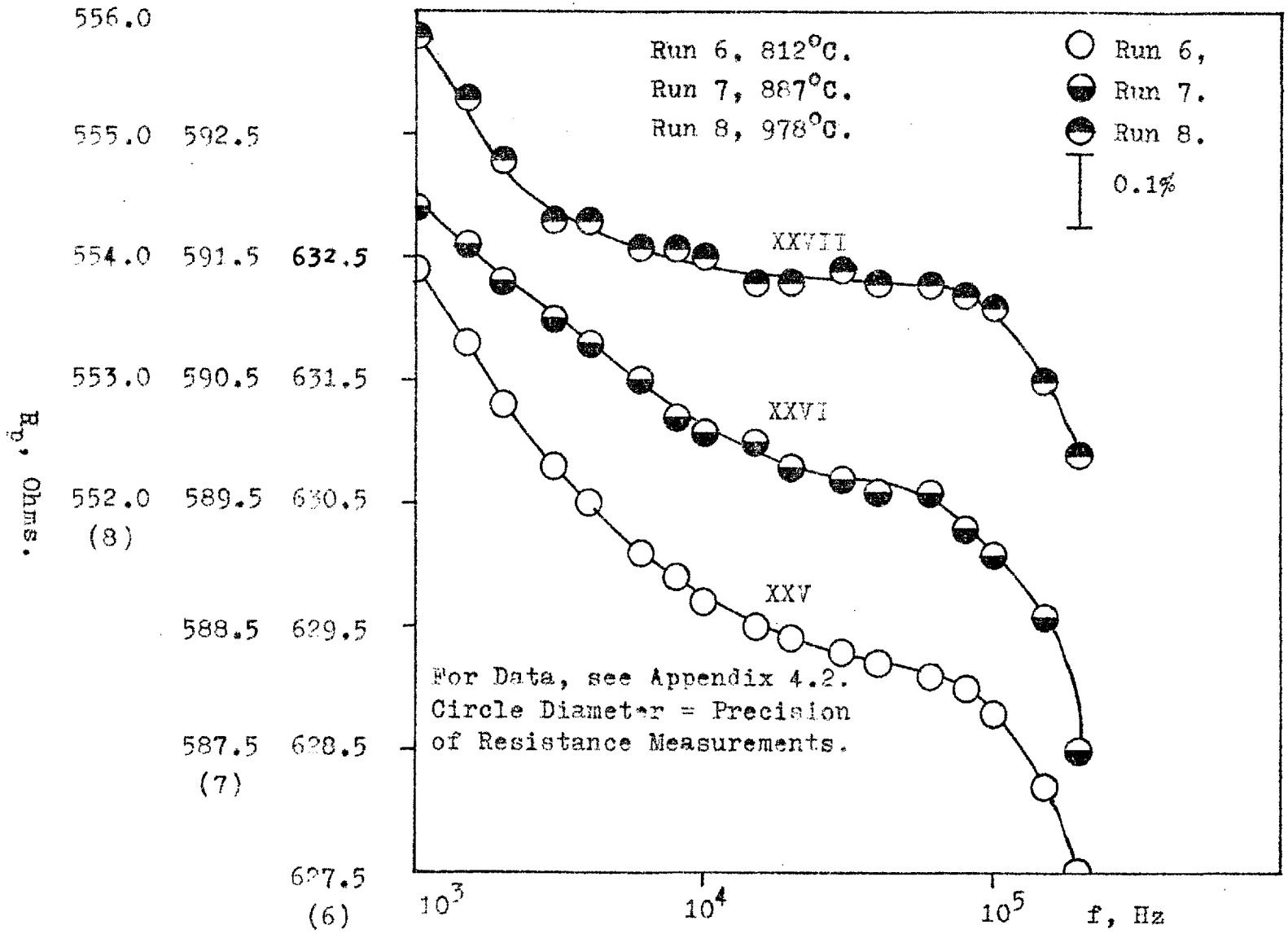


Figure 30. Potassium Chloride, Resistance Plots.

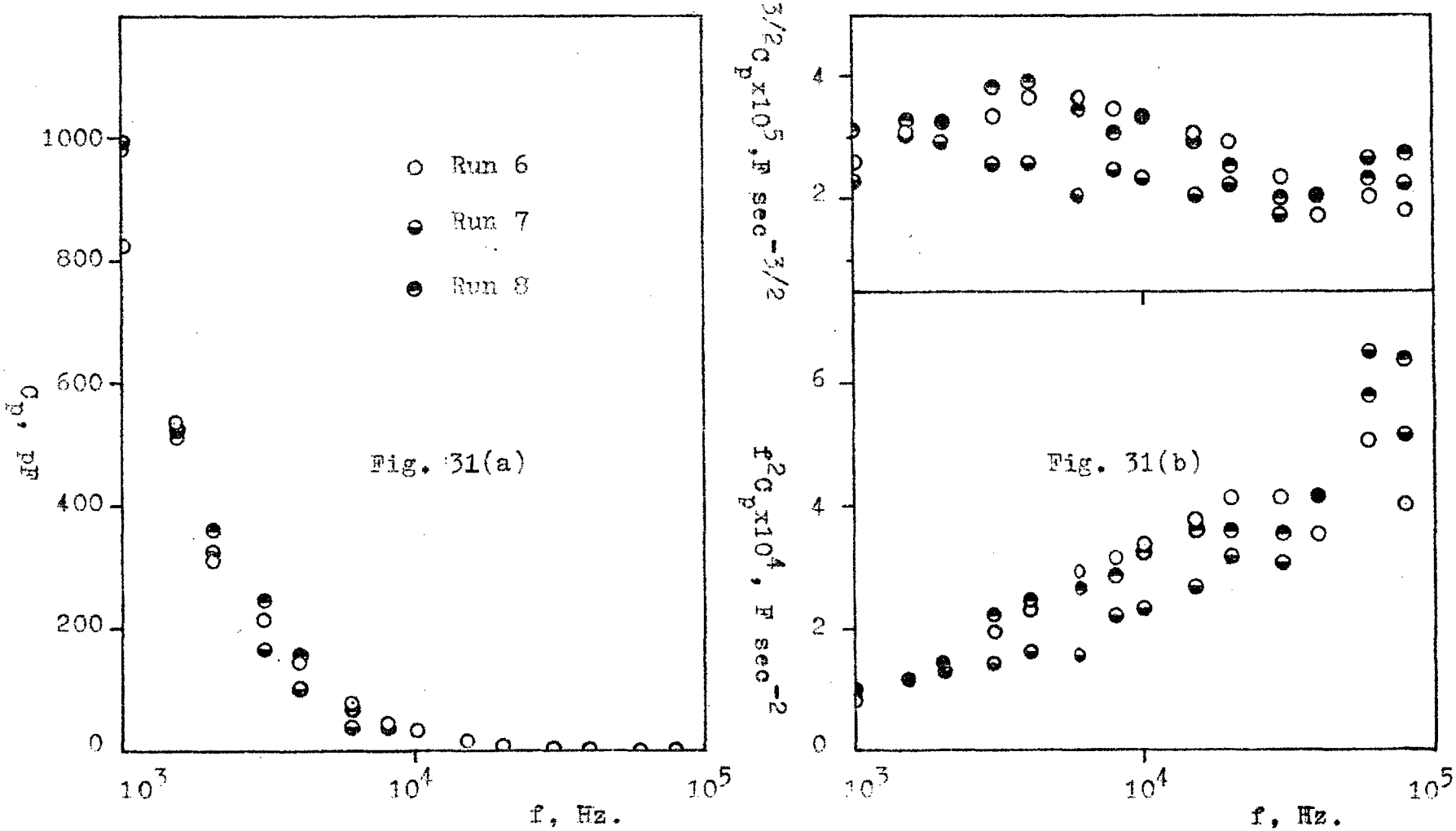


Figure 31. Potassium Chloride, Capacitance Plots.

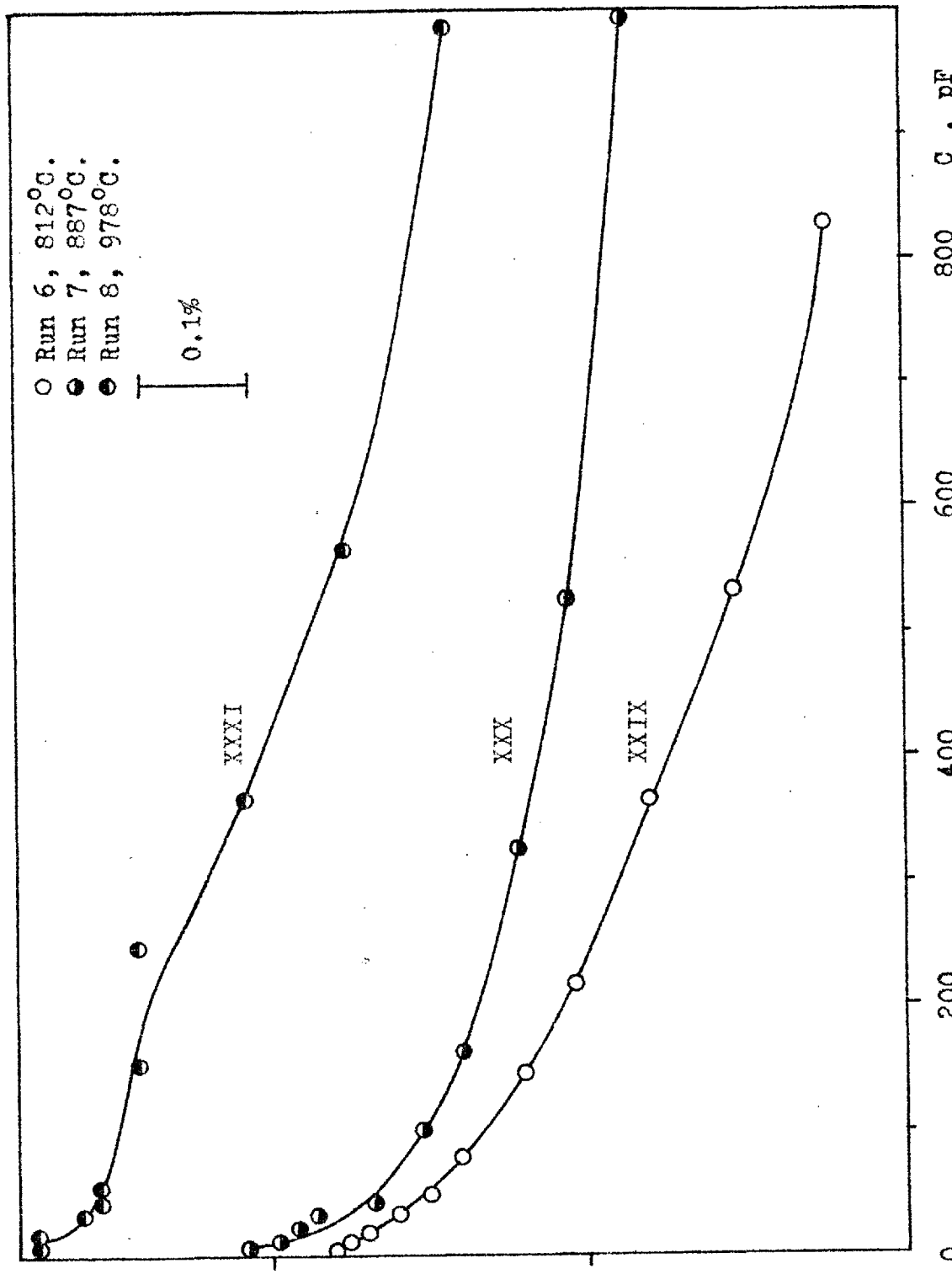


| | | | |
|---|---|---|---|
| Run 6 | 1.590 | 1.585 | 1.580 |
| Run 7 | 1.695 | 1.690 | 1.685 |
| Run 8 | 1.800 | 1.795 | 1.790 |

$G_p \times 10^4$, $ohm^{-1}$

Figure 32. Potassium Chloride, Conductance-Capacitance Plots.

4.2, pp. 205-207). The low frequency limiting slopes do not vary consistently with temperature, and consequently it is not possible to determine the temperature dependence of $\tau$.

However, Fig.30 shows that the dispersion region, and hence $1/\tau$, falls to lower frequencies as the temperature is increased.

Dogonadze and Chizmadzhev [21] assumed that the distribution of charge in a molten salt is of the damped oscillation type, and that alternate layers of oppositely charged ions correspond to this distribution. They obtained an expression showing that $C_{p_o}$ decreased with increasing temperature, and attributed this to a fall in the short range order correlation length and a consequent increase in the blurring of this distribution. However, they were unable to calculate the temperature dependence, and their value of $C_{p_o}$ was somewhat lower than the value of 40 $\mu F/cm^2$ quoted as typical for molten salts.

## MOLTEN SILVER BROMIDE.

A series of experiments (Table 4.4) were carried out on molten KBr, using a cell for which K = 6479 $cm^{-1}$. This cell remained in the furnace throughout, and rapid devitrification damage due to cooling to room temperature was thus avoided.

Table 4.4.

AgBr Runs : Experimental Conditions.

| Run No. | Temp.°C* | A-HCl | A | A-$H_2O$ | Blanketing Gas |
|---|---|---|---|---|---|
| (1) | 733 | - | - | - | Dry Argon |
| (2) | 735 | 12 Hrs. | 2 Hrs. | - | " " |
| (3) | 734 | 3 Hrs. | - | - | A-HCl |
| (4) | 733 | - | 2 Hrs. | - | Dry Argon |
| (5) | 733 | - | - | 18 Hrs. | A-$H_2O$ |

* Three different thermocouples were used for Run (1), (2) and (3), (4) and (5).

The use of HCl might have caused some decomposition of the melt, e.g.,

$$AgBr + HCl \rightleftharpoons AgCl + HBr$$

It was not possible to test the feasibility of this reaction due to the lack of thermodynamic data.

The parallel resistance and capacitance are plotted against frequency in Figs. 33 and 34(a). The relative dispersion of the resistance in all runs except No.3 (curve XXXIV) is strikingly less than that for the KCl runs shown in Fig.27, even though the KCl temperature was 80°C higher. This confirms the observations of Winterhager and Werner [17], and of Buckle and Tsaoussoglou [3] that dispersion is low in univalent heavy metal halide melts. The difference in the positioning of the resistance curves in Fig.33 is probably due simply to small differences in temperature between the runs. As in potassium chloride, the plateau for the run on the water saturated melt (curve XXXVI) is flatter than those for the untreated (curve XXII) and dried (curves XXXIII, XXXV) melts. The minimum is also observed at about 700 Hz, but there is no maximum at 1500 Hz.

The capacitance behaviour is similar in AgBr and KCl melts [cf. Figs. 28(a) with 34(a), 28(b) with 34(b)]. The difference between the curves for the treated and untreated melts may now be attributed to the addition of hydrogen chloride. Any possibility that the capacitance might have increased significantly following the removal of the cell from the furnace during the series of runs on KCl may be discounted in the light of the AgBr results. It is significant that the anomalous resistance behaviour observed

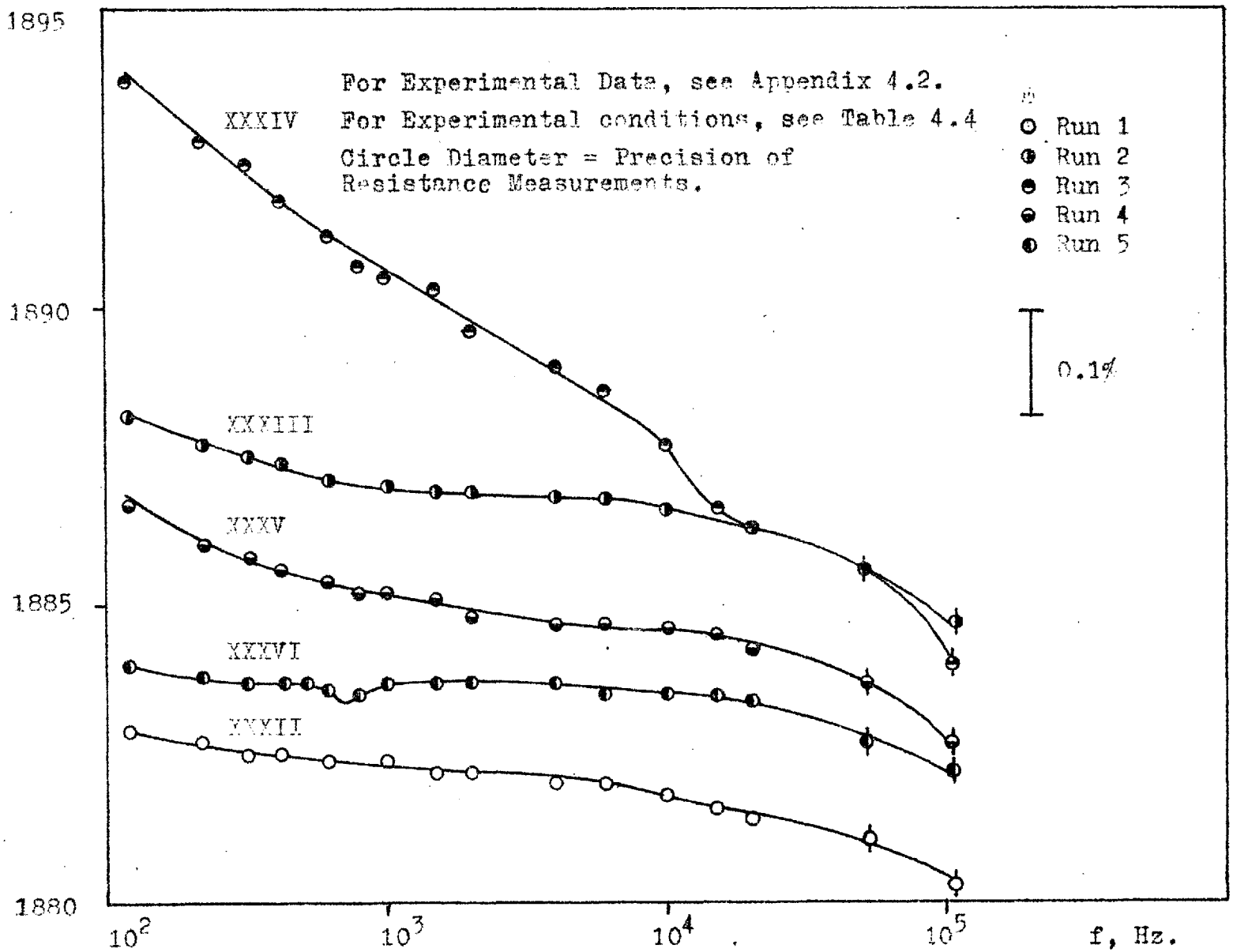


Figure 33. Silver Bromide, Resistance Plots.

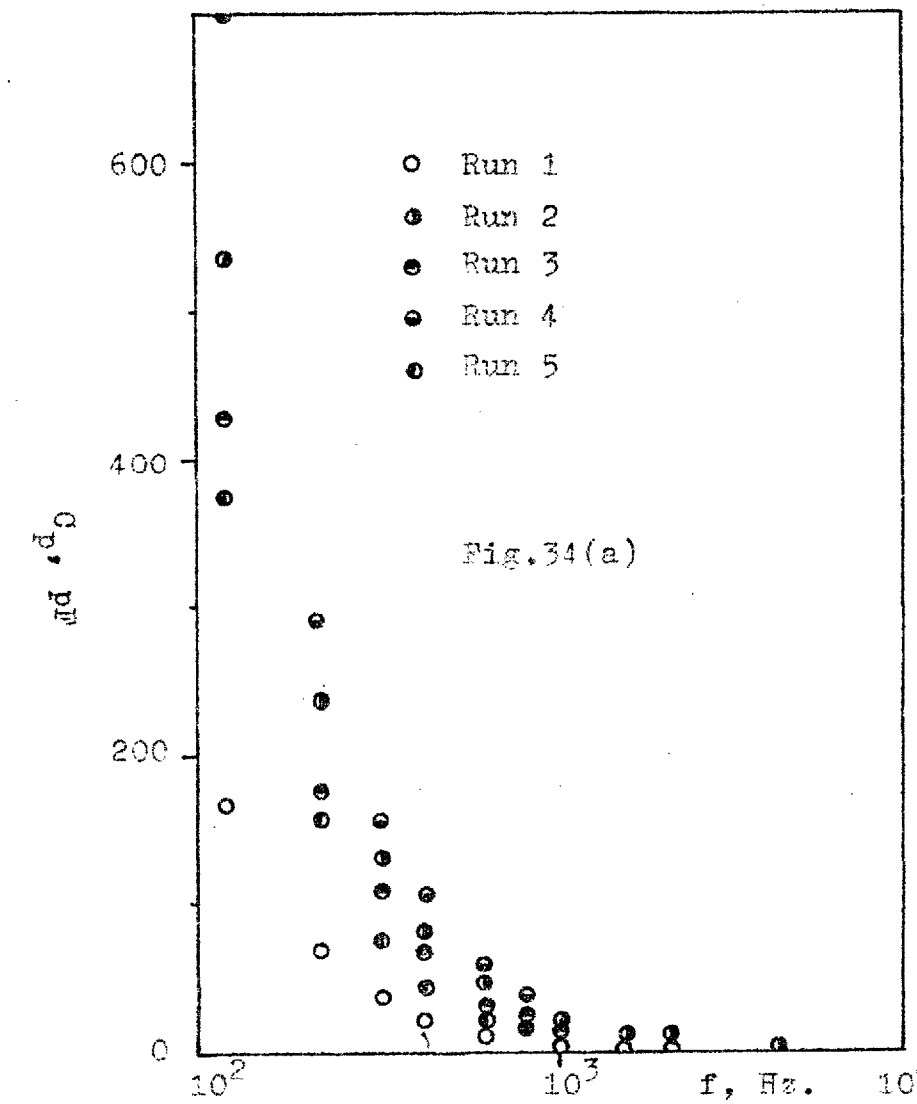


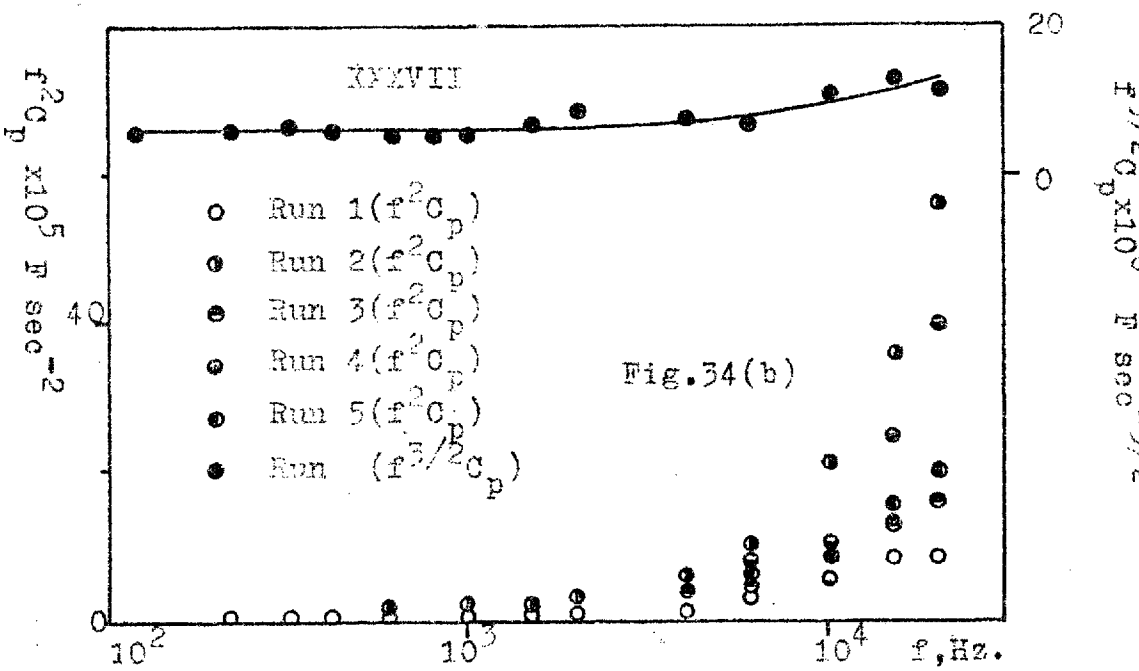


Figure 34. Silver Bromide, Capacitance Plots.

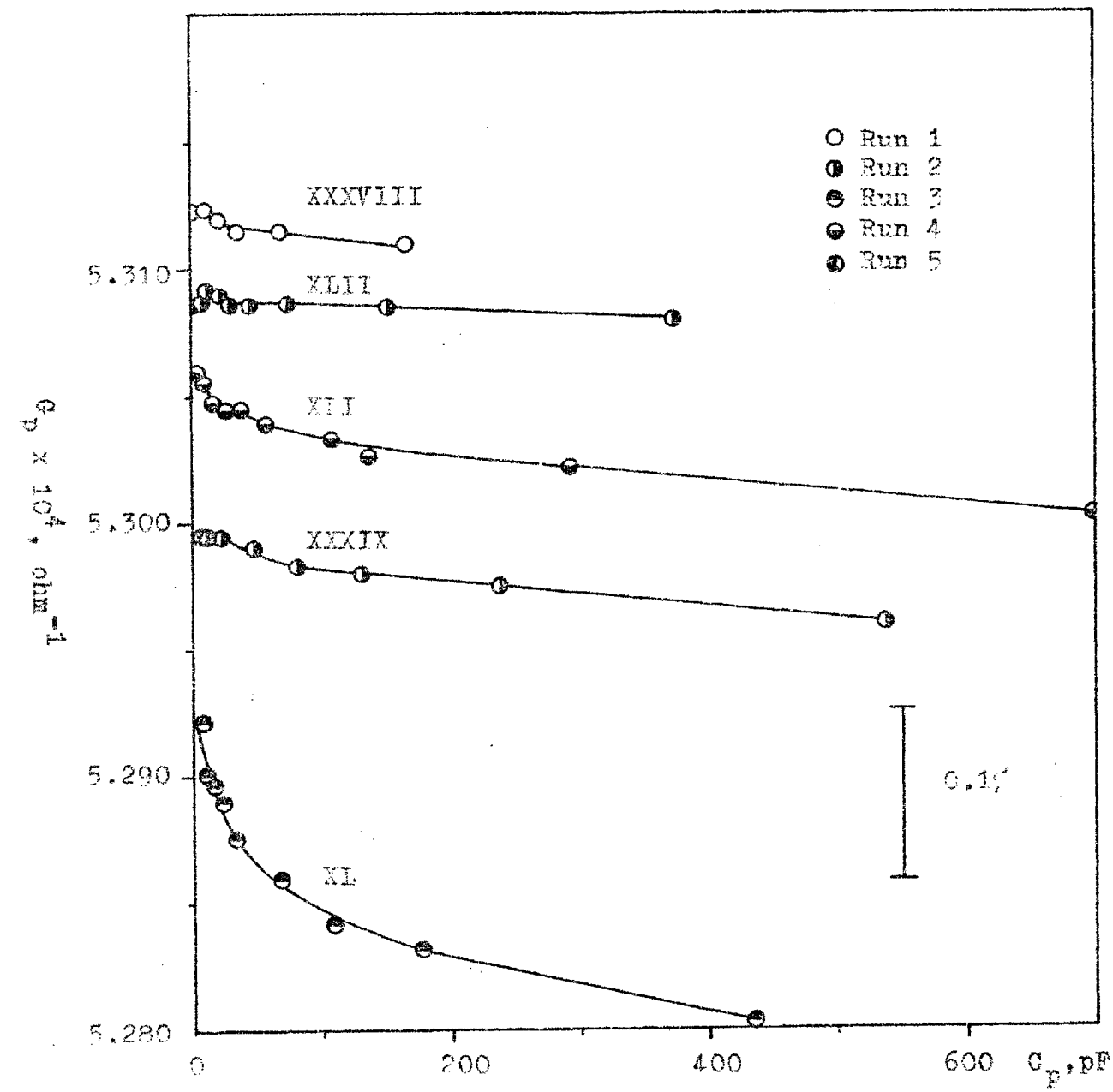


Figure 35. Silver Bromide, Conductance-Capacitance Plots

in Run (3), (Fig.33, curve XXXIV) is not reflected in the capacitance results (Fig.34(a)). The values of the capacitance in AgBr are considerably lower than those in KCl even though the electrode area was the same. Despite the somewhat greater scatter between runs, the approximate proportionality between $C_p$ and $f^{-3/2}$ is still observed, at least at low frequencies [Fig.34(b), curve XXXVII].

The conductance-capacitance curves for AgBr are shown in Fig.35. Those for Runs (1), (2), (4), and (5), curves XXXVIII, XXXIX, XLI, XLII) are not significantly different in shape from the corresponding ones for molten KCl (Fig.29). However, by comparison with the other curves for AgBr, that for Run (3), (Fig.34, curve XL), in which the melt was saturated with hydrogen chloride, shows marked curvature in the low frequency region. Values of $\tau$, $C_{p_0}$, $G_{p\infty}$, and $\kappa_\infty$, calculated from the present results are given in Table 4.5. The theoretical value of $\tau$ may be taken to be of the same order as that given for KCl on p.167, i.e. $10^{-5}$ sec.

Table 4.5.

AgBr Runs : Derived Parameters.

| Run No* | $\tau \times 10^3$ (sec.) | $C_{p_o}$ ($\mu$F) | $G_{p\infty} \times 10^4$ ($ohm^{-1}$) | $\kappa_\infty$ ($ohm^{-1}cm^{-1}$) | $\kappa_\infty$(plateau) ($ohm^{-1}cm^{-1}$) |
|---|---|---|---|---|---|
| (1) | 1.59±.41 | 0.845±.022 | 5.3119±.0003 | 3.442±.002 | 3.364±.002 |
| (2) | 2.07±.24 | 1.048±.012 | 5.2986±.0002 | 3.433±.002 | 3.433±.002 |
| (3) | 0.893±.103 | 0.471±.055 | 5.2850±.0002 | 3.424±.002 | 3.433±.002 |
| (4) | 1.94±.22 | 1.029±.119 | 5.3035±.0002 | 3.436±.002 | 3.436±.002 |
| (5) | 3.22±.38 | 1.762±.204 | 5.3087±.0002 | 3.440±.002 | 3.440±.002 |

* See Table 4.4 for experimental conditions.

Accurate specific conductance data for molten AgBr at this temperature appears to be lacking in previously published literature. However there is reasonable agreement between the present results and the value of $3.4_7$ $ohm^{-1}$ $cm^{-1}$ at 735°C obtained by linear interpolation of the results quoted by Klemm [19].

MOLTEN CADMIUM CHLORIDE.

Due to rapid devitrification of silica in the melt, only one run on $CdCl_2$ was achieved. The salt had been dried at 200°C for 24 hours prior to melting. The results of this run are shown in Fig.36. The relative dispersion

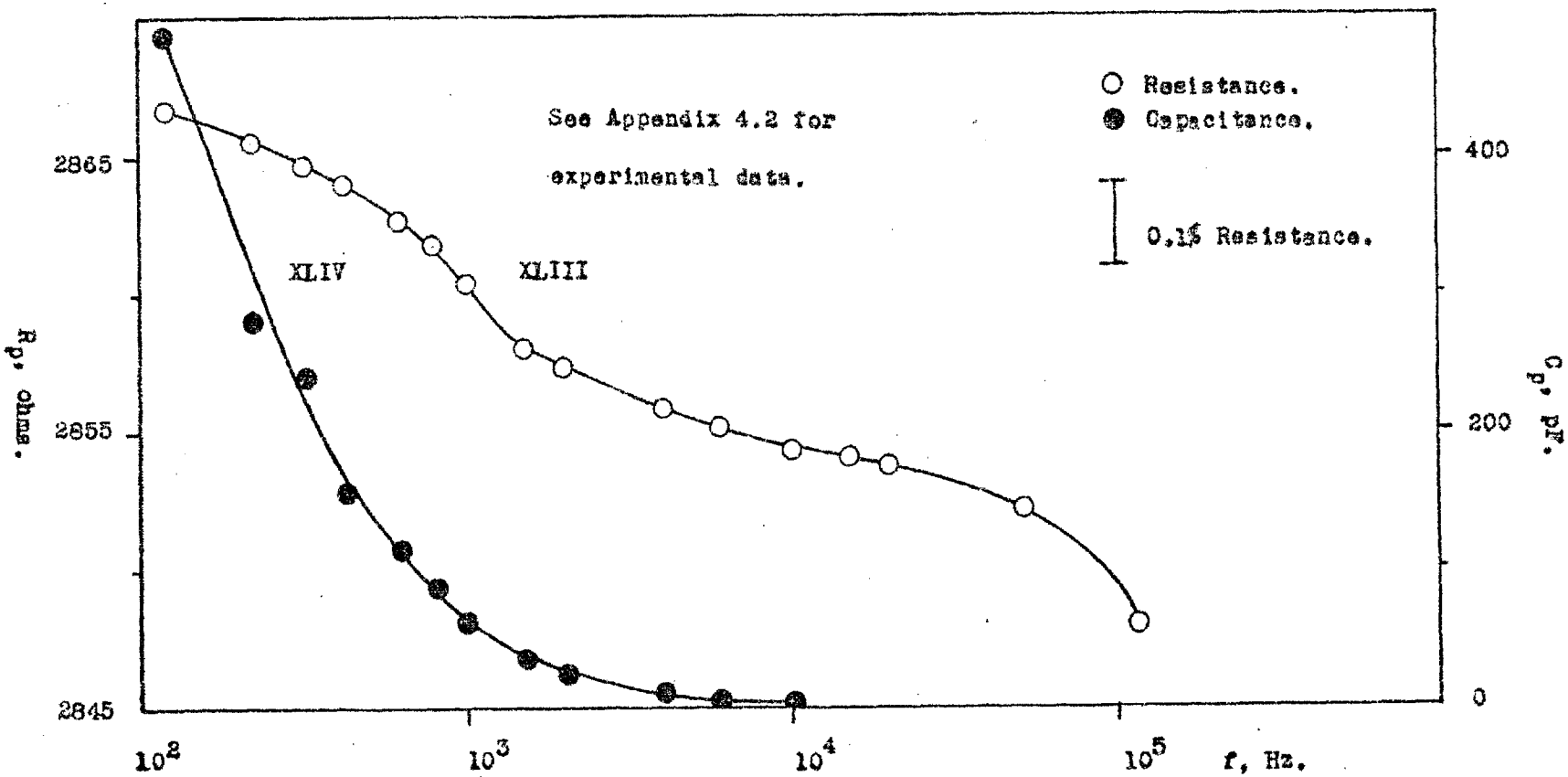


Figure 36. Cadmium Chloride, Resistance and Capacitance Plots.

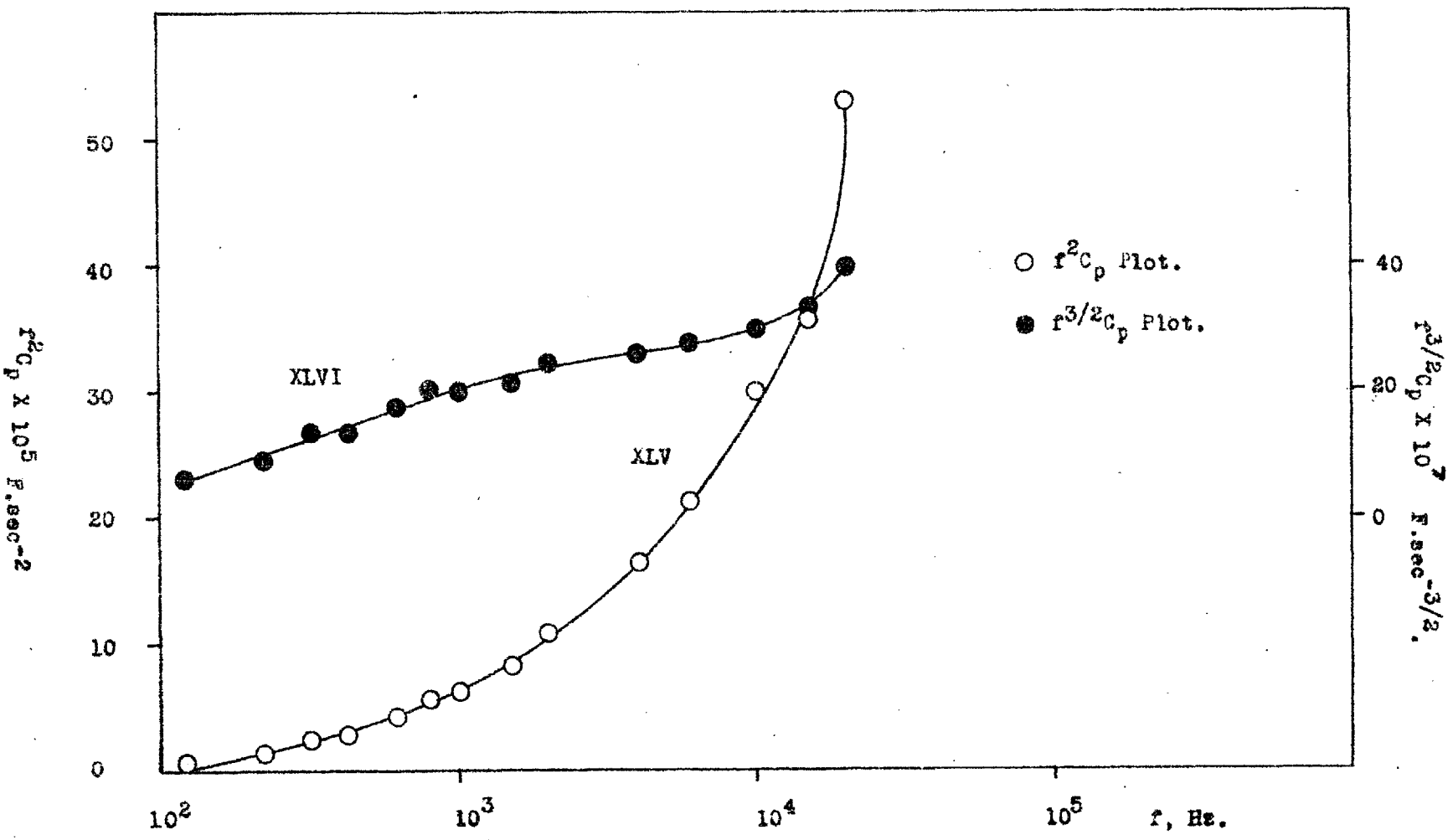


Figure 37. Cadmium Chloride, Capacitance Plots

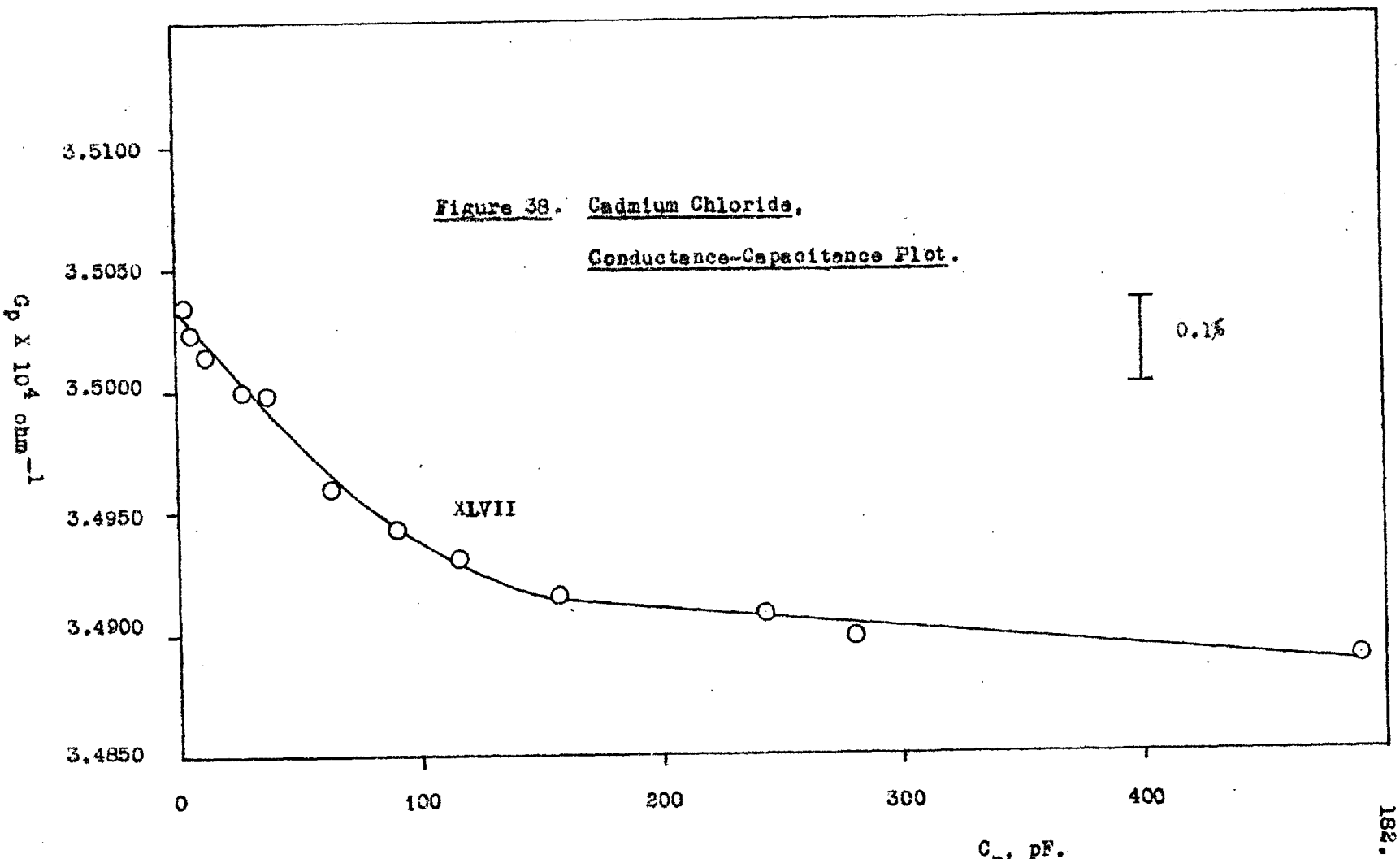


Figure 38. Cadmium Chloride,

Conductance-Capacitance Plot.

of both the resistance and capacitance of a cell for which $K = 6479\ cm^{-1}$ is larger than that observed for the untreated melts of KCl and AgBr. The resistance plot for $CdCl_2$ (Curve XLIII), unlike those for the KCl and AgBr melts, exhibits concave curvature towards the frequency axis. However, the capacitance values (Fig.36, Curve XLIV) show no such anomaly.

The $f^2C_p$ and $f^{3/2}C_p$ versus f plots (Curves XLV and XLVI respectively) are shown in Fig.37. Neither of these products are constant, and the trend of the results indicates that the capacitance depends on a negative power of frequency somewhat smaller than 3/2. The parameters derived from the linear region of the conductance-capacitance plot (Fig.38, Curve XLVII) are: $\tau = (1.20 \pm .07) \times 10^{-3}$ sec., $C_{p_o} = 0.419 \pm .024\ \mu F$, $G_{p_\infty} = (3.4927 \pm .0001) \times 10^{-4}\ ohm^{-1}$, and $K_\infty = 2.263 \pm .001\ ohm^{-1}\ cm^{-1}$.

The result for $K_\infty$ is approximately 1.6% lower than that given by Bockris et al.[2]. In view of the corrosion of the cell, which resulted in a gradual increase in its resistance with time, it is probable that the present result is in error.

# DISCUSSION.

## DISPERSION IN MELTS AND SOLUTIONS.

The successful study of dispersion in ionic melts is made possible by experimental advances achieved in the present research. The use of the bridge described above enabled measurements of extremely high precision to be made, thus revealing effects which would previously have remained undetected. The problem of the lack of temperature stability, which in earlier work distorted the true shape of dispersion curves, has been overcome, as is demonstrated by the excellent reproducibility of resistance measurements (p.127).

Dispersion in capillary cells containing molten salts does not follow all the predictions of diffuse double layer theory. There is linearity between conductance and capacitance, but this is the only point of resemblance as the slopes give values of $\tau$ which are about 100 times greater than predicted. If the double layer theory is applicable to molten salts, the theoretical value of $\tau$ would preclude any appreciable conduction below 1 MHz. This could only be rectified by altering the order of magnitude of one or more of the theoretical parameters, as did Jaffé and Rider[23]. For example, $D_p$ would have to be decreased from $10^{-4}$ to $10^{-8}$ $cm^2$ $sec^{-1}$. The same conclusions are reached by comparing the theoretical $\tau$ with

a value derived from the resistance plateau, taking this to mark the point where $\kappa$ has reached 99.95% of $\kappa_\infty$[3]. Mobility data for melts obtained from audio frequency conductances and from static-field electromigration experiments usually agree quite well [24]. It follows that, in order to keep $\kappa_\infty$ unchanged, only the value of $D_p/\varepsilon_o$ may be altered at will. To justify a change by a factor of $10^{-4}$ in this lumped parameter would be difficult on theoretical grounds.

However, in deducing $u_p$ from experiment, $p_e$ is given the value for a fully dissociated electrolyte. It might be that whereas the product $u_p p_e$ obtained from experiment is correct, the individual values of $u_p$ and $p_e$ are not. For example, if there were association in the melt, the values of $p_e$ and $D_p$ would fall, but $u_p$ would have to be proportionately higher to maintain the observed value of $u_p p_e$. This would result if the associates were multiply charged, e.g.,

$$nM^+ + X^- \rightleftharpoons MnX^{(n-1)+}$$

The increase in $u_p$ would have to be outweighed by the effect on $D_p$ to result in a suitable increase in $\tau$. There is no evidence of any other kind which supports the existence of complex species in simple ionic melts [25]. However, in the absence of any such effect which would sufficiently raise the theoretical value of $\tau$, it must be concluded that

either the conduction observed in audio frequency experiments on melts is not due to ionic migration or there is no diffuse double layer.

Another result of the theory is that the ratio of resistances in two cells of the same length but different bore is independent of frequency. This behaviour was observed earlier in melts [3], but present results show that there is a residual variation of the order of 0.01%. The ratio $R_{n.b}/R_{w.b}$ increases with frequency, n.b and w.b, referring respectively to narrow and wide bores. This deviation also occurs in solution, but, for a given pair of cells, it is very much less than in melts.

These facts show that the dispersion of conductance closely follows a law of the form predicted by the double layer theory. The same cannot be said of the capacitance however, which in melts approximates to the relation $f^n C_p$ = constant, with n = 3/2 and not 2. Such negative capacitance deviations would have to arise by a mechanism completely independent of diffuse layer relaxation. To account for a linear region in the $G_p$ versus $C_p$ plots one might single out another capacitance source as the cause of all the deviations in melts, but it would not explain the finite conductance below 1 MHz. If this could be attributed to charge transfer due to electrolysis, it would also explain the capacitance dispersion, since Friauf [26] found that in the

case where negative carriers are blocked and positive carriers are free to discharge, the capacitance varies as $f^{-3/2}$. However, it cannot explain the linearity between $G_p$ and $C_p$ because for Friauf's case, $(G_{p\infty} - G_p)$ varies as $f^{-1/2}$. Furthermore, it is not reasonable on thermodynamic grounds to expect electrolysis of pure melts at cell e.m.f's of 0.1 volt. The discharge explanation cannot apply to solutions, where deviations from the double layer theory are eliminated by sufficiently widening the bore of the capillary. Jaffe' and Rider [23] were also unsuccessful in explaining their results for solutions by a discharge theory, so that it would appear that the close agreement between the calculated and measured values of $\tau$ is not coincidental.

Since current does not appear to be carried by a charge transfer process, there must be a contribution to the capacitance from the diffuse double layer.

The capacitance deviations and their dependence on bore size in solutions and melts are hard to explain. Deviations from $f^2C_p$ = constant towards $f^{3/2}C_p$ = constant represent anomalously low capacitance at low frequencies, the effect being eliminated in KCl aq. at least by widening the capillary bore. It would seem that this anomaly is caused by a repression of the diffuse layer capacitance, and that the $f^2C_p$ curve is raised on widening the bore until it

merges with the theoretical curve. Comparison of the capacitance results for molten KCl in the two cells shows that for wider bore capillaries either the frequency dependence of the capacitance suppression relaxes out at lower frequencies [Fig.39(a)], or that the amplitude of the error is decreased [Fig.39(b)]. Although it is not possible to differentiate between these alternatives, it seems certain that the capacitance anomaly involves the electrolyte since there was no apparent dispersion in a silica cell at room temperature in which the liquid was replaced by a resistor (p.140, measurement of cell inductance).

A number of effects were examined which might contribute to the depression of the capacitance. None of these is entirely satisfactory in explaining the facts. The wavelength of the applied a.c. signal is too long and the double layer too thin to account for an appreciable distortion of the field linearity at the electrode-electrolyte interface. The skin effect could be responsible for a depression of the capacitance at low frequencies. However, the predictions of the theory for this effect in metallic conductors[27] are contrary to the observed variation of $R_{n.b}/R_{w.b.}$ with frequency, if it is assumed that double layer relaxation is observed in wide bore cells. Moreover, no value of the magnetic permeability could be selected which would simultaneously correct the deviations in both

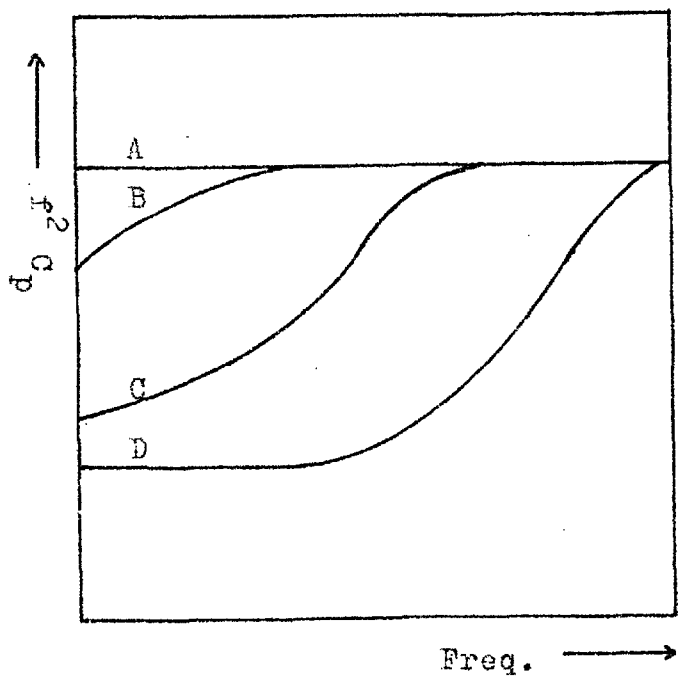


Fig. 39(a).

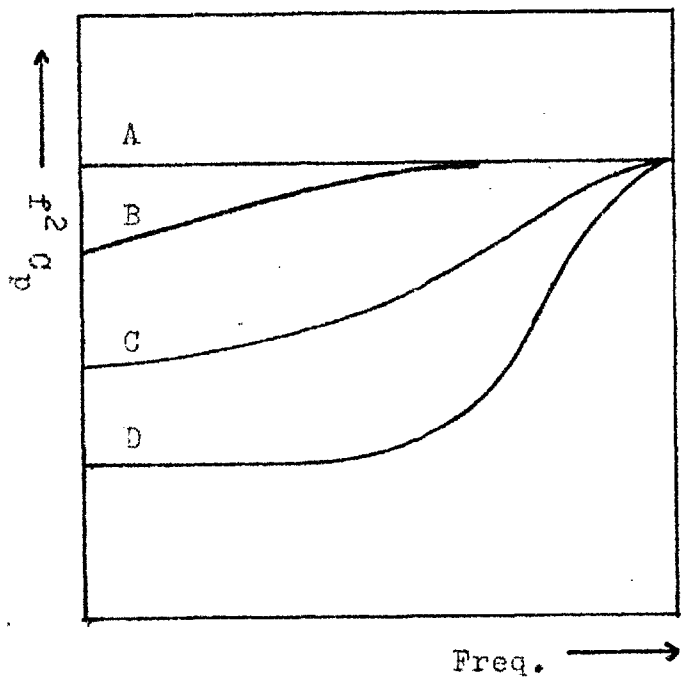


Fig. 39(b).

A is the ideal Diffuse Double Layer Curve,
B,C,D are curves for Narrow Bore Cells (Bore Increasing D,C,B)

Figure 39. Alternative Interpretations of Caracitance Deviations, (a) Change of Frequency Range, (b) Change of Amplitude.

the narrow bore cell resistance and in the capacitance.

The anomalous capacitance behaviour in melts and solutions is not explained by dissipation in the capillary wall since the capacitance of the solid silica cell (p.139) was essentially independent of frequency. It would also appear that the double layer is too thin to be appreciably influenced by distortion of the field by the guard, an effect which would be most marked near the inner electrode. The existence of a Helmholtz layer in pure melts and solutions cannot be discounted, but it is difficult to see how its influence on the capacitance dispersion could be affected by altering the capillary bore. It was not possible to assess the effect of convection, but this should be very small in these cells.

One possibility which has not been investigated is that ions are strongly adsorbed at the silica-melt interface and intensify local deviations in the permittivity $\varepsilon_o$. However, it is difficult to see how the properties of a thin layer could cause the cell capacitance to deviate appreciably from theory in cells of the present size. A more detailed investigation into the influence of cell geometry on dispersion is therefore necessary to resolve this problem.

Despite the reservations expressed above, there does appear to be some evidence in favour of diffuse layer

relaxation in conductance experiments. Dispersion in M.KCl solution is adequately described by the theory in wide bore cells. In melts, it would appear that the capacitance anomalies are reduced by widening the capillary bore. By analogy with the behaviour of the solution, it seems probable that in cells of sufficiently wide bore, dispersion conforming to the predictions of the theory would also be observed.

Further evidence in support of diffuse layer relaxation follows from a consideration of the separate influences of ionic mass and valency on the magnitude of the dispersion in a cell of given length. An increase in ionic mass would result in a decrease in both $u_p$ and $D_p$ due to the greater inertia of the ions, and a decrease in $p_e$ would follow from an increase in ionic radius. The parameter $\mu$ would be unchanged, and if it may be assumed that $\varepsilon_o$ is not appreciably altered, it follows from Eqn.(3.54) that $\tau$ would be increased and consequently that there would be a corresponding lowering of the dispersion over a given frequency range. This is upheld on comparison of the results for KCl and AgBr. On the other hand, with an increase of cation valency, $u_p$ and $\mu$ would increase and ideally $D_p$ and $\varepsilon_o$ would remain unaltered. There results from Eqn.(3.54) a decrease in $\tau$ which would raise the dispersion. Comparison of the results for the melts of

$CdCl_2$ and AgBr, whose molecular weights are not too dissimilar, shows that the predicted trend is again apparently obeyed.

It now remains to consider the implications of the present results in relation to the accurate measurement of specific conductance in melts. The diffuse layer theory may be used to test the validity of calibration for a given cell. Dispersion is correctly accounted for in a wide bore capillary, so that the true limiting conductance may be calculated and the true cell constant derived from reliable data for $\kappa$ of the solution. The value of $\kappa_\infty$ for melts of sufficiently low conductance may be measured in this cell provided the relaxation of the melt also conforms to diffuse double layer theory.

The position for molten salts having specific conductances of the order of 1 $ohm^{-1}$ $cm^{-1}$. is less satisfactory. The use of wide bore capillaries in these melts would result in a low cell resistance, which would lead to the introduction of errors due, for example, to induction. It would however be possible to compensate for this low resistance by connecting an external resistor in series with the cell, but this would decrease the sensitivity. It would seem therefore that in order to obtain accurate conductance data for such melts, the problem of the anomalous capacitance dispersion will have to be overcome.

## THE EFFECT OF ADDITIVES ON DISPERSION.

### WATER.

For water-saturated melts, the gradients of the linear regions of the conductance-capacitance plots are smaller than those for the corresponding untreated and dried melts (Figs. 29, 35). The capacitance changes brought about by humidifying the melts (Figs. 28(a), 34(a)) are far too small to account for this change of slope, which must therefore be attributed to a decrease in the conductance dispersion due to an increase in $\tau$. However, this could not have resulted simply from dilution of the melt by molecular water since, unless this caused a substantial reduction in the transport coefficients, which is unlikely, the effect on $p_e$ and hence on the dispersion would be exceedingly small. It is possible that the preferential adsorption of water at the silica-melt interface considerably enhances its effect on the dispersion. It would be instructive to test this for humidified melts by varying the cell bore.

Regarding the characteristic minimum in the conductance-capacitance plots, it is possible that current was carried by the rotation of water dipoles, and that this effect relaxed out in the region of the dip. The minimum

occurs at 1.5 KHz in both melts and indicates that differences in the interionic forces are insufficient to alter the relaxation time. The amplitude of the effect is greater in KCl, possibly because of greater solubility of water in this melt.

The separate effect of temperature on this process was not investigated in the present work, and it is therefore not possible to evaluate the activation energy. The absence of any such anomalies in the results for KCl aq. shows that at room temperature this effect is either prevented by high energy requirements, or that the relaxation has shifted to a frequency outside the experimental range. Present results do not show which of these alternatives is correct.

HYDROGEN CHLORIDE.

Bubbling A-HCl through molten AgBr produced an increase in capacitance which became very marked on flushing with argon (Fig.34(b)). On the other hand, drying the KCl melt with A-HCl and argon produced an increase in the capacitance only at frequencies below 2KHz (Fig.28(b)). Above this frequency its value was apparently lower than that in the untreated melt. The reason for this is not understood. If this treatment resulted only in the removal of water, resaturation with A-$H_2O$ might be expected to restore the melt to its original condition. However, in

AgBr at least, the capacitance is not restored to its value in the untreated melt. This could indicate that not only was water removed, but also oxide and hydroxide ions. In this case it is apparent that these ions are not formed by reaction of the melt with water, but are present in the original sample. However it cannot be ruled out that the increased capacitance resulted simply from the adsorption of hydrogen chloride at the electrodes.

The conductance-capacitance plot for molten AgBr saturated with hydrogen chloride (Fig.35, curve XL) exhibits strong curvature in the low frequency region, which is eliminated by bubbling dry argon through the melt. This curvature must be due to enhanced conduction since there is no apparent correlation between the curvatures in Figs. 34(b) and 35. Measurements of the Henry's law coefficient for HF in molten NaF - $ZrF_4$ mixtures show that pure NaF will dissolve about 0.1 mole % of HF at 700°C and 1 atmosphere pressure [22]. The solubility of HCl in molten AgBr is not known. However, assuming it is similar, and recalling that the partial pressure of the gas above the melt was considerably less than 1 atmosphere, it seems unlikely that hydrogen chloride dipoles could raise the conductance detectably. This could be supported by the absence of a minimum in the conductance-capacitance plot, but this point is not conclusive because the relaxation time is not known.

Alternatively, the conductance might be raised by the contribution of protons produced by the dissociation of hydrogen chloride. This in turn would be expected to lead to decomposition of the melt, e.g.,

$$HCl \rightleftharpoons H^+ + Cl^-$$

$$H^+ + Br^- \rightleftharpoons HBr \ ,$$

and an accompanying increase in $\kappa$ due to the accumulation of chloride ions. However, no time dependence of the conductance was observed, which suggests that there was no appreciable decomposition.

## CONCLUSIONS.

A theory of diffuse double layer relaxation shows that dispersion should occur in the parallel resistance and capacitance of a conductance cell.

Experimental data for capillary cells give excellent confirmation of the theory in KCl aq. provided the bore is sufficiently large. However, the theory requires the dispersion to be independent of bore.

To obtain reliable dispersion data in melts and solutions it is necessary to exercise great care in the elimination of errors in bridge measurements, and in ensuring a stable and uniform temperature in the cell. To enable dispersion effects of 0.02% in the cell resistance to be followed in melts, the temperature must be controlled to $\pm$ 0.1°C.

In AgBr, KCl, and $CdCl_2$ melts, the observed relations between resistance, capacitance and frequency deviate from those predicted, and dispersion occurs at lower frequencies. Some of the fault may lie with the constants of the theory because the calculated relaxation times would require the conductance to be effectively zero in the experimental frequency range.

Capacitance deviations cannot be explained in terms of the relaxation time since they depend on the bore size.

Until the nature of these deviations is fully understood it will not be possible to obtain closer estimates of the high frequency limiting conductance by the use of capillary cells.

Saturation of melts by water leads to an additional relaxation in the conductance, but this effect is apparently absent in melts as normally prepared for study.

# APPENDIX 4.1.

## EXPERIMENTAL DATA.

## AQUEOUS M.KCl SOLUTION.

RUN USING 0.5 mm BORE SILICA CELL.

| Freq. (KHz) | $R_p$ (ohms) | $C_p$ (pF) | $G_p \times 10^5$ ($ohm^{-1}$) | $f^2 C_p \times 10^6$ (F $sec^{-2}$) | $f^{3/2} C_p \times 10^7$ (F $sec^{-3/2}$) | Temp. (°C) |
|---|---|---|---|---|---|---|
| 200 | 33,740±30 | | | | | $27.31_2$ |
| 150 | 33,460±30 | | | | | $27.32_0$ |
| 100 | 33,210±20 | | | | | $27.31_2$ |
| 70 | 33,080±10 | | | | | $27.31_1$ |
| 50 | 33,087± 5 | | | | | $27.30_2$ |
| 30 | 33,065± 3 | | | | | $27.30_2$ |
| 25 | 33,064± 3 | 0.3±.1 | $3.024_4$ | 190 | 11.9 | $27.29_6$ |
| 20 | 33,064± 3 | 0.3±.1 | $3.024_4$ | 120 | 8.5 | $27.31_1$ |
| 15 | 33,070± 3 | 0.3±.1 | $3.023_9$ | 68 | 5.5 | $27.29_9$ |
| 10 | 33,078± 3 | 0.4±.1 | $3.023_2$ | 40 | 4.0 | $27.29_6$ |
| 5 | 33,080± 5 | 0.6±.1 | $3.023_0$ | 15 | 2.1 | $27.28_5$ |
| 3 | 33,085±10 | 1.0±.2 | $3.022_5$ | 9.0 | 1.6 | $27.26_9$ |
| 2 | 33,135±20 | 1.6±1 | $3.018_0$ | 6.4 | 1.4 | $27.25_4$ |
| 1 | 33,150±20 | 5.4±2 | $3.016_6$ | 5.4 | 1.7 | $27.25_4$ |
| 0.5 | 33,165±30 | 12.2±4 | $3.015_2$ | 3.0 | 1.4 | $27.26_8$ |

Average Temperature, $27.29_3$ °C.

RUN USING 2.5 mm BORE GLASS CELL.

| Freq. (KHz) | $R_p$ (ohms) | $C_p$ (pF) | $G_p \times 10^3$ ($ohm^{-1}$) | $f^2 C_p \times 10^2$ (F $sec^{-2}$) | $f^{3/2} C_p \times 10^5$ (F $sec^{-3/2}$) | Temp. (°C) |
|---|---|---|---|---|---|---|
| 200 | 917.0±.1 | 0.5±.1 | | | | $27.02_2$ |
| 150 | 918.3±.1 | 1.7±.1 | $1.088_9$ | 1.12 | 2.90 | $27.02_2$ |
| 100 | 919.3±.1 | 1.7±.1 | $1.087_8$ | 1.70 | 5.38 | $27.03_2$ |
| 80 | 919.6±.1 | 3.0±.1 | $1.087_4$ | 1.92 | 6.81 | $27.02_8$ |
| 60 | 920.0±.1 | 4.6±.1 | $1.087_0$ | 1.66 | 6.79 | $27.03_4$ |
| 40 | 920.3±.1 | 11.0±.1 | $1.086_6$ | 1.76 | 8.80 | $27.04_2$ |
| 20 | 920.9±.1 | 39.1±.1 | $1.085_9$ | 1.56 | 11.1 | $27.04_3$ |
| 15 | 921.2±.1 | 68.0±.1 | $1.085_5$ | 1.53 | 12.5 | $27.04_4$ |
| 10 | 922.0±.1 | 114.3±.1 | $1.084_6$ | 1.14 | 11.4 | $27.04_5$ |
| 8 | 922.5±.1 | 216.9±.1 | $1.084_0$ | 1.39 | 15.8 | $27.04_3$ |
| 6 | 923.6±.1 | 368.8±.1 | $1.082_7$ | 1.33 | 17.2 | $27.03_2$ |
| 5 | 924.3±.1 | 511.9±.1 | $1.081_9$ | 1.28 | 18.2 | $27.03_2$ |
| 4 | 925.4±.1 | 765.7±.1 | $1.080_6$ | 1.22 | 19.4 | $27.03_2$ |

Average Temperature, $27.03_5$ °C.

# APPENDIX 4.2.

## EXPERIMENTAL DATA.

## MOLTEN SALTS.

### POTASSIUM CHLORIDE.

RUN (1)

| Freq. (KHz) | $R_p$ (ohms) | $C_p$ (pF) | $G_p \times 10^4$ ($ohm^{-1}$) | $f^2 C_p \times 10^5$ ($F\ sec^{-2}$) | Temp. (mV) |
|---|---|---|---|---|---|
| 108 | 2655.8±.1 | | | | 8.060 |
| 51 | 2657.6±.1 | | | | 8.060 |
| 20 | 2658.4±.1 | 0.8±.2 | $3.761_6$ | 32 | 8.061 |
| 15 | 2658.7±.1 | 1.4±.1 | $3.761_2$ | 32 | 8.061 |
| 10 | 2659.1±.1 | 2.8±.1 | $3.760_6$ | 28 | 8.061 |
| 6 | 2659.6±.1 | 3.9±.1 | $3.759_9$ | 14 | 8.061 |
| 4 | 2660.3±.1 | 9.4±.1 | $3.758_9$ | 15 | 8.061 |
| 3 | 2660.8±.1 | 12.7±.1 | $3.758_2$ | 11 | 8.061 |
| 2 | 2661.1±.1 | 20.3±.1 | $3.757_8$ | 8.2 | 8.061 |
| 1.5 | 2661.6±.1 | 28.2±.1 | $3.757_1$ | 6.3 | 8.061 |
| 1 | 2661.7±.1 | 39.2±.1 | $3.756_9$ | 3.9 | 8.061 |
| 0.8 | 2661.7±.1 | 49.3±.3 | $3.756_9$ | 3.2 | 8.062 |
| 0.6 | 2661.8±.1 | 73.7±.5 | $3.756_8$ | 2.7 | 8.062 |
| 0.5 | 2661.9±.1 | 93.5±.5 | $3.756_7$ | 2.3 | 8.063 |
| 0.4 | 2662.1±.1 | 126.3±.5 | $3.756_4$ | 2.0 | 8.063 |
| 0.3 | 2662.4±.1 | 194 ±1 | $3.756_0$ | 1.7 | 8.063 |
| 0.2 | 2663.1±.1 | 355 ±5 | $3.755_0$ | 1.4 | 8.063 |

(N.B. 8.060 mV = 809°C).

RUN (2)

| Freq. (KHz) | $R_p$ (ohms) | $C_p$ (pF) | $G_p \times 10^4$ ($ohm^{-1}$) | $f^2 C_p \times 10^5$ (F $sec^{-2}$) | $f^{3/2} C_p \times 10^6$ (F $sec^{-3/2}$) | Temp. (mV) |
|---|---|---|---|---|---|---|
| 107 | 2693.5± 1 | | | | | 8.127 |
| 51 | 2695.8±.5 | | | | | 8.127 |
| 20 | 2696.6±.2 | 1.0±.2 | $3.708_3$ | 40 | 2.83 | 8.127 |
| 15 | 2696.9±.1 | 1.5±.1 | $3.707_9$ | 34 | 2.76 | 8.127 |
| 10 | 2697.3±.1 | 2.6±.1 | $3.707_4$ | 26 | 2.60 | 8.128 |
| 6 | 2697.6±.1 | 5.4±.1 | $3.706_9$ | 19 | 2.51 | 8.128 |
| 4 | 2698.5±.1 | 10.6±.1 | $3.705_7$ | 17 | 2.69 | 8.128 |
| 3 | 2698.9±.1 | 13.5±.1 | $3.705_2$ | 12 | 2.21 | 8.128 |
| 2 | 2699.2±.1 | 23.2±.1 | $3.704_8$ | 9.3 | 2.07 | 8.128 |
| 1.5 | 2699.4±.1 | 34.3±.1 | $3.704_5$ | 7.7 | 2.00 | 8.128 |
| 1 | 2699.3±.1 | 55.3±.1 | $3.704_6$ | 5.5 | 1.75 | 8.128 |
| 0.8 | 2699.3±.1 | 79.0±.2 | $3.704_6$ | 5.1 | 1.79 | 8.128 |
| 0.6 | 2699.5±.1 | 115.5±.2 | $3.704_3$ | 4.2 | 1.69 | 8.129 |
| 0.51 | 2699.6±.1 | 158.0±.5 | $3.704_2$ | 4.1 | 1.82 | 8.129 |
| 0.41 | 2699.9±.1 | 232.5±.5 | $3.703_8$ | 4.0 | 1.93 | 8.129 |
| 0.36 | 2700.1±.1 | 305 ± 1 | $3.703_5$ | 3.4 | 2.08 | 8.129 |
| 0.31 | 2700.3±.1 | 370 ± 1 | $3.703_2$ | 3.6 | 2.03 | 8.129 |
| 0.26 | 2700.8±.1 | 507 ± 1 | $3.702_6$ | 3.4 | 2.11 | 8.129 |
| 0.21 | 2701.5±.1 | 711 ± 5 | $3.701_6$ | 3.1 | 2.17 | 8.129 |

(N.B. 8.130 mV = 814°C)

RUN (3)

| Freq. (KHz) | $R_p$ (ohms) | $C_p$ (pF) | $G_p \times 10^4$ ($ohm^{-1}$) | $f^2C_p \times 10^5$ ($F\ sec^{-2}$) | Temp. (mV) |
|---|---|---|---|---|---|
| 107 | 2696.5± 1 | | | | 8.129 |
| 51 | 2697.8±.5 | | | | 8.129 |
| 20 | 2698.8±.2 | 1.1±.2 | $3.705_3$ | 44 | 8.129 |
| 15 | 2699.0±.1 | 1.6±.1 | $3.705_0$ | 36 | 8.129 |
| 10 | 2699.4±.1 | 3.1±.1 | $3.704_5$ | 31 | 8.129 |
| 6 | 2699.7±.1 | 6.1±.1 | $3.704_1$ | 22 | 8.129 |
| 4 | 2699.8±.1 | 11.0±.1 | $3.703_9$ | 18 | 8.130 |
| 3 | 2700.3±.1 | 16.3±.1 | $3.703_2$ | 15 | 8.130 |
| 2 | 2700.9±.1 | 27.9±.1 | $3.702_4$ | 11 | 8.130 |
| 1.5 | 2701.2±.1 | 41.4±.1 | $3.702_0$ | 9.3 | 8.130 |
| 1 | 2701.5±.1 | 60.7±.2 | $3.701_6$ | 6.1 | 8.130 |
| 0.8 | 2701.7±.1 | 96.7±.2 | $3.701_3$ | 6.2 | 8.130 |
| 0.6 | 2702.0±.1 | 153.5±.5 | $3.700_9$ | 5.5 | 8.130 |
| 0.52 | 2702.2±.1 | 187.3±.5 | $3.700_6$ | 5.1 | 8.130 |
| 0.42 | 2702.6±.1 | 270 ± 1 | $3.700_1$ | 4.9 | 8.130 |
| 0.36 | 2702.9±.1 | 344 ± 1 | $3.699_7$ | 4.5 | 8.130 |
| 0.32 | 2703.2±.1 | 412 ± 3 | $3.699_3$ | 4.1 | 8.130 |
| 0.27 | 2703.7±.1 | 545 ± 5 | $3.698_6$ | 4.0 | 8.130 |
| 0.22 | 2704.3±.1 | 769 ± 5 | $3.697_8$ | 3.7 | 8.130 |

(N.B. 8.130 mV = 814°C.)

RUN (4)

| Freq. (KHz) | $R_p$ (ohms) | $C_p$ (pF) | $G_p \times 10^4$ | $f^2 C_p \times 10^5$ (F $sec^{-2}$) | Temp. (mV) |
|---|---|---|---|---|---|
| 107 | 2695.5± 1 | | | | 8.134 |
| 51 | 2698.0±.5 | | | | 8.134 |
| 20 | 2699.1±.2 | 1.3±.2 | $3.704_9$ | 31 | 8.134 |
| 15 | 2699.3±.1 | 1.9±.1 | $3.704_6$ | 42 | 8.134 |
| 10 | 2700.1±.1 | 3.0±.1 | $3.703_5$ | 30 | 8.134 |
| 6 | 2700.4±.1 | 5.4±.1 | $3.703_1$ | 19 | 8.134 |
| 4 | 2702.1±.1 | 12.2±.1 | $3.700_8$ | 18 | 8.134 |
| 3 | 2702.3±.1 | 15.6±.1 | $3.700_5$ | 14 | 8.134 |
| 2 | 2702.6±.1 | 25.9±.1 | $3.700_1$ | 10 | 8.134 |
| 1.5 | 2702.8±.1 | 38.1±.1 | $3.699_8$ | 8.6 | 8.134 |
| 1 | 2702.6±.1 | 56.3±.1 | $3.700_1$ | 5.6 | 8.134 |
| 0.8 | 2702.3±.1 | 77.5±.2 | $3.700_5$ | 5.0 | 8.134 |
| 0.6 | 2702.4±.1 | 125.9±.5 | $3.700_4$ | 5.5 | 8.134 |
| 0.52 | 2702.3±.1 | 177.1±.5 | $3.700_5$ | 4.8 | 8.134 |
| 0.42 | 2702.4±.1 | 264.3±.5 | $3.700_4$ | 4.8 | 8.134 |
| 0.37 | 2702.6±.1 | 345 ± 1 | $3.700_1$ | 4.8 | 8.134 |
| 0.32 | 2702.8±.1 | 445 ± 3 | $3.699_8$ | 4.5 | 8.134 |
| 0.27 | 2703.3±.1 | 611 ± 5 | $3.699_1$ | 4.5 | 8.134 |
| 0.22 | 2703.9±.1 | 880 ±10 | $3.698_3$ | 4.7 | 8.134 |

(N.B. 8.130 mV = 814°C)

RUN (5)

| Freq. (KHz) | $R_p$ (ohms) | $C_p$ (pF) | $G_p x10^4$ ($ohm^{-1}$) | $f^2C_p x10^5$ ($F\ sec^{-2}$) | Temp. (mV) |
|---|---|---|---|---|---|
| 107 | 2695.5± 1 | | | | 8.145 |
| 51 | 2697.0±.5 | | | | 8.145 |
| 20 | 2698.1±.2 | 1.0±.2 | $3.706_3$ | 40 | 8.145 |
| 15 | 2698.4±.1 | 1.7±.1 | $3.705_8$ | 38 | 8.145 |
| 10 | 2698.6±.1 | 3.0±.1 | $3.705_6$ | 30 | 8.145 |
| 6 | 2699.0±.1 | 5.9±.1 | $3.705_0$ | 21 | 8.145 |
| 4 | 2699.3±.1 | 10.6±.1 | $3.704_6$ | 19 | 8.145 |
| 3 | 2699.6±,1 | 16.1±.1 | $3.704_2$ | 14 | 8.145 |
| 2 | 2701.2±.1 | 27.3±.1 | $3.702_0$ | 9.5 | 8.145 |
| 1.5 | 2701.4±.1 | 36.9±.2 | $3.701_7$ | 8.3 | 8.145 |
| 1 | 2701.1±.1 | 55.5±.2 | $3.702_1$ | 5.5 | 8.145 |
| 0.8 | 2700.9±.1 | 83.2±.2 | $3.702_4$ | 5.3 | 8.145 |
| 0.6 | 2701.0±.1 | 139.9±.5 | $3.702_3$ | 5.0 | 8.145 |
| 0.52 | 2701.0±.1 | 188.4±.5 | $3.702_3$ | 5.1 | 8.145 |
| 0.42 | 2701.2±.1 | 279 ± 1 | $3.702_0$ | 5.0 | 8.145 |
| 0.37 | 2701.4±.1 | 360 ± 1 | $3.701_7$ | 5.0 | 8.145 |
| 0.32 | 2701.7±.1 | 468 ± 1 | $3.701_3$ | 4.7 | 8.145 |
| 0.27 | 2702.1±.1 | 648 ± 1 | $3.700_8$ | 4.7 | 8.145 |
| 0.22 | 2702.7±.1 | 940 ±10 | $3.700_0$ | 4.5 | 8.145 |

(N.B. 8.145 mV = 815°C)

RUN (6)

| Freq. (KHz) | $R_p$ (ohms) | $C_p$ (pF) | $G_p \times 10^3$ ($ohm^{-1}$) | $f^2 C_p \times 10^4$ (F $sec^{-2}$) | $f^{3/2} C_p \times 10^5$ ($Fsec^{-3/2}$) | Temp. (mV) |
|---|---|---|---|---|---|---|
| 200 | 627.5±.1 | | | | | 8.104 |
| 150 | 628.2±.1 | | | | | 8.104 |
| 100 | 628.8±.1 | | | | | 8.104 |
| 80 | 629.0±.1 | 0.8±.1 | $1.589_8$ | 51.2 | 1.80 | 8.105 |
| 60 | 629.1±.1 | 1.4±.1 | $1.589_5$ | 50.5 | 2.06 | 8.105 |
| 40 | 629.2±.1 | 2.2±.1 | $1.589_3$ | 35.2 | 1.76 | 8.105 |
| 30 | 629.3±.1 | 4.6±.1 | $1.589_0$ | 41.4 | 2.39 | 8.105 |
| 20 | 629.4±.1 | 10.3±.1 | $1.588_8$ | 41.2 | 2.92 | 8.105 |
| 15 | 629.5±.1 | 16.8±.1 | $1.588_5$ | 37.9 | 3.09 | 8.105 |
| 10 | 629.7±.1 | 33.9±.1 | $1.588_0$ | 33.9 | 3.39 | 8.106 |
| 8 | 629.9±.1 | 49.0±.1 | $1.587_5$ | 31.4 | 3.50 | 8.106 |
| 6 | 630.1±.1 | 79.0±.1 | $1.587_0$ | 29.4 | 3.67 | 8.106 |
| 4 | 630.5±.1 | 145.0±.1 | $1.586_0$ | 23.2 | 3.68 | 8.106 |
| 3 | 630.8±.1 | 215.6±.2 | $1.585_2$ | 19.4 | 3.34 | 8.106 |
| 2 | 631.3±.1 | 365.0±.5 | $1.584_0$ | 14.6 | 3.27 | 8.106 |
| 1.5 | 631.8±.1 | 533.3±.5 | $1.582_7$ | 12.0 | 3.10 | 8.106 |
| 1 | 632.4±.1 | 828 ± 1 | $1.581_2$ | 8.3 | 2.61 | 8.106 |

(N.B. 8.10 mV = 812°C)

RUN (7)

| Freq. (KHz) | $R_p$ (ohms) | $C_p$ (pF) | $G_p \times 10^3$ ($ohms^{-1}$) | $f^2 C_p \times 10^4$ (F $sec^{-2}$) | $f^{3/2} C_p \times 10^5$ (F $sec^{-3/2}$) | Temp. (mV) |
|---|---|---|---|---|---|---|
| 200 | 587.5±.1 | | | | | 9.036 |
| 150 | 588.6±.1 | | | | | 9.036 |
| 100 | 589.1±.1 | | | | | 9.036 |
| 80 | 589.3±.1 | 1.0±.1 | $1.696_9$ | 64.0 | 2.26 | 9.036 |
| 60 | 589.6±.1 | 1.8±.1 | $1.696_0$ | 64.9 | 2.65 | 9.036 |
| 40 | 589.6±.1 | 2.6±.1 | $1.696_0$ | 41.6 | 2.08 | 9.036 |
| 30 | 589.7±.1 | 3.4±.1 | $1.695_7$ | 30.6 | 1.77 | 9.036 |
| 20 | 589.8±.1 | 7.9±.1 | $1.695_4$ | 31.6 | 2.24 | 9.036 |
| 15 | 590.0±.1 | 11.8±.1 | $1.694_9$ | 26.6 | 2.07 | 9.037 |
| 10 | 590.1±.1 | 23.4±.1 | $1.694_6$ | 23.4 | 2.34 | 9.037 |
| 8 | 590.2±.1 | 34.7±.1 | $1.694_3$ | 22.3 | 2.48 | 9.038 |
| 6 | 590.5±.1 | 43.9±.1 | $1.693_4$ | 15.8 | 2.04 | 9.038 |
| 4 | 590.8±.1 | 102.0±.2 | $1.692_6$ | 16.4 | 2.58 | 9.039 |
| 3 | 591.0±.1 | 164.0±.2 | $1.692_0$ | 14.8 | 2.54 | 9.039 |
| 2 | 591.3±.1 | 327.2±.5 | $1.691_1$ | 13.1 | 2.93 | 9.039 |
| 1.5 | 591.6±.1 | 527 ± 1 | $1.690_3$ | 11.8 | 3.06 | 9.039 |
| 1 | 591.9±.1 | 993 ± 5 | $1.689_4$ | 9.9 | 3.15 | 9.039 |

(N.B. 9.04 mV = 887°C)

RUN (8)

| Freq. (KHz) | $R_p$ (ohms) | $C_p$ (pF) | $G_p \times 10^3$ ($ohm^{-1}$) | $f^2 C_p \times 10^4$ ($F\ sec^{-2}$) | $f^{3/2} C_p \times 10^5$ ($F\ sec^{-3/2}$) | Temp. (mV) |
|---|---|---|---|---|---|---|
| 200 | 552.4±.1 | | | | | 10.209 |
| 150 | 553.0±.1 | | | | | 10.209 |
| 100 | 553.6±.1 | | | | | 10.210 |
| 80 | 553.7±.1 | 1.2±.1 | $1.806_0$ | 76.9 | 2.71 | 10.210 |
| 60 | 553.8±.1 | 1.6±.1 | $1.805_7$ | 57.8 | 2.35 | 10.210 |
| 40 | 553.8±.1 | 2.6±.1 | $1.805_7$ | 41.6 | 2.08 | 10.210 |
| 30 | 553.9±.1 | 3.9±.1 | $1.805_4$ | 35.1 | 2.03 | 10.211 |
| 20 | 553.8±.1 | 8.9±.1 | $1.805_7$ | 35.6 | 2.52 | 10.212 |
| 15 | 553.8±.1 | 16.0±.1 | $1.805_7$ | 36.0 | 2.95 | 10.212 |
| 10 | 554.0±.1 | 32.4±.1 | $1.805_0$ | 32.4 | 3.24 | 10.212 |
| 8 | 554.1±.1 | 43.1±.1 | $1.804_7$ | 28.6 | 3.09 | 10.212 |
| 6 | 554.1±.1 | 74.0±.1 | $1.804_7$ | 26.6 | 3.45 | 10.213 |
| 4 | 554.3±.1 | 154.0±.2 | $1.804_1$ | 24.6 | 3.90 | 10.213 |
| 3 | 554.3±.1 | 246.7±.5 | $1.804_1$ | 22.2 | 3.82 | 10.214 |
| 2 | 554.8±.1 | 365 ± 1 | $1.802_4$ | 14.6 | 3.27 | 10.214 |
| 1.5 | 555.3±.1 | 566 ± 3 | $1.800_8$ | 12.8 | 3.29 | 10.214 |
| 1 | 555.8±.1 | 985 ± 5 | $1.799_2$ | 9.8 | 3.12 | 10.214 |

(N.B. 10.21 mV = 978°C)

SILVER BROMIDE.

RUN (1)

| Freq. (KHz) | $R_p$ (ohms) | $C_p$ (pF) | $G_p \times 10^4$ ($ohm^{-1}$) | $f^2 C_p \times 10^6$ (F $sec^{-2}$) | Temp. (mV) |
|---|---|---|---|---|---|
| 108 | 1880.3±.2 | | | | 7.136 |
| 51 | 1881.1±.1 | | | | 7.136 |
| 20 | 1881.4±.1 | 0.2±.1 | $5.315_1$ | 80 | 7.136 |
| 15 | 1881.6±.1 | 0.4±.1 | $5.314_6$ | 90 | 7.136 |
| 10 | 1881.8±.1 | 0.6±.1 | $5.314_0$ | 60 | 7.136 |
| 6 | 1882.0±.1 | 1.0±1 | $5.313_4$ | 36 | 7.136 |
| 4 | 1882.0±.1 | 1.0±1 | $5.313_4$ | 16 | 7.136 |
| 2 | 1882.2±.1 | 3.5±.1 | $5.312_9$ | 14 | 7.136 |
| 1.5 | 1882.2±.1 | 4.0±.1 | $5.312_9$ | 10 | 7.136 |
| 1 | 1882.4±.1 | 4.2±.1 | $5.312_3$ | 4.2 | 7.137 |
| 0.62 | 1882.4±.1 | 10.0±.4 | $5.312_3$ | 3.8 | 7.137 |
| 0.42 | 1882.5±.1 | 21.9±.5 | $5.312_0$ | 3.8 | 7.137 |
| 0.32 | 1882.5±.1 | 37 ± 2 | $5.312_0$ | 3.8 | 7.137 |
| 0.22 | 1882.7±.1 | 70 ± 5 | $5.311_5$ | 3.4 | 7.137 |
| 0.12 | 1882.9±.1 | 165 ±10 | $5.310_9$ | 2.4 | 7.137 |

(N.B. 7.14 mV = 733°C)

RUN (2)

| Freq. (KHz) | $R_p$ (ohms) | $C_p$ (pF) | $G_p \times 10^4$ ($ohm^{-1}$) | $f^2 C_p \times 10^6$ (F $sec^{-2}$) | Temp. (mV) |
|---|---|---|---|---|---|
| 108 | 1884.7±.2 | | | | 7.157 |
| 51 | 1885.6±.2 | | | | 7.157 |
| 20 | 1886.2±.1 | 1.4±.1 | $5.301_6$ | 560 | 7.157 |
| 15 | 1886.5±.1 | 1.6±.1 | $5.300_8$ | 360 | 7.157 |
| 10 | 1886.6±.1 | 2.1±.1 | $5.300_5$ | 210 | 7.157 |
| 6 | 1886.8±.1 | 2.4±.1 | $5.299_9$ | 86 | 7.157 |
| 4 | 1886.8±.1 | 3.5±.1 | $5.299_9$ | 62 | 7.157 |
| 2 | 1886.9±.1 | 9.5±.1 | $5.299_6$ | 38 | 7.157 |
| 1.5 | 1886.9±.1 | 12.0±.1 | $5.299_6$ | 27 | 7.157 |
| 1 | 1887.0±.1 | 22.2±.1 | $5.299_4$ | 22 | 7.157 |
| 0.62 | 1887.1±.1 | 47.5±.1 | $5.299_1$ | 18 | 7.157 |
| 0.42 | 1887.4±.1 | 80.8±.1 | $5.298_2$ | 14 | 7.157 |
| 0.32 | 1887.5±.1 | 130 ± 1 | $5.298_0$ | 13 | 7.157 |
| 0.22 | 1887.7±.1 | 238 ± 5 | $5.297_4$ | 11 | 7.157 |
| 0.12 | 1888.2±.1 | 537 ±10 | $5.296_0$ | 7.7 | 7.158 |

(N.B. 7.16 mV = 735°C).

RUN (3)

| Freq. (KHz) | $R_p$ (ohms) | $C_p$ (pF) | $G_p \times 10^4$ ($ohm^{-1}$) | $f^2 C_p \times 10^5$ (F $sec^{-2}$) | $f^{3/2} C_p \times 10^7$ (F $sec^{-3/2}$) | Temp. (mV) |
|---|---|---|---|---|---|---|
| 108 | 1884.0±.2 | | | | | 7.153 |
| 51 | 1885.7±.2 | | | | | 7.153 |
| 20 | 1886.4±.1 | 0.4±.1 | $5.301_1$ | 160 | 11.4 | 7.153 |
| 15 | 1886.8±.1 | 0.7±.1 | $5.299_9$ | 160 | 13.1 | 7.153 |
| 10 | 1887.7±.1 | 1.1±.1 | $5.297_4$ | 110 | 11.0 | 7.152 |
| 6 | 1888.6±.1 | 1.5±.1 | $5.294_9$ | 54 | 6.98 | 7.152 |
| 4 | 1889.0±.1 | 2.9±.1 | $5.293_8$ | 46 | 7.39 | 7.152 |
| 2 | 1889.6±.1 | 9.2±.1 | $5.292_1$ | 37 | 8.22 | 7.152 |
| 1.5 | 1890.3±.1 | 11.1±.2 | $5.290_1$ | 25 | 6.48 | 7.152 |
| 1 | 1890.5±.1 | 16.2±.3 | $5.289_6$ | 16 | 5.13 | 7.151 |
| 0.8 | 1890.7±.1 | 23.0±.4 | $5.289_0$ | 15 | 5.40 | 7.151 |
| 0.62 | 1891.2±.1 | 32.7±.4 | $5.287_6$ | 13 | 5.05 | 7.151 |
| 0.42 | 1891.8±.1 | 68 ± 1 | $5.285_9$ | 12 | 5.86 | 7.151 |
| 0.32 | 1892.4±.1 | 109 ± 1 | $5.284_2$ | 11 | 6.22 | 7.151 |
| 0.22 | 1892.8±.1 | 178 ± 5 | $5.283_1$ | 8.6 | 5.81 | 7.151 |
| 0.12 | 1893.8±.1 | 428 ±10 | $5.280_3$ | 6.2 | 5.61 | 7.151 |

(N.B. 7.15 mV = 734°C).

RUN (4)

| Freq. (KHz) | $R_p$ (ohms) | $C_p$ (pF) | $G_p \times 10^4$ ($ohm^{-1}$) | $f^2 C_p \times 10^5$ (F $sec^{-2}$) | Temp. (mV) |
|---|---|---|---|---|---|
| 107 | 1882.4±.2 | | | | 7.139 |
| 51 | 1883.4±.2 | | | | 7.139 |
| 20 | 1884.3±.1 | 1.0±.1 | $5.307_0$ | 40 | 7.138 |
| 15 | 1884.5±.1 | 1.1±.1 | $5.306_4$ | 25 | 7.138 |
| 10 | 1884.6±.1 | 1.5±.1 | $5.306_1$ | 11 | 7.138 |
| 6 | 1884.7±.1 | 2.8±.1 | $5.305_8$ | 10 | 7.139 |
| 4 | 1884.7±.1 | 4.1±.1 | $5.305_8$ | 6.6 | 7.139 |
| 2 | 1884.8±.1 | 10.8±.1 | $5.305_6$ | 4.3 | 7.139 |
| 1.5 | 1885.1±.1 | 17.4±.2 | $5.304_7$ | 3.9 | 7.139 |
| 1 | 1885.2±.1 | 26.6±.2 | $5.304_4$ | 2.7 | 7.139 |
| 0.8 | 1885.2±.1 | 39.5±.4 | $5.304_4$ | 2.5 | 7.139 |
| 0.62 | 1885.4±.1 | 58.2±.5 | $5.303_9$ | 2.2 | 7.139 |
| 0.42 | 1885.6±.1 | 109 ± 1 | $5.303_3$ | 1.9 | 7.139 |
| 0.32 | 1885.8±.1 | 163 ± 1 | $5.302_7$ | 1.7 | 7.139 |
| 0.22 | 1886.0±.1 | 292 ± 1 | $5.302_2$ | 1.4 | 7.139 |
| 0.12 | 1886.7±.1 | 700 ±10 | $5.300_2$ | 1.0 | 7.139 |

(N.B. 7.14 mV = 733°C).

RUN (5)

| Freq. (KHz) | $R_p$ (ohms) | $C_p$ (pF) | $G_p \times 10^4$ ($ohm^{-1}$) | $f^2 C_p \times 10^6$ ($F\ sec^{-2}$) | Temp. (mV) |
|---|---|---|---|---|---|
| 107 | 1882.2±.2 | | | | 7.144 |
| 51 | 1882.7±.2 | | | | 7.144 |
| 20 | 1883.4±.1 | 0.5±.1 | $5.309_5$ | 200 | 7.144 |
| 15 | 1883.5±.1 | 0.6±.1 | $5.309_2$ | 130 | 7.144 |
| 10 | 1883.5±.1 | 1.1±.1 | $5.309_2$ | 110 | 7.144 |
| 6 | 1883.5±.1 | 1.8±.1 | $5.309_2$ | 65 | 7.144 |
| 4 | 1883.7±.1 | 2.5±.1 | $5.308_7$ | 40 | 7.144 |
| 2 | 1883.7±.1 | 5.0±.1 | $5.308_7$ | 20 | 7.144 |
| 1.5 | 1883.7±.1 | 8.4±.2 | $5.308_7$ | 19 | 7.144 |
| 1 | 1883.7±.1 | 8.4±.2 | $5.308_7$ | 8.4 | 7.144 |
| 0.8 | 1883.5±.1 | 13.7±.5 | $5.309_2$ | 8.8 | 7.144 |
| 0.62 | 1883.6±.1 | 21.6±.5 | $5.308_9$ | 8.3 | 7.144 |
| 0.52 | 1883.7±.1 | 32 ± 1 | $5.308_7$ | 7.2 | 7.144 |
| 0.42 | 1883.7±.1 | 45 ± 1 | $5.308_7$ | 7.9 | 7.144 |
| 0.32 | 1883.7±.1 | 76 ± 1 | $5.308_7$ | 7.7 | 7.144 |
| 0.22 | 1883.8±.1 | 154 ± 1 | $5.308_4$ | 7.4 | 7.144 |
| 0.12 | 1884.0±.1 | 374 ± 1 | $5.307_8$ | 7.4 | 7.144 |

(N.B. 7.14 mV = 733°C).

CADMIUM CHLORIDE.

| Freq. (KHz) | $R_p$ (ohms) | $C_p$ (pF) | $G_p x10^4$ ($ohm^{-1}$) | $f^2C_p x10^6$ (F $sec^{-2}$) | $f^{3/2}C_p x10^7$ (F $sec^{-3/2}$) | Temp. (mV) |
|---|---|---|---|---|---|---|
| 107 | 2848 ± 1 | | | | | 7.204 |
| 51 | 2852.2±.5 | | | | | 7.204 |
| 20 | 2853.8±.2 | 1.4±.2 | $3.504_1$ | 560 | 39.8 | 7.204 |
| 15 | 2854.1±.1 | 1.8±.2 | $3.503_7$ | 410 | 33.1 | 7.203 |
| 10 | 2854.3±.1 | 3.0±.1 | $3.503_5$ | 300 | 30.0 | 7.203 |
| 6 | 2855.2±.1 | 5.9±.1 | $3.502_4$ | 210 | 27.5 | 7.203 |
| 4 | 2855.9±.1 | 10.2±.1 | $3.501_5$ | 160 | 25.9 | 7.203 |
| 2 | 2857.4±.1 | 27.2±.1 | $3.499_7$ | 110 | 24.4 | 7.203 |
| 1.5 | 2858.1±.1 | 37.2±.1 | $3.498_8$ | 84 | 21.7 | 7.204 |
| 1 | 2860.4±.1 | 63.1±.2 | $3.496_0$ | 63 | 20.0 | 7.204 |
| 0.8 | 2861.8±.1 | 89.1±.5 | $3.494_3$ | 57 | 20.2 | 7.204 |
| 0.62 | 2862.7±.1 | 115.3±.5 | $3.493_2$ | 44 | 17.8 | 7.204 |
| 0.42 | 2864.0±.1 | 157.0±.5 | $3.491_6$ | 28 | 13.6 | 7.204 |
| 0.32 | 2864.7±.1 | 243 ± 1 | $3.490_8$ | 25 | 13.9 | 7.204 |
| 0.22 | 2865.5±.1 | 281 ± 5 | $3.489_8$ | 14 | 9.2 | 7.204 |
| 0.12 | 2866.7±.1 | 489 ±10 | $3.488_3$ | 7 | 6.4 | 7.204 |

(N.B. 7.20 mV = 739°C).

## REFERENCES.


1. J.O'M.Bockris, E.H.Crook, H.Bloom and N.E.Richards, Proc.Roy.Soc., 1960, A.255, 558.
2. C.A.Angell and J.W.Tomlinson, Disc. Faraday Soc., 1961, 32, 237.
3. E.R.Buckle and P.E.Tsaoussoglou, J.Chem.Soc., 1964, 667.
4. A.Findlay and J.A.Kitchener, Practical Physical Chemistry, Longmans, London, 8th edit., 1960, p.206.
5. G.Jones and M.J.Prendergast, J.Amer.Chem.Soc., 1937, 59, 731.
6. E.R.Buckle and P.E.Tsaoussoglou, Trans.Faraday Soc., 1964, 60, 2144.
7. E.R.Buckle, P.E.Tsaoussoglou, and A.R.Ubbelohde, ibid., 1964, 60, 684.
8. K.H.Stern and J.A.Stiff, J.Electrochem. Soc., 1964, 111, 813.
9. K.H.Stern, ibid., 1965, 112, 208.
10. R.F.Bartholomew, ibid., 1965, 112, 1120.
11. P.E.Tsaoussoglou, Unpublished Work.

12. S.Glasstone,
Textbook of Physical Chemistry, Macmillan, London, 2nd edit., 1960.

13. Thorpe's Dictionary of Applied Chemistry, edit. Whitely, Longmans, New York, 4th edit., 1938, Vol.II, p.709b.

14. C.P.Smyth,
Dielectric Behaviour and Structure, McGraw-Hill, New York, 1955, p.1.

15. E.R.Van Artsdalen and I.S.Yaffe,
J.Phys.Chem., 1955, 59, 118.

16. P.E.Tsaoussoglou,
Ph.D.Thesis, London, 1965.

17. H.Winterhager and W.Werner,
Forschungsber. Wirtschafts-u. Verkehrsministeriums. Nordrhein-Westfalen, 1956, No.341.

18. I.S.Yaffe and E.R.Van Artsdalen,
J.Phys.Chem., 1956, 60, 1125.

19. A.Klemm,
Molten Salt Chemistry, edit. Blander, Interscience, New York, 1964, p.535.

20. J.Zarzycki and F.Naudin,
Compt. rend., 1963, 256, 1282.

21. R.R.Dogonadze and Yu.A.Chizmadzhev,
Dokl.Akad.Nauk, SSSR, 1964, 157, 944.

22. J.H.Shaffer, W.R.Grimes, and G.M.Watson,
J.Phys.Chem., 1959, 63, 1999.

23. G.Jaffé and J.A.Rider,
J.Chem.Phys., 1952, 20, 1077.

24. E.P.Honig and J.A.A.Ketelaar,
Trans.Faraday Soc., 1966, 62, 190.

25. T.Førland,
Fused Salts, edit. Sundheim, Mc-Graw-Hill,
New York, 1964, p.63.

26. R.J.Friauf,
J.Chem.Phys., 1954, 22, 1329.

27. R.Becker and F.Sauter,
Electromagnetic Fields and Interactions, Transl.
Knudsen, Blackie, London, 1964.

# APPENDIX.

## MEASUREMENT OF THE DENSITY OF MOLTEN CAESIUM CHLORIDE.

Using the pyknometric technique of Buckle, Tsaoussoglou and Ubbelohde[1], the density of pure caesium chloride was measured at a number of temperatures in the range 974 - 1040°C. This was a necessary prerequisite to the future measurement of excess volumes in molten CsCl-MCl, (where M = Tl, Na, K, etc.), in this laboratory.

## EXPERIMENTAL.

### THE PYKNOMETER.

DETAILS OF CONSTRUCTION.

The pyknometer, similar to that used by Buckle et al.[1], was made to specification by Messrs. Johnson Matthey and Co. from iridium of 99.9% purity, and had a capacity of about 2 cc. The main body consisted of a cylinder surmounted by a conical roof (Fig.40 ). When the stopper, provided with an overflow capillary, was inserted into the horizontal mouth, the conical shape of the roof was completed. This, together with the absence of sharp external edges, promoted easy draining of the melt. A length of iridium wire, fused into a bead at the bottom, was threaded through the capillary to facilitate handling of the stopper.

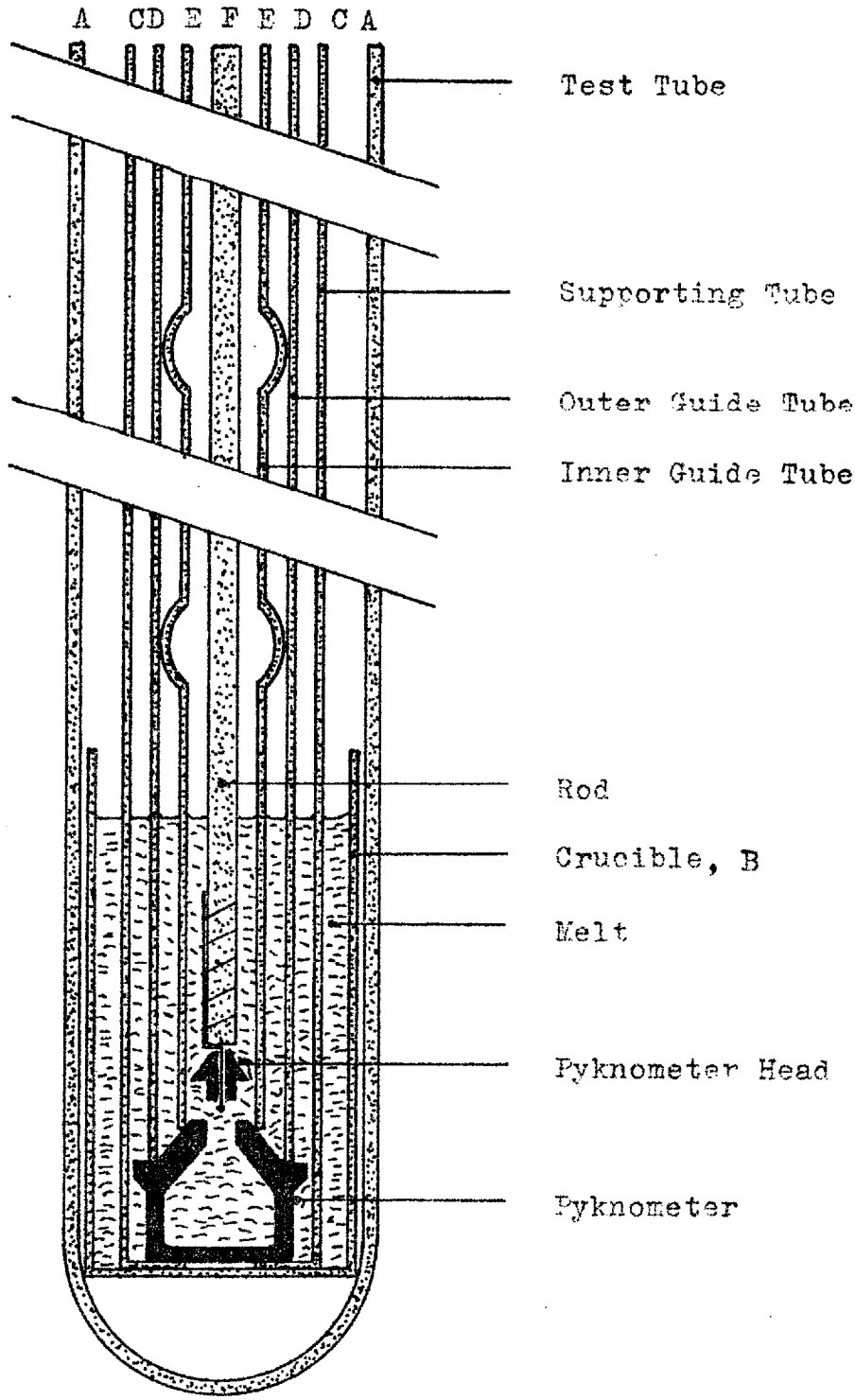


Figure 40. The Pyknometric Technique.

The wire was kinked just above the top of the stopper to restrict relative movement between the two.

CALIBRATION.

A thorough investigation into calibration techniques was undertaken. The pyknometer was first calibrated at room temperature by the method of Buckle et al. (Method 1). In this, the pyknometer was cleaned, dried, and weighed, and the calibrating liquid poured into the mouth. The stopper was then pushed home, and after carefully drying the outside, the pyknometer was reweighed. The results obtained using triple-distilled mercury and distilled water as calibrating liquids showed an unexpectedly high discrepancy of 0.47% (see Table A.1 below). The lower volume, obtained with mercury, was attributed to difficulty in filling the pyknometer due to the high surface tension. This liquid was therefore considered unsuitable for calibration purposes.

A new calibration technique was devised in which the filling conditions in the melt were simulated (Method 2). The pyknometer was lowered on the aluminium carrier tube (Fig. 41) into a beaker containing the calibrating liquid, and air was displaced by lowering and raising a glass rod in the mouth until no more bubbles emerged. The stopper was then placed in position and after a steady temperature

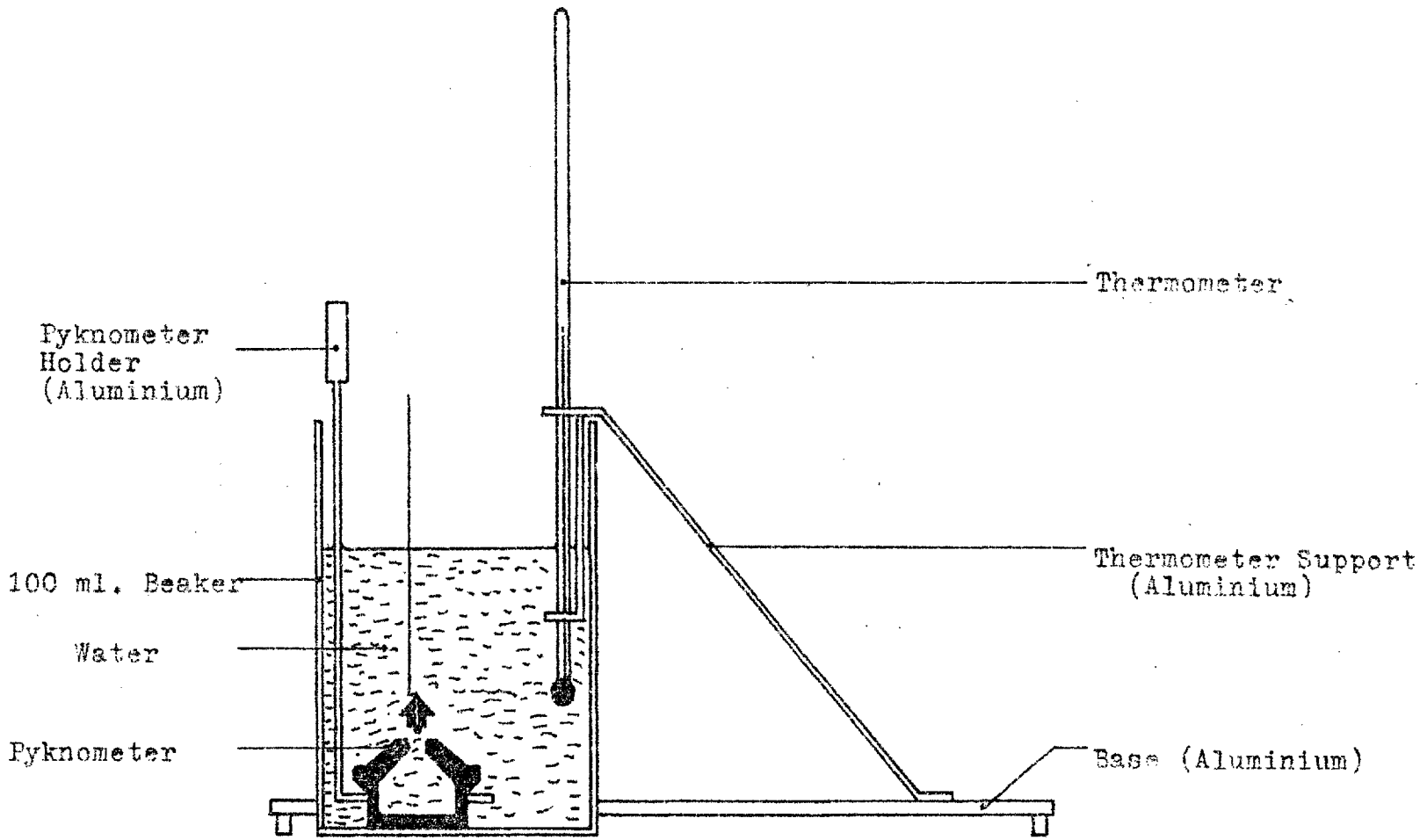


Figure 41. Calibration of the Pyknometer.

had been attained, the pyknometer was removed, dried, and reweighed. The results using this technique are compared with those using that of Buckle et al. in Table A.1.

Table A.1.

| Method | Calibrating Liquid | Temp. °C. | Pyknometer Volume, $cm^3$ | Pyknometer Volume at 20°C. $cm^3$ (a) |
|---|---|---|---|---|
| 1 | Mercury (b) | 20.6 | 2.1607±.0016 | 2.1600 |
| 1 | Water (c) | 19.9 | 2.1704±.0007 | 2.1705 |
| 2 | Water (c) | 21.0 | 2.1690±.0004 | 2.1678 |
| 2 | Toluene (d) | 22.6 | 2.1690±.0005 | 2.1659 |

(a) Iridium expansivity data : Holborn and Valentiner [2].

(b) Mercury density data : Cooke and Stone [3].

(c) Water density data : International Critical Tables.

(d) Toluene (G.P.R.) density data: 0.8637±.0019 g $cm^{-3}$, at 22.6°C. (as measured).

The two determinations using water differ by only 0.12%. However, the standard deviation on the volume of Method 2 is far smaller (12 weighings in each determination) and this value is therefore more reliable. The agreement between the results for water and toluene (Method 2) is considered satisfactory in view of the observed evaporation of the latter.

Two further liquids were examined as to their suitability for calibration purposes. These were benzene, which was rejected on the grounds of its high volatility, and dibutyl phthalate, which was unsuitable because it formed a film on the outside of the pyknometer which was difficult to remove.

In view of these results it was decided to calibrate the pyknometer by Method 2, using distilled water as the calibrating liquid.

## EXPERIMENTAL TECHNIQUE.

The density of molten CsCl (Johnson Matthey, 99.99% purity) was measured using the technique of Buckle et al.[1]. The salt was powdered, heated at 200°C for 24 hours, and stored under vacuum ($10^{-3}$ - $10^{-5}$ mm Hg) to remove most of the moisture. The melt was contained in a transparent vitreosil silica crucible (Fig.40,B), 100 mm long and 27 mm bore, supported inside a silica test tube A, as described above (p.147). Argon, previously dried with an acetone-Cardice mixture, and silica gel and Anhydrone, was admitted through the side-arm.

At the beginning of an experiment the pyknometer, supported on four projections in the silica carrying tube C, 520 mm long and 23 mm bore, was held just above the melt and allowed to attain the temperature of the furnace.

During this period a second stream of dried argon was admitted at the top of the carrier tube assembly to prevent possible oxidation of the pyknometer. A second tube D, 520 mm long and 14 mm bore, rested on the flange of the pyknometer keeping it upright. The pyknometer was then immersed in the melt and filled, using a silica rod to promote displacement of the gas. A series of stirrings over 5 min. was effective in dislodging any bubbles [1]. The stopper, attached to the silica rod F of 2 mm diameter by platinum wire wound tightly its lifting wire, was lowered inside a third tube E which rested on the cone of the pyknometer. This guide tube, 560 mm long and 8 mm bore, was expanded in three places along its length to give a close sliding fit inside the second tube. Its bore was thereby aligned with the mouth of the pyknometer. The stopper was raised and lowered several times in the mouth to expel any bubbles trapped in the capillary before being finally pushed home. Fiducial marks scratched on the rod and guide tube were helpful during this operation. The inner guide tube was then withdrawn, and a thermocouple (see p.132) lowered into the melt above the pyknometer.

At least 3½ hours was required for the attainment of a stable and uniform temperature distribution in the melt, (cf. refs. 1,4). Then, after first removing the thermocouple, the assembly was rapidly withdrawn from the

from the test tube by lifting the carrying tube. Residual melt was drained by raising the guide tube and pushing the pyknometer up and down. After cooling in air the pyknometer was removed from the carrying tube and the lifting wire detached from the rod. The pyknometer was then carefully cleaned of the last traces of adherent salt, and weighed.

To empty the pyknometer, the lifting wire was tied to the rod and the whole lowered once more into the furnace on the carrying tube. When the contents had melted the stopper was withdrawn and the pyknometer was lifted out, inverted, and returned to the furnace. The molten contents were expelled by shaking. Drainage was fairly complete, and the last traces of salt were removed by rinsing in hot water. Complete expulsion of the contents was verfied by weighing.

## RESULTS.

The density of pure Caesium Chloride measured at a number of temperatures is given in Table A.2.

Table A.2.

Density of Caesium Chloride.

| Temperature | Density, g $cm^{-3}$ This Work. | Density, g $cm^{-3}$ Van Artsdalen and Yaffe[4] |
|---|---|---|
| 974 | 2.4376 | 2.4409 |
| 977 | 2.4434 | 2.4377 |
| 1027 | 2.3950 | 2.3844 |
| 1040 | 2.3695 | 2.3706 |

Apart from the values at 1027°C, which differ by 0.5%, there is agreement to better than ± 0.1% between the present results and the extrapolated data of Van Artsdalen and Yaffe[4], i.e.,

$$\rho = 3.4782 - 1.0650 \times 10^{-3} T, \quad g\ cm^{-3}$$

Std. Dev. 0.0006 $g\ cm^{-3}$

670 - 905°C.

The density data are plotted as a function of temperature in Fig.42.

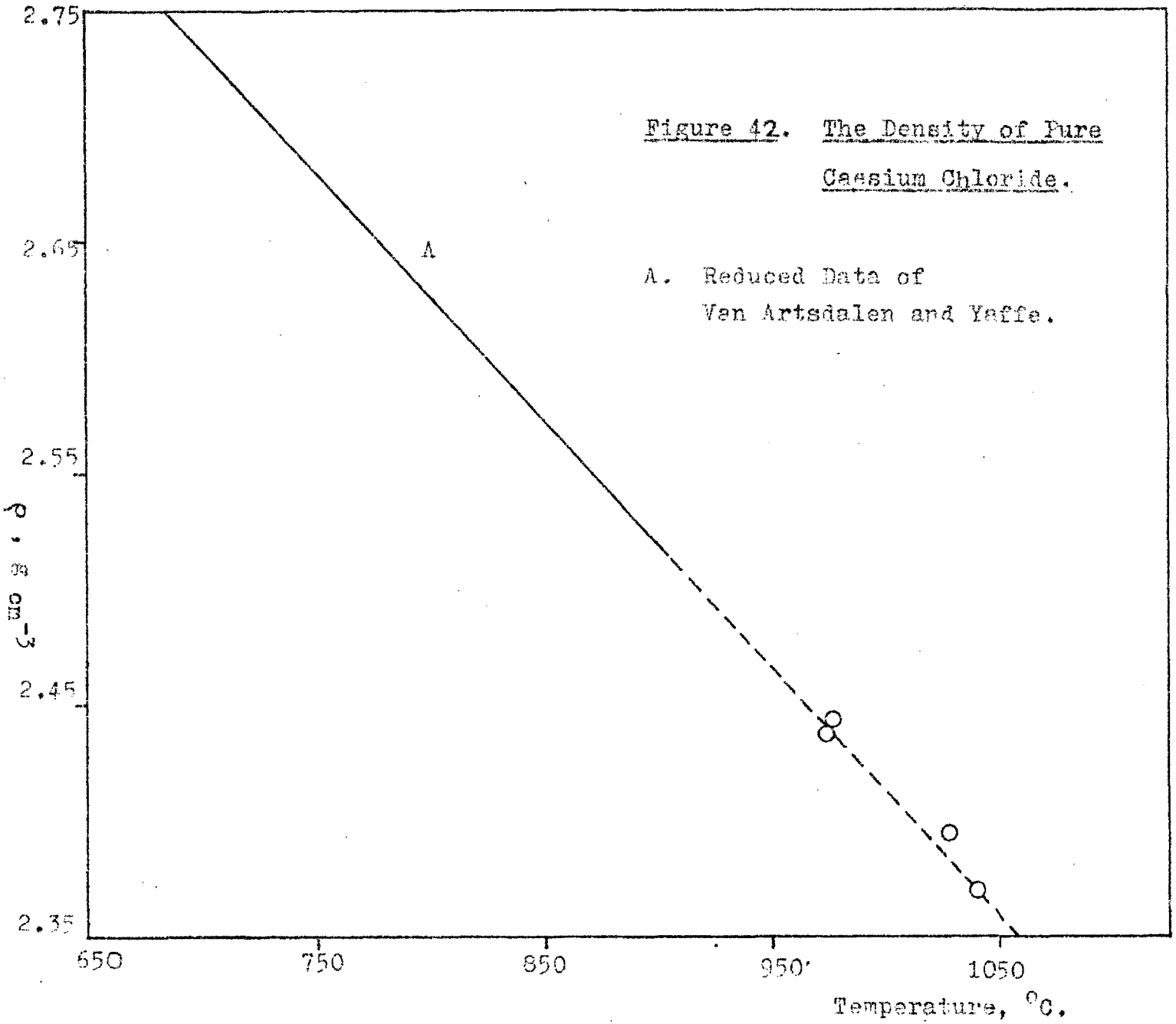


Figure 42. The Density of Pure Caesium Chloride.

A. Reduced Data of Van Artsdalen and Yaffe.

## REFERENCES.

1. E.R.Buckle, P.E.Tsaoussoglou , and A.R.Ubbelohde,
Trans.Faraday Soc., 1964, 60, 684.

2. L.Holborn and S.Valentiner,
Ann.Phys., 1907, 22, 1.

3. A.H.Cooke and N.W.B.Stone,
Phil.Trans., 1957, A250, 279.

4. E.R.Van Artsdalen and I.S.Yaffe,
J.Phys.Chem., 1956, 60, 1125.

# INDEX.

Page No

Page No.

Page No.